Dressed molecules in resonantly interacting ultracold atomic Fermi gases

G. M. Falco and H. T. C. Stoof
Institute for Theoretical Physics, Utrecht University, Leuvenlaan 4, 3584 CE Utrecht, The Netherlands
(Received 9 March 2006; published 12 February 2007)

We present a detailed analysis of the two-channel atom-molecule effective Hamiltonian for an ultracold two-component homogeneous Fermi gas interacting near a Feshbach resonance. We particularly focus on the two-body and many-body properties of the dressed molecules in such a gas. An exact result for the many-body T matrix of the two-channel theory is derived by both considering coupled vertex equations and functional-integral methods. Making use of this result allows us to incorporate exactly into the many-body theory the two-body physics of the Feshbach scattering by means of simple analytical formulas without any fitting parameters. New interesting many-body effects are discussed in the case of narrow resonances. We give also a description of the BEC-BCS crossover above and below T_C. The effects of different approximations for the self-energy of the dressed molecules are discussed. The single-channel results are derived as a special limit for broad resonances. Moreover, through an analytic analysis of the BEC limit, the relation between the composite boson of the single-channel model and the dressed-molecule of the two-channel model is established.

DOI: 10.1103/PhysRevA.75.023612 PACS number(s): 03.75.−b, 67.40.−w, 39.25.+k

I. INTRODUCTION

Since the achievement of the first Bose-Einstein condensate in a trapped dilute gas of alkali-metal atoms in 1995 [1–3], the area of ultracold atomic gases is one of the most active fields of research in physics. The experimental realization of this new state of matter has been made possible by trapping an atomic gas cloud in a magnetic trap and lowering its temperature down to about 10–100 nK by means of a combination of laser-cooling and evaporative-cooling techniques.

The extraordinary progress in the technology of trapping and cooling alkali-metal atoms has been applied in the last two years also to study superfluidity in fermionic gases. However, in a BCS superconductor, the critical temperature of the superfluid transition is exponentially small with respect to the Fermi temperature, which is the temperature scale associated with the onset of degeneracy in the gas. For this reason, the fermionic analog of the Bose-Einstein condensation transition temperature, i.e., the Bardeen-Cooper-Schrieffer (BCS) critical temperature for Bose-Einstein condensation of Cooper pairs, cannot be reached by means of current techniques. Moreover, the BCS phase does not affect the density distribution of the gas in the same manner as in a trapped Bose gas. As a result it is not easy to detect the pair correlations of the Cooper pairs characterizing the superfluid properties of the gas. Fortunately, the use of Feshbach resonances in atomic Fermi gases [4–9], has solved [15,16] both of these problems simultaneously.

Near a Feshbach resonance two atoms can virtually form a long-lived bound molecular state during an *s*-wave collision. The scattering process consists of two incoming atoms in an energetically open channel, which has a different hyperfine state than the bound state in the closed channel. The coupling between the open and the closed channels is physically provided by the exchange interaction, i.e., the difference between the singlet ${}^1\Sigma_g^+$ and triplet ${}^3\Sigma_u^+$ potentials of the two alkali-metal atoms in the electronic ground state. Moreover, the two channels have a different Zeeman shift in a magnetic field because of the difference in hyperfine state. Therefore, the energy difference between the closed-channel bound molecular state and the two-atom continuum threshold is experimentally adjustable by tuning the magnetic field. As a result, the *s*-wave scattering length, and hence the magnitude and sign of the interatomic interactions, can be precisely controlled over a wide range.

The possibility of tuning the interactions in a system is rather unusual in condensed-matter physics and has triggered many new experimental developments. In particular, Feshbach resonances provide a remarkable opportunity to study strongly interacting fermions. By varying the interaction strength between the fermionic atoms, the crossover from a Bose-Einstein condensate of molecules to a BCS superfluid of loosely bound pairs [10–14] has been explored [15–23]. These experiments have revealed evidence of fermionic pair condensation [15,16] and superfluidity [21]. Moreover, in a magnetized Fermi gas the phase separation between a superfluid paired component and the normal unpaired fermions has also been observed [22,23].

A Feshbach resonance in atomic and nuclear physics is a multichannel problem. Already in 1962, Feshbach [4] developed a general method to solve the multichannel elastic scattering equations in the presence of a bound state, using a formalism based on projection-operator techniques. His approach reduces the solution of the multichannel problem of the colliding particles to a single-channel problem, namely the scattering of a particle from an optical potential. In general, the price of this simplification is a complicated nonlocal and energy-dependent optical potential. Neglecting the possible occupation of the bound state energy level and the energy dependence of the optical potential ultimately leads to a many-body theory with a local interaction described by a single adjustable parameter, namely the *s*-wave scattering length a. This is usually called the *single-channel* approximation [10–14,25–41] in the literature related to the study of cold atoms near Feshbach resonances. A different many-body approach, which allows for the population of the bound molecular state and thus preserves the multichannel nature of the Feshbach problem, has also been considered by many

authors. This is based on a *two-channel* low-energy effective Hamiltonian [42–61], where the effects of the resonant scattering are described by a bosonic molecular field coupled to the atoms in the Fermi sea. This bosonic field describes the bound state in the closed channel near the continuum of the open-channel scattering states. As a result of the coupling with the atoms, the physical bosonic degree of freedom in the system is not this bare molecule but the so-called dressed molecule [47], namely the bare molecule "dressed" by the coupling to the continuum of scattering states. The wave-function of the latter is always a superposition sharing a component in the closed channel and one in the open channel. The probability of the bare closed-channel component is denoted by Z. Note that, in this language, the single-channel model is a different model that has $Z=0$ from the outset.

In this work we begin a systematic analysis of a two-channel many-body theory for a mixture of fermionic atoms near a Feshbach resonance based on the dressed-molecule picture. This long paper represents both an extension and a unifying description of our previous results discussed in [49,52,59]. While details about the derivation of the results obtained in these short papers are given, also several results are presented here. The paper is organized as follows. In Sec. II we introduce the physics of Feshbach resonant scattering in ultracold atomic gases. This preliminary analysis is based on a microscopic atomic physics Hamiltonian with spin-dependent interactions in the presence of an external magnetic field.

In Sec. III we introduce the low-energy effective quantum field theory above the superfluid critical temperature based on the atom-molecule Hamiltonian. The field theory is then solved in the so-called many-body T-matrix approximation. We show that this approach incorporates exactly the two-body scattering properties in the presence of a Feshbach resonance. In the two-body limit, we find new and general analytic expressions for the binding energy and the closed-channel component Z of the dressed molecules, which reproduce experimental data without any fitting parameters. Next we generalize the results of the many-body T-matrix approximation by means of functional integral techniques, which is important in order to go beyond the approximation of this paper.

In the limit of a very broad resonance the many-body T matrix of the single-channel approximation is recovered. Moreover, new interesting many-body effects are also discussed in particular in connection with the possibility of having narrow resonances.

In Sec. IV and Sec. V the physics of the BEC-BCS crossover is investigated. Section IV considers the problem of determining the superfluid critical temperature T_c approaching the transition from above, while in Sec. V we turn our attention to the description of the crossover in the superfluid phase below T_c. In both regimes, we give a systematic analysis of the crossover equations both in the mean field approximation [11] and beyond mean field, at the level of the Gaussian fluctuations [12,13,34] and according to a self-consistent approach [14]. We focus especially on the BEC limit of the crossover, where analytical calculations are possible. In the case of broad resonances, we show that the dressed-molecule approach [52,57] is consistent with the single-channel model results. The relation between the *composite boson* of the single-channel model and the dressed molecule of the two-channel approach is established also at the mathematical level.

II. FESHBACH RESONANCES IN ATOMIC FERMI GASES

Before discussing the many-body physics in a resonant Fermi gas, which is the main subject of this paper, we consider the scattering of two atoms at the Feshbach resonance in the absence of a medium. This is a necessary step in order to include exactly the two-body physics in the more general many-body treatment. At low temperatures only s-wave scattering is important in the gas, since the centrifugal barrier prevents higher-order partial waves to enter the interaction region. Due to the Pauli principle occurring in a gas of fermionic particles, interaction effects can therefore only be observed when we consider a mixture of two spin states. For this reason we only consider such mixtures in the following.

Feshbach resonances occur in atomic physics when studying collisions of ultracold atoms under variation of an external magnetic field [62,63]. In the presence of an external magnetic field B the spin-dependent part of the single-atom Hamiltonian is

$$H_{\rm int} = \left(\frac{a_{\rm hf}}{\hbar^2}\right)\mathbf{s}\cdot\mathbf{i} + \mathbf{B}\cdot\frac{2\mu_e\mathbf{s}-\mu_N\mathbf{i}}{\hbar}, \tag{1}$$

where the energy $a_{\rm hf}$ depends on the atomic species and characterizes the hyperfine interaction between the electronic spin $\mathbf{s}$ and the nuclear spin $\mathbf{i}$. The two constants μ_e and μ_N are, respectively, the electronic and nuclear magnetic moments of the alkali atom of interest and we always have that $\mu_e \gg \mu_N$.

The diagonalization of this Hamiltonian yields the hyperfine states, which, at zero magnetic field, have the magnitude f of the total atomic spin $\mathbf{f}=\mathbf{s}+\mathbf{i}$ and its projection on the z-axis m_f as good quantum numbers. At high magnetic fields $B \gg a_{\rm hf}/\mu_e$, the hyperfine interaction can be treated as a perturbation, and, to lowest order, the electronic and nuclear spin projections m_s and m_i are the good quantum numbers. At intermediate values of the magnetic field, where the Feshbach resonances are often observed, the atomic eigenstates are a linear combination of the latter states, that schematically can be written as

$$c_{-1/2}\left|m_s=-\tfrac{1}{2};m_i=m_f+\tfrac{1}{2}\right\rangle + c_{1/2}\left|m_s=\tfrac{1}{2};m_i=m_f-\tfrac{1}{2}\right\rangle.$$

This implies that only the total spin projection m_f is a good quantum number. Without much loss of generality, we consider a gas of ^{6}Li atoms from now on. This species is most widely used in current experiments with trapped ultracold Fermi gases. The ^{6}Li isotope has nuclear spin $i=1$, which gives in increasing order of energy, the six hyperfine states

$$|1\rangle = \sin\theta_+\left|\tfrac{1}{2};0\right\rangle - \cos\theta_+\left|-\tfrac{1}{2};1\right\rangle,$$

$$|2\rangle = \sin\theta_-\left|\tfrac{1}{2};-1\right\rangle - \cos\theta_-\left|-\tfrac{1}{2};0\right\rangle,$$

$$|3\rangle = \left|-\tfrac{1}{2};-1\right\rangle,$$

$$|4\rangle = \cos\theta_-\left|\tfrac{1}{2};-1\right\rangle + \sin\theta_-\left|-\tfrac{1}{2};0\right\rangle,$$

$$|5\rangle = \cos\theta_+\left|\tfrac{1}{2};0\right\rangle + \sin\theta_+\left|-\tfrac{1}{2};1\right\rangle,$$

$$|6\rangle = \left|\tfrac{1}{2};1\right\rangle, \tag{2}$$

with $\sin\theta_\pm = 1/\sqrt{1+(Q^\pm+R^\pm)^2/2}$, $Q^\pm=(\mu_n+2\mu_e)B/a_{\rm hf}\pm 1/2$, and $R^\pm=\sqrt{(Q^\pm)^2+2}$. Here the states $|m_s;m_i\rangle$ have a well-defined projection of the electron and nuclear spin, respectively.

So far, we have considered only the spin degrees of freedom of a single atom. The spin-dependent Hamiltonian of two noninteracting atoms is [64]

$$H_{\rm int} = \left(\frac{a_{\rm hf}}{\hbar^2}\right)(\mathbf{s}_1\cdot\mathbf{i}_1+\mathbf{s}_2\cdot\mathbf{i}_2) + \mathbf{B}\cdot\frac{2\mu_e\cdot\mathbf{S}-\mu_N\cdot\mathbf{I}}{\hbar}, \tag{3}$$

where $\mathbf{S}=\mathbf{s}_1+\mathbf{s}_2$ and $\mathbf{I}=\mathbf{i}_1+\mathbf{i}_2$ are the total electronic and nuclear spin, respectively. In view of the ongoing experiments, we consider in the following a hyperfine mixture of the states $|1\rangle$ and $|2\rangle$. Hence, the incoming channel for two-atom scattering is the antisymmetric state

$$|\{12\}\rangle \equiv \frac{1}{\sqrt{2}}[|1\rangle_1|2\rangle_2 - |2\rangle_1|1\rangle_2]. \tag{4}$$

This combination can only be trapped in a far-off resonance optical trap [66] and not in a magnetic trap. It is, however, the most favorable mixture experimentally, because it cannot decay through inelastic two-body collisions. For future reference it is useful to rewrite this state as the linear superposition

$$\begin{aligned}|\{12\}\rangle = {}& \sin\theta_+\sin\theta_-|1,1;1,-1\rangle + \sin\theta_+\cos\theta_-\left(\frac{1}{\sqrt{3}}|0,0;0,0\rangle\right.\\ & \left. - \sqrt{\frac{2}{3}}|0,0;2,0\rangle\right) + \cos\theta_+\sin\theta_-\left(\frac{1}{\sqrt{3}}|0,0;0,0\rangle\right.\\ & \left. + \frac{1}{\sqrt{6}}|0,0;2,0\rangle - \frac{1}{\sqrt{2}}|1,0;1,0\rangle\right)\\ & + \cos\theta_+\cos\theta_-|1,-1;1,1\rangle \end{aligned} \tag{5}$$

of the basis states $|SM_S;IM_I\rangle$, which diagonalize the second term in the right-hand side of Eq. (3). The quantum numbers M_S and M_I represent the total electronic and nuclear spin projection along the direction of the magnetic field, respectively.

The central interaction for two colliding atoms depends on the magnitude of the total electronic spin. It can be written as [64]

$$\mathrm{V_C} = \mathrm{V_S}\cdot\mathrm{P_S} + \mathrm{V_T}\cdot\mathrm{P_T}, \tag{6}$$

where $\mathrm{P_{S,T}}$ are the projection operators onto the singlet and triplet states and $\mathrm{V_{S,T}}$ the corresponding interatomic potentials. The singlet and triplet potentials $\mathrm{V_{S,T}}$ are by now rather accurately known from atomic-physics measurements. The central interaction $\mathrm{V_C}$ is diagonal in the basis $|SM_S;IM_I\rangle$ but induces transitions between different hyperfine levels. More precisely, the central interaction can be rewritten as

$$\mathrm{V_C} = \mathrm{V_{dir}} + \mathrm{V_{exch}}, \tag{7}$$

with the direct interaction given by

$$\mathrm{V_{dir}} = \frac{(\mathrm{V_S}+\mathrm{V_T})}{2}, \tag{8}$$

and the exchange interaction expressed as

$$\mathrm{V_{exch}} = \frac{(\mathrm{P_S}-\mathrm{P_T})(\mathrm{V_S}-\mathrm{V_T})}{2}. \tag{9}$$

If we describe a collision in the hyperfine basis, it is this latter interaction that is responsible for the coupling of different hyperfine states in the quantum collision of cold alkali-metal atoms. Only transitions where the quantum number M_S+M_I is conserved are allowed, since the central interaction cannot change the total electron or nuclear spin. Therefore, the state $|\{12\}\rangle$ couples only to the states

$$\begin{aligned}|\{14\}\rangle = {}& \sin\theta_+\cos\theta_-\frac{1}{\sqrt{2}}|1,1;1,-1\rangle + \left(\sqrt{\frac{2}{3}}\sin\theta_+\sin\theta_-\right.\\ & \left. + \frac{1}{\sqrt{6}}\cos\theta_+\cos\theta_-\right)|0,0;2,0\rangle + \left(\frac{1}{\sqrt{3}}\cos\theta_+\cos\theta_-\right.\\ & \left. - \frac{1}{\sqrt{3}}\sin\theta_+\sin\theta_-\right)|0,0;0,0\rangle\\ & - \cos\theta_+\cos\theta_-\frac{1}{\sqrt{2}}|1,0;1,0\rangle\\ & - \cos\theta_+\sin\theta_-|1,-1;1,1\rangle, \end{aligned}$$

$$\begin{aligned}|\{25\}\rangle = {}& \cos\theta_+\sin\theta_-|1,1;1,-1\rangle - \left(\frac{1}{\sqrt{3}}\sin\theta_+\sin\theta_-\right.\\ & \left. - \frac{1}{\sqrt{3}}\cos\theta_+\cos\theta_-\right)|0,0;0,0\rangle - \left(\sqrt{\frac{2}{3}}\cos\theta_+\cos\theta_-\right.\\ & \left. + \frac{1}{\sqrt{6}}\sin\theta_+\sin\theta_-\right)|0,0;2,0\rangle\\ & + \frac{1}{\sqrt{2}}\sin\theta_+\sin\theta_-|1,0;1,0\rangle\\ & - \sin\theta_+\cos\theta_-|1,-1;1,1\rangle, \end{aligned}$$

$$\begin{aligned}|\{45\}\rangle = {}& \cos\theta_+\cos\theta_-|1,1;1,-1\rangle - \left(\frac{1}{\sqrt{3}}\cos\theta_+\sin\theta_-\right.\\ & \left. + \frac{1}{\sqrt{3}}\sin\theta_+\cos\theta_-\right)|0,0;0,0\rangle + \left(\sqrt{\frac{2}{3}}\cos\theta_+\sin\theta_-\right.\\ & \left. - \frac{1}{\sqrt{6}}\sin\theta_+\cos\theta_-\right)|0,0;2,0\rangle\\ & + \frac{1}{\sqrt{2}}\sin\theta_+\cos\theta_-|1,0;1,0\rangle\\ & + \sin\theta_+\sin\theta_-|1,-1;1,1\rangle, \end{aligned}$$

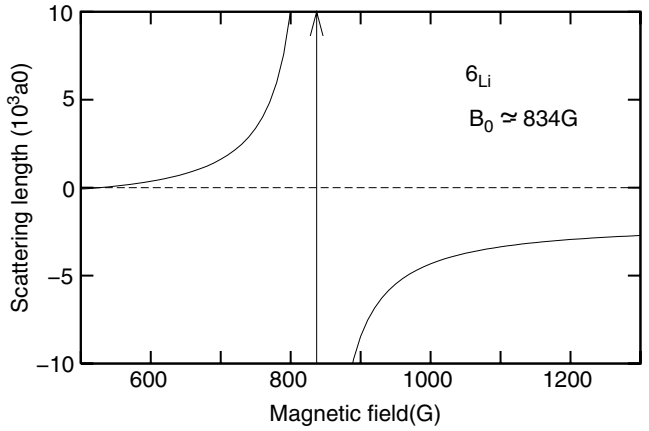

FIG. 1. Scattering length as a function of the magnetic field for two ^{6}Li atoms in the hyperfine states $|1\rangle$ and $|2\rangle$ near the broad resonance at 834 G [65].

$$|\{36\}\rangle = \frac{1}{\sqrt{3}}|0,0;0,0\rangle + \frac{1}{\sqrt{6}}|0,0;2,0\rangle + \frac{1}{\sqrt{2}}|1,0;1,0\rangle. \tag{10}$$

The magnetic field dependence of the s-wave scattering length $a(B)$ in the $|\{12\}\rangle$ channel is obtained by solving the system of five coupled-channels equations for these channels [64]. The scattering length exhibits several resonances as an effect of the interplay between the different channels in the scattering process. A very broad resonance occurring at 834 G is shown in Fig. 1.

Physically, this Feshbach resonance at 834 G arises when the energy of the atoms with the incoming spin wavefunction $|\{12\}\rangle$, which in this high magnetic field region is almost purely triplet, coincides with the energy of a bound-state energy in the singlet potential V_S. It is convenient for this purpose to rewrite the the spin-dependent part of the total Hamiltonian as

$$H_{\text{spin}} = \mathbf{B}\cdot\frac{2\mu_e\cdot\mathbf{S}-\mu_N\cdot\mathbf{I}}{\hbar} + \frac{a_{\text{hf}}}{\hbar^2}(\mathbf{s}_1\cdot\mathbf{i}_1+\mathbf{s}_2\cdot\mathbf{i}_2) + V_C \equiv H_Z$$
$$+ \frac{a_{\text{hf}}}{\hbar^2}(\mathbf{s}_1\cdot\mathbf{i}_1+\mathbf{s}_2\cdot\mathbf{i}_2) + V_C \equiv H_Z + H_{\text{hf}} + V_C, \tag{11}$$

because the states $|SM_S;IM_I\rangle$ diagonalize the H_Z+V_C operator. The hyperfine interaction H_{hf} is, however, not diagonal on the $|SM_S;IM_I\rangle$ states. The latter couples states with I and S quantum numbers differing at most by one. Classically, it gives rise to the independent single-atom precessions of $\mathbf{s}_i$ and $\mathbf{i}_i$ about their sum vector $\mathbf{f}_i$. During the collision of two lithium atoms, the hyperfine coupling H_{hf} can induce transitions to others, spin-flipped collision channels. A Feshbach resonance occurs when one of these supports a bound molecular state $\phi_m(\mathbf{r})|S'M'_S;I'M'_I\rangle$ with energy E_m, which lies near the continuum level of the incident $|\{12\}\rangle$ channel. The channel of the metastable bound state is said to be closed because, due to energy conservation, atoms can be observed asymptotically only in the incident open channel. The situation is illustrated in Fig. 2.

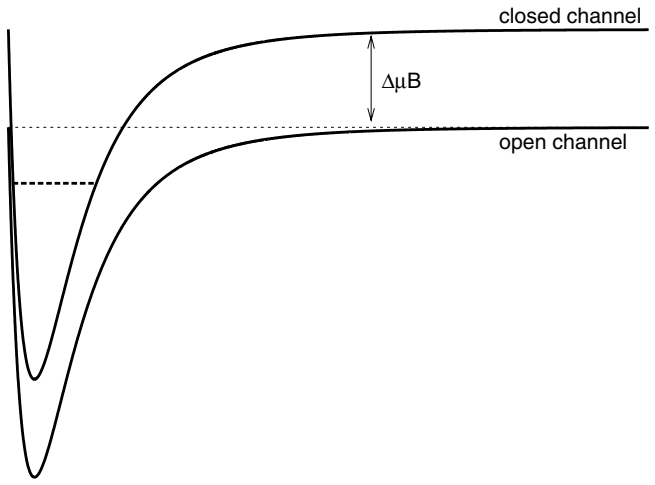

FIG. 2. Illustration of a Feshbach resonance. The upper potential curve describes, as a function of the interparticle separation, the closed channel interaction potential that contains the bound state responsible for the Feshbach resonance. The lower potential curve corresponds to the open-channel interaction potential.

At the high magnetic fields where the resonance occurs, the hyperfine interaction represents a small perturbation, and the total spin projections M_S and M_I are rather good quantum numbers. Therefore, we can approximate the basis $|\{ij\}\rangle$ with the basis $|SM_S;IM_I\rangle$. More precisely, in the limit of high magnetic field we have $\sin\theta_\pm \simeq 0$ and the six states in Eq. (2) can be approximated by

$$|1\rangle \simeq \left|-\tfrac{1}{2};1\right\rangle,$$
$$|2\rangle \simeq \left|-\tfrac{1}{2};0\right\rangle,$$
$$|3\rangle \simeq \left|-\tfrac{1}{2};-1\right\rangle,$$
$$|4\rangle \simeq \left|\tfrac{1}{2};-1\right\rangle,$$
$$|5\rangle \simeq \left|\tfrac{1}{2};0\right\rangle,$$
$$|6\rangle \simeq \left|\tfrac{1}{2};1\right\rangle, \tag{12}$$

which implies that the scattering channel $|\{12\}\rangle$ is almost the pure triplet state [see Eq. (5)]:

$$|\{12\}\rangle \simeq -|1,-1;1,1\rangle. \tag{13}$$

When the magnetic field is tuned between 800 G and 900 G, the energy of the incoming channel $|\{12\}\rangle$ lies near the $v=38$ molecular bound state energy of the singlet potential V_S. As a result a Feshbach resonance occurs which turns out to be very broad. The closed channel $|0,0;0,0\rangle$, supporting the bare molecular state, can be written by using Eq. (10) and taking the limit of high magnetic fields as

$$|0,0;0,0\rangle \simeq \frac{1}{\sqrt{3}}(|\{36\}\rangle + |\{25\}\rangle + |\{14\}\rangle). \tag{14}$$

The width of the resonance is thus determined by the matrix element

$$\langle 0,0;0,0|H_{\rm hf}|1,-1;1,1\rangle,$$

which describes the overlap induced by the hyperfine coupling between the spin wavefunctions of the closed and the open channel. The total atom-molecule coupling involves of course also the overlap between the relevant spatial wavefunctions of the atomic potentials.

Another resonance, a very narrow one, occurs at about 549 G when the energy of the open channel approaches the energy of the same $v=38$ bound state of the singlet potential, but now in the channel

$$|0,0;2,0\rangle \simeq \frac{1}{\sqrt{3}}\left(\frac{1}{\sqrt{2}}|\{36\}\rangle - \sqrt{2}|\{25\}\rangle + \frac{1}{\sqrt{2}}|\{14\}\rangle\right), \tag{15}$$

calculated also from Eq. (10) in the limit of high magnetic field, i.e., approximating $\sin\theta_{\pm}\simeq 0$ and $\cos\theta_{\pm}\simeq 1$ at lowest order in $a_{\rm hf}/\mu_e B$. The matrix element related to the width of the resonance is in this approximation

$$\langle 0,0;2,0|H_{\rm hf}|1,-1;1,1\rangle,$$

which is of the same order as the matrix element in Eq. (15). Hence, the different width of these two resonances does not originate from the overlap in the spin parts of the wavefunctions but in the overlap of the wavefunctions of the spatial degrees of freedom.

In the absence of the hyperfine coupling the energy difference between the closed and the open channels is linear in the magnetic field, i.e.,

$$\epsilon_{\rm m}(B) = E_{\rm m} + 2\mu_B B, \tag{16}$$

where we have used that the difference in magnetic moment $\Delta\mu$ between the closed singlet channel and the open triplet channel is twice the Bohr's magneton or $\Delta\mu=2\mu_B$. The hyperfine coupling produces a shift in the position of the magnetic field at which the resonance occurs [67]. It is this shifted value B_0 that is observed experimentally. The exact location of the resonance can be used to redefine the energy difference between the bound state in the closed channel and the threshold continuum. This is

$$\delta(B) = \Delta\mu(B - B_0), \tag{17}$$

and is called the detuning because it represents the variable that can be tuned experimentally by varying the magnetic field. At large negative detuning, the binding energy $\epsilon_{\rm m}(B)$ of the diatomic molecules, i.e., the energy you need to break up a molecule, goes linearly in the magnetic field B as $\epsilon_{\rm m}(B) \simeq \delta(B)$. Near resonance, the hyperfine coupling leads to a quadratic magnetic-field dependence of the binding energy according to Wigner's formula [24]

$$\epsilon_{\rm m}(B) = -\frac{\hbar^2}{ma^2(B)}, \tag{18}$$

where the total scattering length $a(B)$ diverges near resonance as

$$a(B) = a_{\rm bg}\left(1 - \frac{\Delta B}{B - B_0}\right). \tag{19}$$

The width of the resonance ΔB is a phenomenological parameter taken from experiments and the scattering length $a_{\rm bg}$ describes the nonresonant scattering in the open channel. At positive detuning, there no longer exists a bound state because the molecule decays into two free atoms due to the coupling with the atomic continuum.

So far we have seen that Feshbach resonances in atom-atom scattering involve intermediate states that are molecular bound states. For these molecules, the electronic and nuclear spins have been flipped compared to the spin of the colliding atoms by virtue of the interplay between hyperfine and exchange interactions. Next we consider briefly some of the ways that the ultracold gases at Feshbach resonance can be experimentally investigated. This account is, however, by no means complete. We discuss only the experimental results which are relevant in connection with the theory we want to discuss in the following.

Ultracold gases of fermionic atoms are trapped and cooled in optical traps [68–73]. The optical potential has the advantage to trap atoms in any spin state, as well as the molecules created from these atoms. The Fermi temperature T_F of these systems is usually of the order of $0.1-1$ μK. Cooling fermionic atoms down to temperatures $T \ll T_F$ below quantum degeneracy is problematic under normal conditions, because the standard evaporative cooling stops to work in the degenerate regime. However, in a mixture with two different spin states, the large cross section for elastic scattering near the Feshbach resonance can be used for efficient evaporative cooling, expecially at negative scattering lengths above the resonance where inelastic loss is negligible [74]. This permits experiments to reach temperatures down to $0.05T_F$.

By sweeping an external magnetic field across a Feshbach resonance, it is possible to create bosonic diatomic molecules. If the temperature of the gas is comparable or lower than the binding energy of the molecular state, an almost pure ultracold molecular gas forms. At even lower temperatures, the molecules form a Bose-Einstein condensate. The process is reversible because the gas can be converted back to atoms by reversing the sweep. These molecules are vibrationally highly excited states and would usually undergo fast relaxational decay into deeply bound states by molecule-molecule and atom-molecule collisions. This does occur for Feshbach molecules made with bosonic atoms [75,76]. In that case, the lifetime of the molecules can be increased only by trapping the sample in an optical lattice [77,78]. However, $^6Li_2$ and $^{40}K_2$ molecules, consisting of fermionic atoms, show very long lifetimes [68–71].

The origin of such a long lifetime has been explained by Petrov *et al.* in [79] as follows. The size of the deeply bound state is of the order of the characteristic range of the interaction r_0. The relaxation requires the presence of at least three fermions at distances of about r_0 from each other. As there are only two different spin states, two particles are

necessarily identical and the Pauli exclusion principle prevents this from happening and thus suppresses the relaxation probability.

The bound Feshbach molecule has a magnetic moment which differs from that of the unbound atoms pairs because its wavefunction is a superposition of the open and the closed channels. The difference in magnetic moment facilitates Stern-Gerlach selection of molecules and atoms. Jochim *et al.* [71] describe a purification scheme based on a Stern-Gerlach technique that efficiently removes all the atoms, while leaving all molecules trapped. The basic idea of this method consists in applying a magnetic field gradient B' perpendicularly to the axis of the optical dipole trap. The magnetic field pulls out of the trap particles for which the magnetic force is larger than the trapping force. The value B'_{at} at which all the atoms are lost turns out to be smaller than the value B'_{mol} at which molecules start to spill out of the the trap. This means that in principle one can remove all the atoms while keeping the total number of molecules constant. The magnetic moment of the bound molecules can be estimated from the relation $\mu_{\mathrm{mol}}=2\mu_{\mathrm{at}}B'_{\mathrm{mol}}/B'_{\mathrm{at}}$, where $2\mu_{\mathrm{at}}$ is the magnetic moment of two unbound atoms in the open channel. In a gas of ^{6}Li atoms at low density and at high magnetic fields, the latter is almost completely in the triplet state which implies $2\mu_{\mathrm{at}}=2\mu_B$. We have mentioned this experiment because the magnetic moment of the Feshbach molecule at negative detuning near the resonance will be one of the crucial quantities in order to verify that our theory incorporates the two-body physics exactly.

The long lifetime of the molecules makes it possible to observe a Bose-Einstein condensate of K_2 [68] and Li_2 [72,73] Feshbach molecules. Zwierlein *et al.* create in [73], for example, the Bose-Einstein condensate of Li_2 Feshbach molecules by operating additional evaporative-cooling cycles on the molecular side of the resonance. It is important to point out that in all these experiments, the condensed molecules are not detected directly by standard imaging techniques. In [73] the molecular density is inferred from absorption images at zero magnetic field taken with and without dissociating the molecules on the positive-detuning side of the resonance. The onset of Bose-Einstein condensation is characterized by an abrupt change from a smooth distribution to a bimodal distribution [1,2]. Differently, in [68] Greiner *et al.* deduce the existence of a molecular component from radio-frequency spectroscopy by coupling the closed-channel component to a third hyperfine state initially unoccupied. In all cases, quantitative information about the temperature, the total number of atoms and the condensate fraction, is obtained by fitting the density profiles using a Bose-Einstein distribution for the broad normal component and a Thomas-Fermi [80,81] distribution for the narrow condensate component.

The success in creating a molecular condensate leads to the new possibility of exploring the BEC-BCS crossover in ultracold atomic Fermi gases by tuning the magnetic field near a Feshbach resonance. In a dilute gas at very low temperatures the scattering length describes the interactions of the atoms. Hence, changing the scattering length by sweeping the magnetic field across the resonance, makes it possible to change the sign and the strength of interactions in the gas. For positive detuning, no bound molecular state exists. At large positive detuning, the total scattering length is usually small and negative. In this case, the gas will undergo a Bardeen-Cooper-Schrieffer phase transition for sufficiently low temperatures. This state is characterized by a Bose-Einstein condensate of Cooper pairs that are largely delocalized in coordinate space. Their extension is much larger than the interparticle distance between two atoms.

When approaching the resonance, the scattering length diverges and the gas enters a strong-coupling regime, defined by the condition $k_F|a|>1$, where k_F is the Fermi momentum of the gas. At resonance, the scattering length jumps from $-\infty$ to $+\infty$, which is the hallmark of a formation of a zero-energy bound state. At large negative detuning the superfluid gas turns into a Bose Einstein condensate of tightly bound molecules. The evolution between the two limits is called a *crossover* because the same $U(1)$ symmetry is always broken and there is therefore no difference between the symmetries of the two phases. The molecular condensate obtained in [20,68,72,73] represents one extreme of the BEC-BCS crossover. The investigation of the BCS side is more difficult because the fermionic superfluid transition hardly affects the density profile of the gas in the trap [26]. Therefore, it cannot be detected by simple imaging techniques.

Several ideas have been put forward in order to point out a clear signature of the superfluid transition [26,82–86]. However, it turns out that the Feshbach resonance itself makes it possible to study pairing effects in momentum space directly. The method, introduced by Regal *et al.* at JILA in [15], uses the Feshbach resonance to transfer slowly compared to the two-body physics but fast compared to the many-body physics, the fermionic ^{40}K pairs onto the bare molecular state. This enables them to detect the condensate component of the gas also on the positive side of the resonance. The results of the experiment of Regal *et al.* give the molecular condensate fraction after the sweep as a function of temperature and magnetic field. The experiments reveal a few-percent condensate fraction on the positive side of the resonance. The fraction depends on the initial temperature T of the gas and seems to have a threshold at about $B-B_0 \simeq 0.5$ G. This is the magnetic field at which $k_F|a(B)|$ is about 1.

The condensate component has been interpreted by Regal *et al.* as a fermionic condensate. In doing so, they make use the absence of a two-body bound state on the positive side of the resonance. Hence the fermionic condensation must be understood as a "macroscopic occupation of a single quantum state, in which the underlying Fermi statistic of the paired particles plays an essential role." A similar experiment has been realized a few months later by Zwierlein *et al.* [16] at MIT using ^{6}Li atoms. Surprisingly, they observe a much larger molecular condensate fraction than in the experiment at JILA. The origin of this difference still lacks an explanation. Both experiments are performed in axially elongated traps, which should exclude trapping effects as a main reason.

III. ATOM-MOLECULE THEORY FOR FESHBACH-RESONANT INTERACTIONS

Thus far, we have introduced the basic atomic physics of the Feshbach resonance in the language of two-body quan-

tum mechanics. We turn now to the main topic of this paper that is to develop a many-body formulation of the theory. For an incoherent equal mixture of fermionic atoms in two different hyperfine states, and in the vicinity of a Feshbach resonance at low temperatures and densities, it is possible to derive [42,43,45,47] a low-energy effective quantum field theory in terms of the atom-molecule Hamiltonian

$$H = \sum_{\mathbf{k},\sigma\in\{\uparrow,\downarrow\}} (\epsilon_{\mathbf{k}} - \mu) a^{\dagger}_{\mathbf{k},\sigma} a_{\mathbf{k},\sigma} + \frac{1}{V}\sum_{\mathbf{k},\mathbf{k}',\mathbf{q}} V_{\mathrm{bg}}(\mathbf{q}) a^{\dagger}_{\mathbf{k}+\mathbf{q},\uparrow} a^{\dagger}_{\mathbf{k}'-\mathbf{q},\downarrow} a_{\mathbf{k}',\downarrow} a_{\mathbf{k},\uparrow} + \sum_{\mathbf{k}} \left(\frac{\epsilon_{\mathbf{k}}}{2} + \delta_{\mathrm{bare}} - 2\mu \right) b^{\dagger}_{\mathbf{k}} b_{\mathbf{k}} + \frac{1}{\sqrt{V}} \sum_{\mathbf{k},\mathbf{q}} [g^{*}(\mathbf{q}) b^{\dagger}_{\mathbf{k}} a_{\mathbf{k}/2+\mathbf{q},\downarrow} a_{\mathbf{k}/2-\mathbf{q},\uparrow} + \mathrm{H.c.}]. \tag{20}$$

Here, V is the volume, $a^{\dagger}_{\mathbf{k},\sigma}$ is the creation operator of an atom with momentum $\hbar\mathbf{k}$ in the hyperfine state $|\sigma\rangle$ with chemical potential μ. In the case of ^{6}Li gas, the hyperfine states denoted by $|\sigma\rangle$ are the two states $|1\rangle$ and $|2\rangle$ discussed above. The operator $b^{\dagger}_{\mathbf{k}}$ is the creation operator of a bare Feshbach molecule with momentum $\hbar\mathbf{k}$. Here and in the following, the bare molecule refers to the molecular state in the closed channel in the absence of coupling between the open and the closed channels. In addition, V_{bg} is the nonresonant or background interaction between the atoms in the open channel that give rise to the background scattering length a_{bg}. The last two terms of the Hamiltonian in Eq. (20) describe the formation of a molecule from two atoms and the time-reverse process. The strength of this coupling is given by the bare atom-molecule coupling $g(\mathbf{k})$. Both g and V_{bg} depend in principle also on the external magnetic field B. The energy $\delta_{\mathrm{bare}} = \epsilon_{\mathrm{bare}} + \Delta\mu B$ is the bare detuning, where ϵ_{bare} is the energy of a bare molecule with zero total momentum when the external magnetic field is absent, and $\Delta\mu$ is the difference in magnetic moment between the bare molecule and two atoms in the states $|\uparrow\rangle$ and $|\downarrow\rangle$. Bare quantities must be eliminated with a renormalization procedure in favor of experimentally known parameters in order to apply this Hamiltonian to a realistic gas. For example, we will show how the bare detuning δ_{bare} is related to the expression for the detuning given in Eq (17). In the next section such a procedure is introduced for the normal state of the atomic gas in the framework of a many-body formalism based on imaginary-time Green's function techniques [87,88].

A. Many-body T matrix

The dynamical and thermodynamical properties of an atomic gas interacting near a Feshbach resonance are determined by the exact (four-point) interaction vertex function $\Gamma_{\uparrow,\downarrow}$. The latter describes the collisions of two atoms with spin $|\uparrow\rangle$ and $|\downarrow\rangle$, in the presence of many-body correlations introduced by the medium. Unfortunately, in the language of imaginary-time Green's function techniques, the exact $\Gamma_{\uparrow,\downarrow}$ is given by an infinite series of Feynman diagrams and cannot be obtained in general. Therefore, we have to introduce some approximations and to restrict ourselves to the relevant subset of Feynman graphs. We assume that the average distance between the fermions is much larger than the range of the interactions r_0, i.e., $k_F r_0 \ll 1$. Hence only two-particle collisions are expected to be important and we can neglect three-particle and more particle collisions. For a dilute system of fermions with short-range interactions we thus have to consider the ladder approximation [89–91], which sums exactly over all two-body processes. In this approximation only the particle-particle channel [87] is relevant and the vertex function Γ is reduced to the so-called many-body T matrix. This satisfies a Bethe-Salpeter equation of the type

$$\mathrm{T}^{\mathrm{MB}}(\mathbf{k}_f,\mathbf{k}_i,\mathbf{K},\Omega_n) = \mathrm{V}_{\mathrm{eff}}(\mathbf{k}_f,\mathbf{k}_i,\mathbf{K},\Omega_n) - \frac{1}{\hbar}\frac{k_B T}{\hbar V}\sum_{\mathbf{k},\omega_n} \mathrm{V}_{\mathrm{eff}}(\mathbf{k}_f,\mathbf{k},\mathbf{K},\Omega_n) \times G_{\uparrow}\left(\frac{\mathbf{K}}{2}+\mathbf{k},\frac{\Omega_n}{2}+\omega_n\right) \times G_{\downarrow}\left(\frac{\mathbf{K}}{2}-\mathbf{k},\frac{\Omega_n}{2}-\omega_n\right)\mathrm{T}^{\mathrm{MB}}(\mathbf{k},\mathbf{k}_i,\mathbf{K},\Omega_n), \tag{21}$$

where G_{σ} is the exact atomic Green's function. The effective atom-atom interaction is given by

$$\mathrm{V}_{\mathrm{eff}}(\mathbf{k}_f,\mathbf{k}_i,\mathbf{K},\Omega_n) = \mathrm{V}_{\mathrm{bg}}(\mathbf{k}_f-\mathbf{k}_i) + g^{*}(\mathbf{k}_f)\frac{G_0(\mathbf{K},\Omega_n)}{\hbar} g(\mathbf{k}_i), \tag{22}$$

where

$$\frac{G_0(\mathbf{K},\Omega_n)}{\hbar} = \left(i\hbar\Omega_n - \frac{\epsilon_{\mathbf{K}}}{2} + 2\mu - \delta_{\mathrm{bare}} \right)^{-1} \tag{23}$$

is the bare molecular propagator. Here $\hbar\mathbf{k}_f$ and $\hbar\mathbf{k}_i$ are the relative momenta of the incoming and outcoming particles of the scattering process, $\hbar\mathbf{K}$ is the total momentum of the two fermions, and $\Omega_n = 2\pi k_B T n/\hbar$ is the total bosonic Matsubara frequency of the fermion pair propagator and of the molecule.

In general, it is very difficult to solve this equation directly because the interaction $V_{\mathrm{bg}}(\mathbf{k})$ and the atom-molecule coupling $g(\mathbf{k})$ are included with all their details and are known only numerically from very complicated atomic physics measurements. Nevertheless, as we will show, in a dilute gas ($k_F \ll r_0^{-1}$) at very low temperatures, the vertex function T^{MB} can be calculated without explicitly solving the Bethe-Salpeter equation in all its complexity. This is achieved in a number of steps. First, we replace the complicated physical atomic potentials with a pseudopotential that leads to a more simple structure of the scattering equations. Then we try to eliminate the parameters of this pseudopotential from the theory in favor of an equal number of parameters that can be measured experimentally. The theory eventually works because all the relevant information to describe the low-energy physics of the system has been condensed into the phenomenological parameters.

When atoms are colliding at ultralow temperatures, the problem simplifies considerably. At these temperatures they

move so slowly that their kinetic energy is much smaller than the energy $\hbar^2/mr_0^2$, related to the range of the interaction r_0. This condition can be expressed as

$$\lambda_{\mathrm{th}}(T) \gg r_0, \tag{24}$$

where $\lambda_{\mathrm{th}}(T)=(2\pi\hbar^2/mk_BT)^{1/2}$ is the thermal de Broglie wavelength. As a result, the wave numbers of the relative momenta $\hbar\mathbf{k}_f$ and $\hbar\mathbf{k}_i$ are much smaller than the characteristic wave number r_0^{-1}, i.e.,

$$|\mathbf{k}_f|, |\mathbf{k}_i| \ll r_0^{-1}, \tag{25}$$

and from scattering theory it is known that for low energy the T matrix of a two-body collision becomes independent of the relative momenta $\mathbf{k}_f, \mathbf{k}_i$. Therefore, we can try to neglect their explicit dependence in Eq. (21) by replacing the physical potentials with pointlike interactions $V_{\mathrm{bg}}\delta(\mathbf{x}-\mathbf{x}')$ and $g_{\mathrm{bare}}\delta(\mathbf{x}-\mathbf{x}')$. This implies that the effective interaction in Eq. (22) can be rewritten as

$$\mathrm{V}_{\mathrm{eff}}(\mathbf{K},\Omega_n) = \mathrm{V}_{\mathrm{bg}} + g_{\mathrm{bare}}\frac{G_0(\mathbf{K},\Omega_n)}{\hbar}g_{\mathrm{bare}}. \tag{26}$$

It turns out that under these conditions the many-body T matrix is also independent of $\mathbf{k_f}$ and $\mathbf{k_i}$ and may be taken out of the integral. This gives

$$\mathrm{T}^{\mathrm{MB}}(\mathbf{K},\Omega_n) = \mathrm{V}_{\mathrm{eff}}(\mathbf{K},\Omega_n) + \mathrm{V}_{\mathrm{eff}}(\mathbf{K},\Omega_n)\Pi(\mathbf{K},\Omega_n)\mathrm{T}^{\mathrm{MB}}(\mathbf{K},\Omega_n), \tag{27}$$

where the kernel

$$\hbar\Pi(\mathbf{K},\Omega_n) = -\frac{k_BT}{\hbar V}\sum_{\mathbf{k},\omega_n} G_{\uparrow}\left(\frac{\mathbf{K}}{2}+\mathbf{k},\frac{\Omega_n}{2}+\omega_n\right) \times G_{\downarrow}\left(\frac{\mathbf{K}}{2}-\mathbf{k},\frac{\Omega_n}{2}-\omega_n\right) \tag{28}$$

contains an unphysical ultraviolet divergence because the internal integration over $\mathbf{k}$ in the Bethe-Salpeter equation in Eq. (27) gives a contribution for every momenta while in the original expression in Eq. (21) the natural continuum cutoff around $\hbar/r_0^{-1}$ of the physical potentials cuts off the high-momentum tail. The T-matrix renormalization procedure consists of eliminating this divergency by means of the bare unknown constants δ_{bare}, V_{bg}, and g_{bare} from Eq. (27). To this purpose we introduce the full molecular propagator

$$G(\mathbf{q},\omega_n)^{-1} = G_0^{-1}(\mathbf{q},\omega_n) - \Sigma_{\mathrm{m}}(\mathbf{q},\omega_n) \tag{29}$$

by using the molecular self-energy defined as

$$\hbar\Sigma_{\mathrm{m}}(\mathbf{q},\omega_n) = g_{\mathrm{bare}}\Pi(\mathbf{q},\omega_n)g^{\mathrm{MB}}(\mathbf{q},\omega_n). \tag{30}$$

Here we have used for the momentum dependence of the exact atom-molecule coupling g^{MB} the same assumptions as for T^{MB}. For the same reason as above, there is also an unphysical ultraviolet divergency in the self-energy of the molecular propagator that can be eliminated by a simple subtraction in the self-energy. This leads to the renormalization of the bare detuning δ_{bare} to the physical detuning $\delta(B)=\Delta\mu(B-B_0)$ defined in Eq. (17) of the previous section.

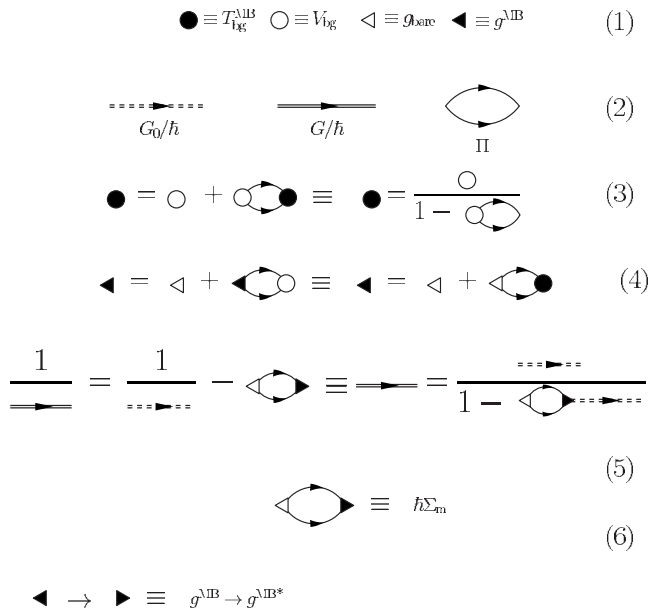

FIG. 3. The first two lines define the symbols we use in our diagrammatic notation. The next four lines represent, respectively, (3) Eq. (32), (4) Eq. (31), (5) Eq. (29), and (6) Eq. (30).

The desired renormalized atom-molecule coupling g^{MB} is connected to the many-body T matrix by the relation [47]

$$g^{\mathrm{MB}}(\mathbf{K},\Omega_n) = g_{\mathrm{bare}} + g_{\mathrm{bare}}\Pi(\mathbf{K},\Omega_n)\mathrm{T}_{\mathrm{bg}}^{\mathrm{MB}}(\mathbf{K},\Omega_n), \tag{31}$$

where the many-body T matrix for the background processes satisfies

$$\mathrm{T}_{\mathrm{bg}}^{\mathrm{MB}}(\mathbf{K},\Omega_n) = \mathrm{V}_{\mathrm{bg}} + \sum_{\mathbf{k}} \mathrm{V}_{\mathrm{bg}}\Pi(\mathbf{K},\Omega_n)\mathrm{T}_{\mathrm{bg}}^{\mathrm{MB}}(\mathbf{K},\Omega_n). \tag{32}$$

This means that we have dressed the bare atom-molecule coupling with all the two-body background interactions. The set of equations (29)–(32) is represented in Fig. 3 by means of a diagrammatic notation.

By formally solving Eq. (27) and using Eqs. (29), (31), and (32) to eliminate G_0, V_{bg} and g_{bare}, it is possible, by some straightforward algebra, to obtain the desired result

$$\mathrm{T}^{\mathrm{MB}}(\mathbf{K},\Omega_n) = \mathrm{T}_{\mathrm{bg}}^{\mathrm{MB}}(\mathbf{K},\Omega_n) + g^{\mathrm{MB}^*}(\mathbf{K},\Omega_n)\frac{G(\mathbf{K},\Omega_n)}{\hbar}g^{\mathrm{MB}}(\mathbf{K},\Omega_n), \tag{33}$$

where all the bare quantities have been eliminated from the theory. A nice derivation of this formula by means of an algebra of diagrams is shown in Fig. 4.

This result represents a generalization of the solution of the standard many-body T matrix for a dilute ultracold gas of atoms and molecules at the Feshbach resonance [89–91]. This solution describes the scattering of a pair of atoms at (complex) energy $i\hbar\Omega_n$, while the dependence on the center-of-mass momentum $\mathbf{K}$ incorporates the Pauli-blocking effects of the medium. As we have anticipated, at this level the solution is still somewhat formal because we have only eliminated the bare coupling constants in terms of the renor-

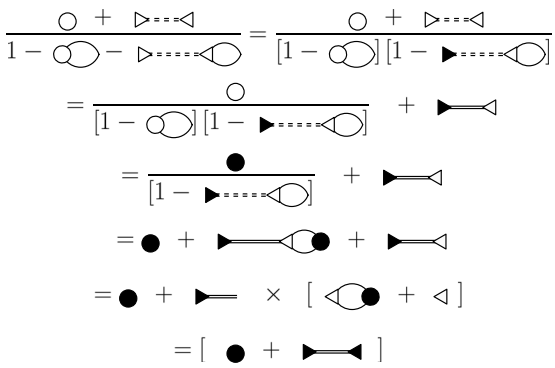

FIG. 4. Diagrammatic calculation of the many-body T matrix. The derivation starts from the definition of the many-body T matrix in Eq. (27) in terms of the bare quantities of the theory. The many-body T matrix in terms of the renormalized couplings and propagators follows exactly from the algebra defined in Fig. 3 based on the exact relations in Eqs. (29)–(32).

malized ones. The next step consists in relating the renormalized quantities, such as $\mathrm{T}_{\mathrm{bg}}^{\mathrm{MB}}$ and g^{MB}, to the two-body parameters, which can be measured by experiments.

B. Two-atom properties of the many-body theory

In the two-body limit [92–94] there are only two fermions present so that in an infinite volume, the particle density tends to zero, i.e., $k_F=0$, and there are no many-body effects anymore. This limit can be achieved by letting $T\to 0$ and $i\hbar\Omega_n\to E$ while the chemical potential is fixed to $\mu=0$. The dressed fermion propagator G_σ can be replaced by the free atomic propagator

$$G_{\sigma,0}(\mathbf{k},E)=\frac{\hbar}{E-\epsilon_{\mathbf{k}}}, \tag{34}$$

and the dependence on the total momentum $\mathbf{K}$ drops out everywhere. The many-body T matrix in Eq. (33) becomes the two-body T matrix and Eq. (33) can be rewritten as

$$\mathrm{T}^{2\mathrm{B}}(E)=\mathrm{T}_{\mathrm{bg}}^{2\mathrm{B}}(E)+g^{2\mathrm{B}*}(E)\frac{G^{2\mathrm{B}}(E)}{\hbar}g^{2\mathrm{B}}(E), \tag{35}$$

where the two-particle dressed molecular propagator at zero momentum is given by

$$G^{2\mathrm{B}}(E)^{-1}\equiv G^{2\mathrm{B}}(\mathbf{0},E)^{-1}=G_0(\mathbf{0},E)^{-1}-\Sigma_{\mathrm{m}}^{2\mathrm{B}}(\mathbf{0},E). \tag{36}$$

The on-shell energy-dependent T_{bg} matrix

$$\mathrm{T}_{\mathrm{bg}}^{2\mathrm{B}}(E)=\frac{4\pi\hbar^2 a_{\mathrm{bg}}(B)}{m}\frac{1}{1-a_{\mathrm{bg}}(B)\sqrt{\frac{-Em}{\hbar^2}}} \tag{37}$$

is obtained by solving Eq. (32) in the vacuum, which reduces to the well-known Lippmann-Schwinger equation [24]

$$\mathrm{T}_{\mathrm{bg}}^{2\mathrm{B}}(E)=\mathrm{V}_{\mathrm{bg}}+\sum_{\mathbf{k}}\mathrm{V}_{\mathrm{bg}}\frac{1}{E-2\epsilon_{\mathbf{k}}}\mathrm{T}_{\mathrm{bg}}^{2\mathrm{B}}(E). \tag{38}$$

The background scattering length $a_{\mathrm{bg}}(B)$ is the quantity which is measurable experimentally and is defined by $\mathrm{T}_{\mathrm{bg}}^{2\mathrm{B}}(0)=4\pi\hbar^2 a_{\mathrm{bg}}/m$. Noting that Eqs. (31) and (32) lead to $g^{2\mathrm{B}}(E)=g_{\mathrm{bare}}\mathrm{T}_{\mathrm{bg}}^{2\mathrm{B}}(E)/\mathrm{V}_{\mathrm{bg}}$, we conclude that the same kind of energy dependence can also be used for the atom-molecule coupling constant, i.e.,

$$g^{2\mathrm{B}}(E)=g\frac{1}{1-a_{\mathrm{bg}}(B)\sqrt{\frac{-Em}{\hbar^2}}}, \tag{39}$$

where $g=g^{2\mathrm{B}}(0)$ is also inferred from experiments. The evaluation of the molecular self-energy in the vacuum will complete the definition of the $\mathrm{T}^{2\mathrm{B}}$ in terms of measurable quantities.

As we have seen in the previous section, the molecular self-energy in the dressed molecular propagator contains an unphysical ultraviolet divergency. This can be eliminated by rewriting the two-body propagator in Eq. (36) as

$$\begin{aligned}G^{2\mathrm{B}}(\mathbf{k},E)^{-1}&=G_0(\mathbf{k},E)^{-1}+\Sigma_{\mathrm{m}}^{2\mathrm{B}}(\mathbf{0},0)-\Sigma_{\mathrm{m}}^{2\mathrm{B}}(\mathbf{k},E)-\Sigma_{\mathrm{m}}^{2\mathrm{B}}(\mathbf{0},0)\\&=\frac{E-\epsilon_{\mathbf{k}}/2-\delta(B)}{\hbar}-\Sigma_{\mathrm{m}}^{2\mathrm{B}}(\mathbf{k},E)+\Sigma_{\mathrm{m}}^{2\mathrm{B}}(\mathbf{0},0),\end{aligned} \tag{40}$$

where the energy-independent but infinite shift $\Sigma^{2\mathrm{B}}(\mathbf{0},0)$ has renormalized the bare detuning δ_{bare} to the physical detuning $\delta(B)$ according to

$$\delta(B)=\delta_{\mathrm{bare}}+\hbar\Sigma_{\mathrm{m}}^{2\mathrm{B}}(\mathbf{0},0)\equiv\Delta\mu(B-B_0) \tag{41}$$

in such a manner that the position of the resonance in the magnetic field is now precisely at the observed magnetic field value B_0. The renormalized molecular self-energy can now be calculated by performing a simple integration [47]

$$\hbar\Sigma_{\mathrm{m}}^{2\mathrm{B}}(\mathbf{k},E)-\hbar\Sigma_{\mathrm{m}}^{2\mathrm{B}}(\mathbf{0},0)=\frac{\eta(B)}{1+|a_{\mathrm{bg}}(B)|\sqrt{\frac{-Em}{\hbar^2}}}\sqrt{-E}, \tag{42}$$

where the quantity $\eta^2=(g^2m^{3/2}/4\pi\hbar^3)^2$ defines an important energy scale in the problem which is related to the width of the Feshbach resonance. Note that as a result of the internal integration over $\mathbf{k}$ the background scattering length appears as an absolute value in the self-energy [47]. This turns out to be very important in the case of negative background scattering length when we calculate the binding energy of the molecule. The two-body molecular propagator takes the final form

$$\hbar G^{2\mathrm{B}}(E^+)^{-1}=E^+-\delta(B)-\frac{\eta(B)}{1+|a_{\mathrm{bg}}(B)|\sqrt{\frac{-Em}{\hbar^2}}}\sqrt{-E}. \tag{43}$$

Using this expression in Eq. (35) we recover the effective atom-atom resonant interaction in the limit of zero-energy scattering. This is given by

$$T^{2B}(0) = \frac{4\pi\hbar^2 a(B)}{m} = \frac{4\pi\hbar^2 a_{bg}(B)}{m} - \frac{g^2(B)}{\delta(B)}$$
$$\equiv \frac{4\pi\hbar^2}{m}[a_{bg}(B) + a_{res}(B)], \quad (44)$$

where $a(B)$ is the total effective scattering length that diverges at $B=B_0$.

When the background scattering length can be considered as a constant for the magnetic field range across the Feshbach resonance, such as is certainly the case for a narrow resonance, the total effective scattering length can be rewritten as

$$a(B) = a_{bg}\left(1 - \frac{\Delta B}{B - B_0}\right) \quad (45)$$

with the width of the resonance ΔB defined through the relation $\Delta B = mg^2/4\pi\hbar^2|a_{bg}|\Delta\mu$. For the broad resonance at 834 G in an atomic ^{6}Li gas, however, the background scattering length exhibits a strong dependence on the external magnetic field B [95] and it is not sufficiently accurate to use Eq. (45) [59]. The energy of the molecule is given by $E_{\mathbf{k}} = \epsilon_m(B) + \epsilon_{\mathbf{k}}/2$, where the energy of the zero-momentum molecular level $\epsilon_m(B)$ is determined by the pole of the retarded molecular propagator given in Eq. (43) at zero kinetic energy. This is equivalent to finding the zero of the equation

$$\epsilon_m - \delta(B) - \frac{\eta(B)}{1 + |a_{bg}(B)|\sqrt{\frac{-\epsilon_m^+ m}{\hbar^2}}}\sqrt{-\epsilon_m^+} = 0. \quad (46)$$

For negative detuning $\delta(B) < 0$ the molecular propagator has a real and negative pole corresponding to the bound-state energy. The real solution of Eq. (46) can be calculated analytically by solving the equivalent algebraic equation. We find

$$\epsilon_m = -\frac{1}{9}\left(-\sqrt{\epsilon_{bg}} - \frac{2^{1/3}\alpha}{(\gamma + \sqrt{4\alpha^3 + \gamma^2})^{1/3}} + \frac{(\gamma + \sqrt{4\alpha^3 + \gamma^2})^{1/3}}{2^{1/3}}\right)^2, \quad (47)$$

where the coefficients are $\alpha = 3\delta - \epsilon_{bg} + 3\eta\sqrt{\epsilon_{bg}}$ and $\gamma = -18\delta\sqrt{\epsilon_{bg}} - 2\epsilon_{bg}^{3/2} + 9\eta\epsilon_{bg}$. The energy ϵ_{bg}, associated to the background scattering length a_{bg}, is defined as

$$\epsilon_{bg}(B) = \frac{\hbar^2}{m a_{bg}(B)^2}. \quad (48)$$

Interestingly, it can be shown that the solution of Eq. (47) is equivalent to the solution of the equation for the binding energy given by Eq. (4) in [99] in the limit when the effective range r_0 can be neglected. Therefore, in the case of a very large background scattering length, our theory reproduces correctly the nontrivial energy dependence due to the interplay between the resonant background interaction and the Feshbach resonance [95,100].

In the limit of a vanishing background scattering length $a_{bg} \to 0$, the solution of Eq. (47) reduces to [47]

$$\epsilon_m(B) = \delta(B) + \frac{\eta^2}{2}\left(\sqrt{1 - \frac{4\delta(B)}{\eta^2}} - 1\right). \quad (49)$$

The bound-state energy of the dressed molecule as a function of the magnetic field $\epsilon_m(B)$ of Eq. (47), is shown in Figs. 5(a), 6(a), and 7(a) for three different resonances. Near resonance the binding energy goes to zero and the square-root term in Eq. (46), which describes the dressing effects of the open channel, dominates the linear term. In this approximation the location of the pole is at

$$\epsilon_m(B) = -\frac{\hbar^2}{m a^2(B)}, \quad (50)$$

according to the Wigner's formula in Eq. (18) for the binding energy in resonant scattering. At large negative detuning, far away from resonance, the dressing effects of the coupling with the open channel represent only a small perturbation. In this limit, the energy of the Feshbach molecule approaches the binding energy of the bare molecule which scales linearly with the magnetic field as

$$\epsilon_m(B) \simeq \delta(B). \quad (51)$$

In general the residue of the pole of the molecular Green's function $G^{2B}(E^+)$ is given by

$$Z(B) = \left(1 - \frac{\partial\hbar\Sigma^{2B}(z)}{\partial z}\right)^{-1}_{z=\epsilon_m(B)} = \left(1 + \frac{\eta(B)}{2\sqrt{|\epsilon_m(B)|}\left(1 + \sqrt{\frac{|\epsilon_m(B)|}{\epsilon_{bg}(B)}}\right)^2}\right)^{-1} \quad (52)$$

and is always smaller than 1, because physically the wavefunction of the dressed molecular state near the Feshbach resonance is given by the linear superposition

$$\langle \mathbf{r}|\chi_m; \text{dressed}\rangle \simeq \sqrt{Z(B)}\chi_m(\mathbf{r})|\text{closed}\rangle + \sqrt{1 - Z(B)}\frac{1}{\sqrt{2\pi a(B)}}\frac{e^{-r/a(B)}}{r}|\text{open}\rangle, \quad (53)$$

where $\chi_m(\mathbf{r})$ denotes the wavefunction of the bare molecular state in the closed channel of the Feshbach problem. The quantity Z is plotted in Figs. 5(b), 6(b), and 7(b) for the three different Feshbach resonances already considered. The dressed molecular state therefore only contains with an amplitude $\sqrt{Z(B)}$ the bare molecular state $|\chi_m; \text{bare}\rangle$ of the closed channel. The remaining $\sqrt{1-Z(B)}$ component is carried by the continuum of the scattering states in the open channel.

The density of states of the dressed molecule can be calculated from the imaginary part of the Green's function [87]. The density of states at negative detuning is shown in Fig. 8(a). The probability Z corresponds to the wavefunction renormalization constant of the bare molecule in the closed channel. It goes linearly in $|B-B_0|$ to zero near resonance, where the dressing due to the open channel is maximum. It goes to one monotonically at large negative detunings where

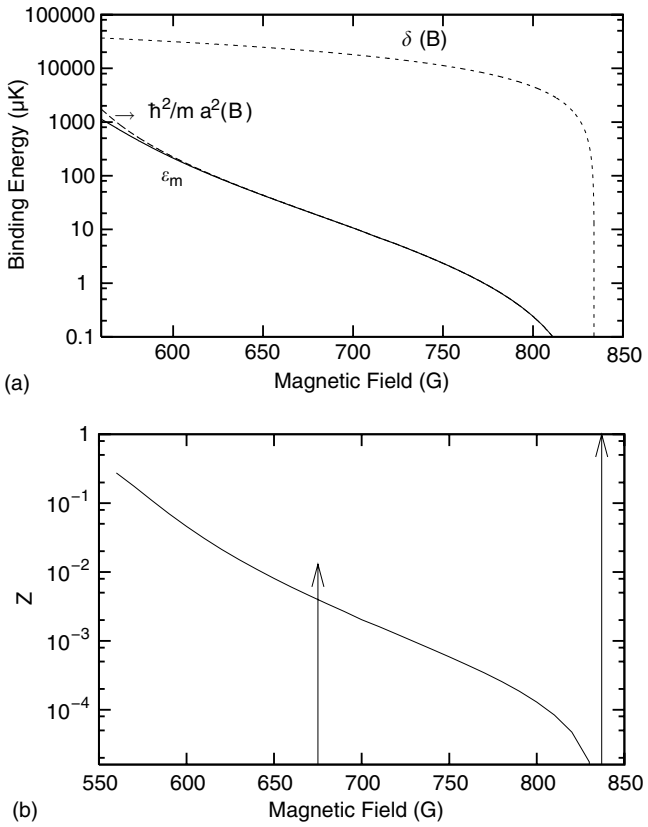

FIG. 5. (a) Binding energy $\epsilon_m(B)$ and (b) the probability $Z(B)$ as a function of the magnetic field near the broad resonance at 834 G in a mixture of ^{6}Li atoms in the hyperfine states $|1\rangle$ and $|2\rangle$. In (a) the full line shows the binding energy obtained from Eq. (47). The dashed line merging at about 600 G with the full line represents the binding energy approximated according to the Wigner formula in Eq. (50). The detuning $\delta(B)$ is shown by the dotted line for comparison. In (b), the full line represents the value of Z calculated from Eq. (52). The short arrow at about 675 G indicates the magnetic-field scale associated with the energy $\epsilon_{bg}=\hbar^2/ma_{bg}^2$, while the long arrow on the right side of the picture indicates the location of the resonance. The curve for the binding energy is calculated for the most recent measured value of the location of the resonance at $B_0 \simeq 834$ G. We are not aware of more recent publications of the binding energy data incorporating this position of the resonance. However, our theory is in perfect agreement with the coupled-channel calculations and the experimental data reported in [71] when just shifting the location of the resonance to $B_0 \simeq 850$ G [71]. This result was reported in [59]. The curve for Z agrees perfectly with the experimental data of [20] in the range of validity of the two-body approximation (see also Fig. 24).

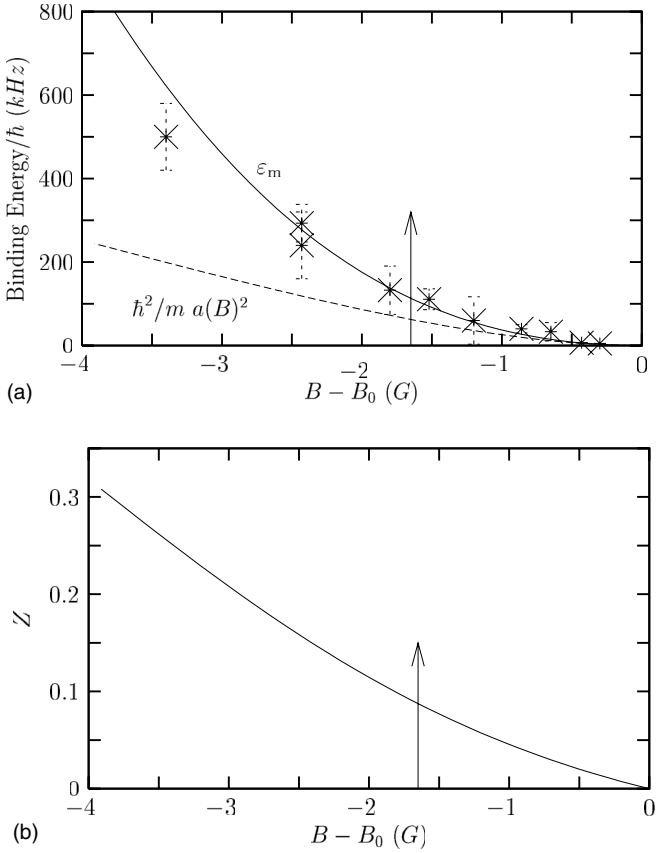

FIG. 6. (a) Binding energy and (b) the probability Z as a function of the magnetic field near the resonance at 224 G in a mixture of ^{40}K atoms in the hyperfine states $|f;m_f\rangle=|9/2;-9/2\rangle$ and $|f;m_f\rangle=|9/2;-5/2\rangle$. The dashed line in (a) represents the binding energy approximated according to the Wigner formula in Eq. (50). The stars represent the experimental data taken from [96]. The arrow at about $B-B_0=-1.6$ G indicates the magnetic field associated with the energy ϵ_{bg}. The curves are calculated using the the same experimental parameters $a_{bg}=174\ a_0$, $\Delta\mu=1.27\ \mu_B$, and $\Delta B=9.7$ G as in [53]. Note that for this resonance the high-field approximation discussed in Sec. II is not valid and the structure of the spin states of the ^{40}K atoms is thus more complicated.

the eigenstate of the Feshbach problem approaches the bare molecule of the closed channel. (See also the right sides of Figs. 5–7). For a broad resonance, we usually have that $\eta^2 > \epsilon_{bg}$. In this case the "crossover" between these two regimes takes place at detunings such that

$$|\epsilon_m| \simeq \epsilon_{bg}. \tag{54}$$

When a_{bg} is small the turning point between the quadratic and the linear regime is given by the condition $|\epsilon_m| \simeq \eta^2$. The quantity Z is also related to the magnetic moment μ_{mag} of the dressed molecules. Taking the derivative on both sides with respect to the magnetic field B in Eq. (46) we have that

$$\frac{\partial \epsilon_m}{\partial B} - \Delta\mu - \frac{\partial \hbar \Sigma^{2B}}{\partial \epsilon_m}\frac{\partial \epsilon_m}{\partial B} = 0, \tag{55}$$

where we recall again that $\Delta\mu$ is the difference in the magnetic moment between the atomic pair and the bare molecule and closed channel in absence of coupling. Using the definition of Z, Eq. (55) can be rewritten as

$$Z(B)\Delta\mu = \frac{\partial \epsilon_m}{\partial B} \equiv \Delta\mu - \mu_{mag}(B). \tag{56}$$

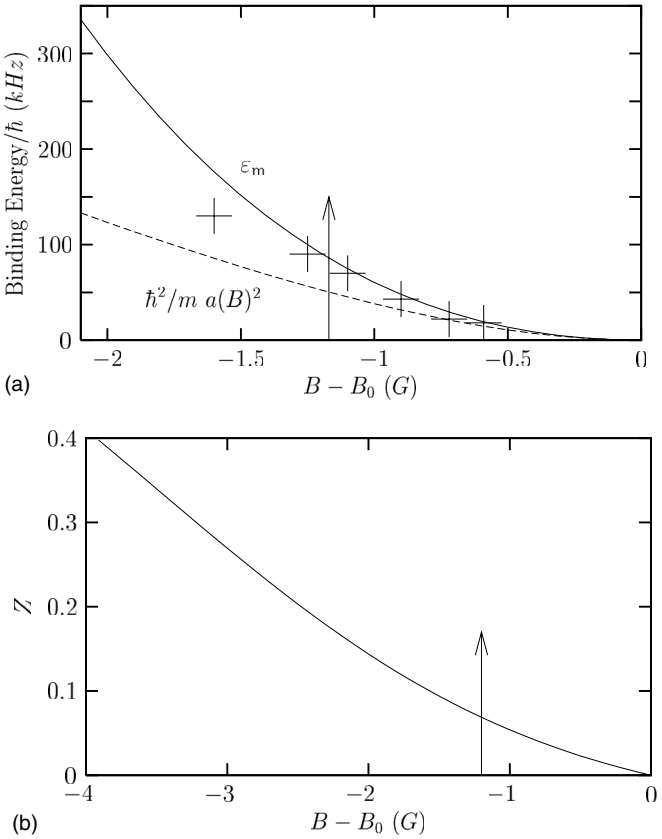

FIG. 7. (a) Binding energy and (b) the probability Z as a function of the magnetic field near the resonance at 202.1 G in a mixture of ^{40}K atoms in the hyperfine states $|f;m_f\rangle=|9/2;-9/2\rangle$ and $|f;m_f\rangle=|9/2;-7/2\rangle$. The dashed line in (a) represents the binding energy approximated according to the Wigner formula in Eq. (50). The crosses represent the experimental data taken from [96]. The arrow at about $B-B_0=-1.2$ G indicates the magnetic field associated with the energy ϵ_{bg}. The curves are calculated using the experimental parameters $a_{bg}=174\ a_0$, $\Delta\mu=(16/9)\mu_B$ and $\Delta B=7.8$ G as in [97,98]. Note that also for this resonance the high-field approximation discussed in Sec. II is not valid and the structure of the spin states of the ^{40}K atoms is thus more complicated.

Therefore the change of the difference in magnetic moments due to the dressing of the molecule near resonance is given by the relation

$$\mu_{\rm mag}(B) = \Delta\mu[1 - Z(B)] \tag{57}$$

and is automatically included in our theory [47]. The curve of Eq. (57) is in very good agreement [59] with the measurement of the dressed-molecule magnetic moment in ^{6}Li gas taken if [71] and discussed earlier in Sec. II.

For positive detuning $\delta(B)>0$ the solution of Eq. (46) has a negative imaginary part, in agreement with the fact that the molecule decays when its energy is above the two-atom continuum threshold. The molecular density of states at positive detuning does no longer have a delta function at negative energy but is given by a Lorentzian-like curve depicted in Fig. 8(b). The analytic expression which gives the maximum in the density of states ϵ_m at positive detuning can be easily calculated in the limit of $a_{bg}=0$ and reads [56]

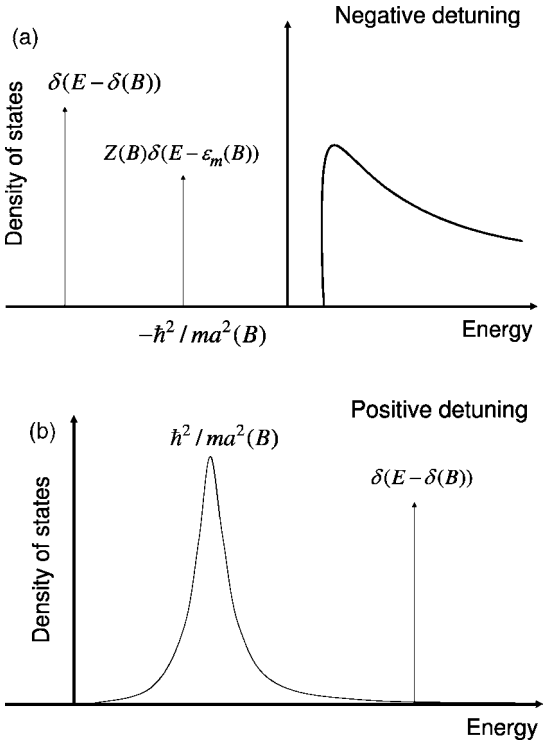

FIG. 8. Molecular density of states in the two-body limit at (a) negative detuning and (b) positive detuning. In (a) the delta function at $E=\epsilon_m(B)$ indicates the real dressed molecular state at negative energies, while the delta function at $E=\delta(B)$ denotes the energy of the bare molecular level in the absence of coupling between the open and the closed channels. The broad continuum distribution at positive energies is associated with the scattering states in the open channel. The absence of a true bound state at positive detuning is shown in (b) by the nonzero width of the molecular level at $E\simeq\epsilon_m(B)\simeq\hbar^2/ma(B)^2$. However, due to the interchannel coupling the maximum of the density of states distribution is shifted with respect to the value $E=\delta(B)$ in the absence of coupling.

$$\epsilon_m = \frac{1}{3}\left(\delta - \frac{\eta^2}{2} + \sqrt{\frac{\eta^4}{4} - \eta^2\delta + 4\delta^2}\right). \tag{58}$$

At large positive detuning, the peak of the Lorentzian distribution is located at the detuning. Near resonance, it is shifted from the detuning by the nonzero coupling, and located at $\hbar^2/ma^2(B)$. This is up to a sign exactly the position of the real pole at small negative detuning.

C. Reexamination of the many-body T matrix: Functional integral approach

The approximation developed to solve the two-body scattering problem, based on Eq. (33), can be generalized rather straightforwardly to include the Pauli-blocking effects on the many-body T matrix and on the molecular propagator. Nevertheless, for completeness we prefer here to rederive the many-body T matrix approach also by means of functional-

integral methods [88,101,102]. The reasons for this are twofold. First, it simplifies considerably the many-body calculations in order to go beyond the mean-field approximation. Second, as we will see, it helps in connecting our theory with the other studies developed in the literature.

The path integral expression for the grand-canonical partition function of the effective atom-molecule model in Eq. (20) is

$$\mathcal{Z} = \int d[\phi_{\mathrm{m}}^*]d[\phi_{\mathrm{m}}]\left(\prod_{\sigma} d[\psi_{\sigma}^*]d[\psi_{\sigma}]\right)e^{-S[\phi_{\mathrm{m}}^*,\phi_{\mathrm{m}},\psi_{\sigma}^*,\psi_{\sigma}]/\hbar} \tag{59}$$

with the Euclidean action given by

$$\begin{aligned} S[\phi_{\mathrm{m}}^*,\phi_{\mathrm{m}},\psi_{\sigma}^*,\psi_{\sigma}] = & \int_0^{\hbar\beta} d\tau \int d\mathbf{x} \sum_{\sigma} \psi_{\sigma}^*(\mathbf{x},\tau)\left(\hbar\frac{\partial}{\partial\tau} - \frac{\hbar^2\nabla^2}{2m} - \mu\right)\psi_{\sigma}(\mathbf{x},\tau) \\ & + \int_0^{\hbar\beta} d\tau \int d\mathbf{x}\phi_{\mathrm{m}}^*(\mathbf{x},\tau)\left(\hbar\frac{\partial}{\partial\tau} - \frac{\hbar^2\nabla^2}{2(2m)} + \delta_{\mathrm{bare}}(B) - 2\mu\right)\phi_m(\mathbf{x},\tau) \\ & + \int_0^{\hbar\beta} d\tau \int d\mathbf{x} \int d\mathbf{x}' V_{\mathrm{bg}}(\mathbf{x}-\mathbf{x}')\psi_{\uparrow}^*(\mathbf{x},\tau)\psi_{\downarrow}^*(\mathbf{x}',\tau)\psi_{\downarrow}(\mathbf{x}',\tau)\psi_{\uparrow}(\mathbf{x},\tau) \\ & + \int_0^{\hbar\beta} d\tau \int d\mathbf{x} \int d\mathbf{x}' [g^*(\mathbf{x}-\mathbf{x}')\phi_{\mathrm{m}}^*((\mathbf{x}+\mathbf{x}')/2,\tau)\psi_{\downarrow}(\mathbf{x}',\tau)\psi_{\uparrow}(\mathbf{x},\tau) + \mathrm{c.c.}], \end{aligned} \tag{60}$$

where ϕ_{m} denotes the molecular bosonic field, the Grassmann fields ψ_{σ} represent the fermionic atoms in the two atomic hyperfine states, and $\beta = 1/k_B T$. By means of the Hubbard-Stratonovich transformation

$$e^{-(\psi_{\uparrow}\psi_{\downarrow}|V_{\mathrm{bg}}|\psi_{\downarrow}\psi_{\uparrow})} = \int d[\Delta]d[\Delta^*]e^{+(\Delta|\psi_{\downarrow}\psi_{\uparrow})+(\psi_{\uparrow}\psi_{\downarrow}|\Delta)+(\Delta|V_{\mathrm{bg}}^{-1}|\Delta)} \tag{61}$$

we can introduce the auxiliary field $\Delta(\mathbf{x},\tau)$, which describes the quantum fluctuations in the particle-particle channel according to the ladder approximation. Using this identity, we can rewrite the full action as

$$\begin{aligned} S[\phi_{\mathrm{m}}^*,\phi_{\mathrm{m}},\psi_{\sigma}^*,\psi_{\sigma},\Delta^*,\Delta] = & \int_0^{\hbar\beta} d\tau \int d\mathbf{x} \sum_{\sigma} \psi_{\sigma}^*(\mathbf{x},\tau)\left(\hbar\frac{\partial}{\partial\tau} - \frac{\hbar^2\nabla^2}{2m} - \mu\right)\psi_{\sigma}(\mathbf{x},\tau) \\ & + \int_0^{\hbar\beta} d\tau \int d\mathbf{x}\phi_{\mathrm{m}}^*(\mathbf{x},\tau)\left(\hbar\frac{\partial}{\partial\tau} - \frac{\hbar^2\nabla^2}{2(2m)} + \delta_{\mathrm{bare}}(B) - 2\mu\right)\phi_m(\mathbf{x},\tau) - \frac{|\Delta(\mathbf{x},\tau)|^2}{V_{\mathrm{bg}}} \\ & + \int_0^{\hbar\beta} d\tau \int d\mathbf{x}[g_{\mathrm{bare}}\phi_{\mathrm{m}}(\mathbf{x},\tau) - \Delta(\mathbf{x},\tau)]\psi_{\uparrow}^*(\mathbf{x},\tau)\psi_{\downarrow}^*(\mathbf{x},\tau) \\ & + \int_0^{\hbar\beta} d\tau \int d\mathbf{x}[g_{\mathrm{bare}}\phi_{\mathrm{m}}^*(\mathbf{x},\tau) - \Delta^*(\mathbf{x},\tau)]\psi_{\downarrow}(\mathbf{x},\tau)\psi_{\uparrow}(\mathbf{x},\tau). \end{aligned} \tag{62}$$

Note that we have made the replacements $V_{\mathrm{bg}}(\mathbf{x}-\mathbf{x}') = V_{\mathrm{bg}}\delta(\mathbf{x}-\mathbf{x}')$ and $g(\mathbf{x}-\mathbf{x}') = g_{\mathrm{bare}}\delta(\mathbf{x}-\mathbf{x}')$ as in Eq. (26) above.

Recalling the definition of the noninteracting atomic Green's function [88]

$$\left\{\hbar\frac{\partial}{\partial\tau} - \frac{\hbar^2\nabla^2}{2m} - \mu\right\}G_{\sigma,0}(\mathbf{x},\tau;\mathbf{x}',\tau') = -\hbar\delta(\mathbf{x}-\mathbf{x}')\delta(\tau-\tau') \tag{63}$$

and using a 2×2 matrix (Nambu-space) notation, the dressed atomic Green's function can be written as

$$\begin{aligned} \mathbf{G}_{\mathrm{f}}^{-1}(\mathbf{x},\tau;\mathbf{x}',\tau') = & \begin{bmatrix} G_{\uparrow,0}^{-1}(\mathbf{x},\tau;\mathbf{x}',\tau') & 0 \\ 0 & -G_{\downarrow,0}^{-1}(\mathbf{x}',\tau';\mathbf{x},\tau) \end{bmatrix} - \frac{1}{\hbar}\begin{bmatrix} 0 & g_{\mathrm{bare}}\phi_{\mathrm{m}}(\mathbf{x},\tau) - \Delta(\mathbf{x},\tau) \\ g_{\mathrm{bare}}^*\phi_{\mathrm{m}}^*(\mathbf{x},\tau) - \Delta^*(\mathbf{x},\tau) & 0 \end{bmatrix}\delta(\mathbf{x}-\mathbf{x}') \\ & \times\delta(\tau-\tau') \equiv \mathbf{G}_{\mathrm{f},0}^{-1}(\mathbf{x},\tau;\mathbf{x}',\tau') - \mathbf{\Sigma}_{\mathrm{f}}(\mathbf{x},\tau;\mathbf{x}',\tau'). \end{aligned} \tag{64}$$

The integration over the atomic fields now involves a Gaussian integral which adds the formal result $-\hbar\mathrm{Tr}[\ln(-\mathbf{G}_{\mathrm{f}})]$ to the effective action, that can be treated perturbatively. The effective Gaussian action is obtained by keeping terms up to the quadratic level in the Δ and ϕ_{m} fields. It reads

$$S[\Delta^*,\Delta,\phi_m^*,\phi_m] = \int_0^{\hbar\beta} d\tau \int d\mathbf{x}\Delta(\mathbf{x},\tau)^*\left(-\frac{1}{V_{bg}}\right)\Delta(\mathbf{x},\tau) + \frac{\hbar}{2}\mathrm{Tr}(\mathbf{G}_{f,0}\boldsymbol{\Sigma}_f)^2 + \int_0^{\hbar\beta} d\tau \int d\mathbf{x}\phi_m^*(\mathbf{x},\tau) \times\left(\hbar\frac{\partial}{\partial\tau} - \frac{\hbar^2\nabla^2}{2(2m)} - \delta_{bare}(B) - 2\mu\right)\phi_m(\mathbf{x},\tau), \tag{65}$$

where the trace $\mathrm{Tr}(\mathbf{G}_{f,0}\Sigma_f)^2$ can be rewritten as

$$\mathrm{Tr}(\mathbf{G}_{f,0}\boldsymbol{\Sigma}_f)^2 = \frac{2}{\hbar^2}\int_0^{\hbar\beta} d\tau \int d\mathbf{x}\int_0^{\hbar\beta} d\tau' \int d\mathbf{x}' \times[-g_{bare}\phi_m(\mathbf{x}',\tau') + \Delta(\mathbf{x}',\tau')]\hbar\Pi_0(\mathbf{x},\tau;\mathbf{x}',\tau') \times[-g_{bare}^*\phi_m^*(\mathbf{x},\tau) + \Delta^*(\mathbf{x},\tau)] \tag{66}$$

if we introduce the free pair propagator

$$\hbar\Pi_0(\mathbf{x},\tau;\mathbf{x}',\tau') = -G_{\uparrow,0}(\mathbf{x},\tau;\mathbf{x}',\tau')G_{\downarrow 0}(\mathbf{x},\tau;\mathbf{x}',\tau') \tag{67}$$

in coordinate space. Using as a definition of the pairing-field propagator

$$-\hbar G_{\Delta_{bg}}^{-1}(\mathbf{x},\tau;\mathbf{x}',\tau') = -\frac{\delta(\mathbf{x}-\mathbf{x}')\delta(\tau-\tau')}{V_{bg}} + \Pi_0(\mathbf{x},\tau;\mathbf{x}',\tau') \tag{68}$$

the effective Gaussian action in Eq. (65) can be put finally into the form

$$S[\Delta^*,\Delta,\phi_m^*,\phi_m] = \int d\tau \int d\mathbf{x} \int d\tau' \int d\mathbf{x}'\Big[\Delta^*(\mathbf{x}',\tau') \times[-\hbar G_{\Delta_{bg}}^{-1}(\mathbf{x},\tau;\mathbf{x}',\tau')]\Delta(\mathbf{x},\tau) + \phi_m^*(\mathbf{x}',\tau')\Big(-\hbar G_0^{-1}(\mathbf{x},\tau;\mathbf{x}',\tau') + \frac{1}{\hbar}g_{bare}\hbar\Pi_0(\mathbf{x},\tau;\mathbf{x}',\tau')g_{bare}\Big)\phi_m(\mathbf{x},\tau) - \frac{1}{\hbar}\Delta^*(\mathbf{x},\tau)\hbar\Pi_0(\mathbf{x},\tau;\mathbf{x}',\tau')g_{bare}\phi_m(\mathbf{x}',\tau') - \frac{1}{\hbar}\phi_m^*(\mathbf{x},\tau)g_{bare}\hbar\Pi_0(\mathbf{x},\tau;\mathbf{x}',\tau')\Delta(\mathbf{x}',\tau')\Big], \tag{69}$$

which represents a generalization to the two-channel atom-molecule model of the Gaussian fluctuation theory developed in [13] for a single-channel resonantly interacting Fermi gas. From Eqs. (68) and (32) we see that the Fourier transform of the pair propagator $G_{\Delta_{bg}}$ can be identified with the many-body T_{bg} matrix. It can be easily calculated by performing the sum over the Matsubara frequencies in Π_0 and using the Lippmann-Schwinger equation in Eq. (38) at $E=0$. We obtain [13,91]

$$\hbar G_{\Delta_{bg}}^{-1}(\mathbf{K},\Omega_n) = \mathrm{T}_{bg}^{\mathrm{MB}^{-1}}(\mathbf{K},\Omega_n) = -\frac{1}{V}\sum_{\mathbf{k}}\left(\frac{1-N_{\mathbf{K}/2+\mathbf{K}}-N_{\mathbf{K}/2-\mathbf{k}}}{i\hbar\Omega_n+2\mu-2\epsilon_{\mathbf{k}}-\epsilon_{\mathbf{K}}/2}+\frac{1}{2\epsilon_{\mathbf{k}}}\right) + \frac{m}{4\pi\hbar^2 a_{bg}}. \tag{70}$$

The Fermi distribution factors $N_{\mathbf{k}}$ describe the effects of Pauli blocking in the medium.

The renormalized pair propagator G_Δ, which includes the effects of the resonant scattering, is calculated by integrating out also the molecular field in Eq. (69). After some algebra, which involves the definitions in Eqs. (26)–(32), we recover the expected result

$$G_\Delta(\mathbf{K},\Omega_n)/\hbar = \mathrm{T}^{\mathrm{MB}}(\mathbf{K},\Omega_n) = \mathrm{T}_{bg}^{\mathrm{MB}}(\mathbf{K},\Omega_n) + g^{\mathrm{MB}^*}(\mathbf{K},\Omega_n)\frac{G(\mathbf{K},\Omega_n)}{\hbar}g^{\mathrm{MB}}(\mathbf{K},\Omega_n), \tag{71}$$

where $G(\mathbf{K},\Omega_n)$ is the full molecular propagator. Note that in this derivation we have assumed $\Pi=\Pi_0$ which corresponds to neglecting many-body effects in fermionic atomic propagators. Nevertheless, this restriction would disappear if we consider the complete series in the expansion of the $-\hbar\mathrm{Tr}[\ln(-\mathbf{G}_f)]$ term. At the saddle point $\Delta(\mathbf{x},\tau)=0$, there are no contributions coming from the $\hbar\mathrm{Tr}[\ln(-\mathbf{G}_f)]$ term, and the solution of the pair propagator reduces to

$$\hbar G_\Delta^{-1}(\mathbf{K},\Omega_n) = \left(\frac{4\pi\hbar^2 a_{bg}}{m} + \frac{g_{bare}^2}{i\hbar\Omega_n+2\mu-\delta_{bare}-\epsilon_{\mathbf{K}}/2}\right)^{-1}. \tag{72}$$

Thus the Feshbach molecule makes the pair field dynamical, even before including the fluctuations around the saddle point, in contrast with the usual BCS theory, where the dynamics of the pair field is generated only via the $\hbar\mathrm{Tr}[\ln(-\mathbf{G}_f)]$ term. As we will see in two next sections, this can have a large effect on the bare molecular component above the resonance in the case of a narrow resonance $\eta^2 \leqslant \epsilon_F$.

D. Many-body T matrix for a very broad resonance

For a very broad resonance, the dynamics of the molecular boson close to resonance is dominated by the self-energy in the molecular propagator in Eq. (29). The dynamics of the bare boson, given by the term $i\hbar\omega$ in the free propagator, is then effectively screened by dressing effects. This can be explicitly verified by carefully studying the low-energy behavior of the exact many-body T matrix in Eq. (71).

At fixed density the width of the BEC-BCS crossover region, delimited by

$$|k_F a(B)| \simeq \sqrt{\epsilon_F}\frac{\eta}{|\delta(B)|} \leqslant 1, \tag{73}$$

is determined by the energy scale η^2, related to the width of the specific resonance under consideration. As the latter in-

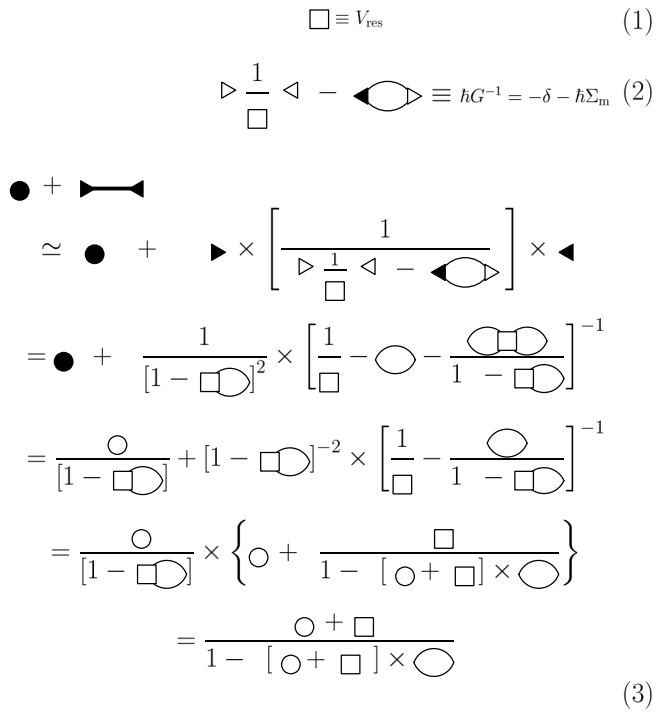

FIG. 9. (1) Diagrammatic representation of the bare resonant interaction introduced in Eq. (76). (2) Approximated form of the molecular propagator defined in Eq. (75). (3) Diagrammatic derivation of the formula in Eq. (77).

creases, so does the range of the magnetic fields which spans the crossover region. Within this range the detuning in general turns out, except of course very close to resonance, to be much larger than the other energy scales:

$$|\delta(B)| \gg |2\mu|, \epsilon_{\mathrm{m}}. \tag{74}$$

To put it more precisely, at positive detuning it is $\delta(B) \gg 2\mu \simeq 2\epsilon_F$, where ϵ_F is the Fermi energy. At negative detuning, the chemical potential approaches half the molecular binding energy $2|\mu| \simeq |\epsilon_{\mathrm{m}}| \ll |\delta(B)|$. Furthermore, at low energies $\hbar\omega \simeq \epsilon_F$ and low momenta $\hbar|\mathbf{q}| \simeq \hbar k_F$, we have $\hbar\omega \ll \hbar\Sigma_{\mathrm{m}}(\mathbf{q},\omega) \simeq \eta\Pi(\mathbf{q},\omega)$ due to the large coupling η. Under these conditions, the full molecular propagator in Eq. (29) and (71) can be approximated by

$$\hbar G(\mathbf{q},\omega)^{-1} \simeq -\delta_{\mathrm{bare}} - \hbar\Sigma_{\mathrm{m}}(\mathbf{q},\omega). \tag{75}$$

Introducing also

$$\mathrm{V}_{\mathrm{res}} = -\frac{g_{\mathrm{bare}}^2}{\delta_{\mathrm{bare}}} \tag{76}$$

as a new definition of the bare resonant part of the potential and using the set of relations in Eqs. (26)–(32), we obtain without any further approximation

$$\begin{aligned}\mathrm{T}^{\mathrm{MB}}(\mathbf{K},\omega) &\simeq \mathrm{T}_{\mathrm{bg}}^{\mathrm{MB}}(\mathbf{K},\omega) + g^{\mathrm{MB}^*}(\mathbf{K},\omega) \\ &\times \frac{1}{-\delta_{\mathrm{bare}} - \hbar\Sigma_{\mathrm{m}}(\mathbf{K},\omega)} g^{\mathrm{MB}}(\mathbf{K},\omega) \\ &= \frac{\mathrm{V}_{\mathrm{bg}} + \mathrm{V}_{\mathrm{res}}}{1 - (\mathrm{V}_{\mathrm{bg}} + \mathrm{V}_{\mathrm{res}})\Pi(\mathbf{K},\omega)}.\end{aligned} \tag{77}$$

This is the formal solution of a Bethe-Salpeter equation for the many-body T matrix of the bare interaction $\mathrm{V}_{\mathrm{bg}} + \mathrm{V}_{\mathrm{res}}$ [89–91]. A derivation of Eq. (77) based on the diagrammatic calculus developed in Sec. III B is shown in Fig. 9. Renormalizing the bare interactions to the two-body T matrix as in Eq. (70) this equation can be rewritten as [13]

$$\begin{aligned}\hbar G_{\Delta}^{-1}(\mathbf{K},\Omega_n) = \mathrm{T}^{\mathrm{MB}^{-1}}(\mathbf{K},\Omega_n) &\simeq \frac{m}{4\pi\hbar^2 a(B)} \\ &- \frac{1}{V}\sum_{\mathbf{k}} \left(\frac{1 - N_{\mathbf{K}/2+\mathbf{k}} - N_{\mathbf{K}/2-\mathbf{k}}}{i\Omega_n + 2\mu - 2\epsilon_{\mathbf{k}} - \epsilon_{\mathbf{K}}/2} + \frac{1}{2\epsilon_{\mathbf{k}}} \right).\end{aligned} \tag{78}$$

In the limit of zero-energy scattering in the vacuum it reduces to the atom-atom effective interaction in Eq. (44):

$$\frac{4\pi\hbar^2 a(B)}{m} = \frac{4\pi\hbar^2 a_{bg}(B)}{m} - \frac{g^2(B)}{\delta(B)} \equiv \frac{4\pi\hbar^2}{m}[a_{\mathrm{bg}}(B) + a_{\mathrm{res}}(B)] \tag{79}$$

that we obtain by integrating out the molecular field from the very beginning in the original action in Eq. (60). This shows that for a very broad resonance, the low-energy behavior of the many-body T matrix in Eq. (71) in most of the BEC-BCS crossover region determined by Eq. (73), does not differ significantly from the many-body T matrix of a *single-channel* interaction with scattering length $a(B)$. A detailed analysis of the analytic structure of the many-body T matrix (78) has been carried out by Combescot in [30,31].

However, even for a broad resonance, a complete approach to investigate the physics across the Feshbach resonance cannot neglect the closed channel from the beginning. This is essentially for two reasons. First, at sufficiently negative detuning, where the systems approaches a gas of weakly interacting bare molecules with binding energy linear in the magnetic field, the closed channel dominates. In that regime, the approximation introduced in Eq. (75) fails because the analytic expression of the two-body scattering amplitude contained in Eq. (77) has the wrong pole structure in the complex plane in order to reproduce the correct binding energy. The pole which denotes the binding energy of the molecular state follows Wigner's formula $\epsilon_{\mathrm{m}}(B) = -\hbar^2/ma^2(B)$, which is quadratic in the detuning, at every magnetic field below resonance. Therefore only a two-channel model can allow a full description at every magnetic field across the resonance. Second, near the resonance the gas consists of a mixture of atoms and dressed molecules which can in principle be measured separately. Dressed molecules have nonzero components on two different spin state configurations, even above the Feshbach resonance, which can also be measured by experiments [20]. Thus, even when the dressing

effect is so strong that the wavefunction contains almost completely only atomic scattering states in the open channel, the distinction between the two different components can be crucial for the interpretation of the experiments.

E. Many-body molecular self-energy

The physics of the dressed molecules is described by the molecular propagator in the presence of the medium. The effective Gaussian action for the molecules is obtained by integrating out the pairing field $\Delta(\mathbf{x},\tau)$ in Eq. (69). In this manner we obtain

$$S[\phi_{\mathrm{m}}^*,\phi_{\mathrm{m}}] = \int d\tau \int d\mathbf{x} \int d\tau' \int d\mathbf{x}' \phi_{\mathrm{m}}^*(\mathbf{x}',\tau') \times \left[-\hbar G_0^{-1}(\mathbf{x},\tau;\mathbf{x}',\tau') + \frac{1}{\hbar} g_{\mathrm{bare}} \hbar \Pi_0 \left(g_{\mathrm{bare}} + \frac{1}{\hbar^2} G_{\Delta_{\mathrm{bg}}}(\mathbf{x},\tau;\mathbf{x}',\tau') \hbar \Pi_0 g_{\mathrm{bare}} \right) \right] \phi_{\mathrm{m}}(\mathbf{x},\tau). \quad (80)$$

When we recall the definition of the pairing propagator $G_{\Delta_{\mathrm{bg}}}$ in Eq. (68) and Eqs. (31) and (32), we observe that the effect of the Gaussian integration over the field Δ consists of dressing the atom-molecule coupling constant with ladder diagrams. Therefore, we obtain the renormalized molecular propagator

$$S[\phi_{\mathrm{m}}^*,\phi_{\mathrm{m}}] = \int d\tau \int d\mathbf{x} \int d\tau' \int d\mathbf{x}' \phi_{\mathrm{m}}^*(\mathbf{x}',\tau') \times \left(-\hbar G_0^{-1}(\mathbf{x},\tau;\mathbf{x}',\tau') + \frac{1}{\hbar} g \hbar \Pi_0(\mathbf{x},\tau;\mathbf{x}',\tau') g^{\mathrm{MB}} \right) \phi_{\mathrm{m}}(\mathbf{x},\tau). \quad (81)$$

By repeating the same renormalization procedure of the ultraviolet divergencies described above in Eqs. (40) and (41), the many-body molecular propagator can be rewritten as

$$\hbar G^{\mathrm{MB}^{-1}}(\mathbf{k},E) = E + 2\mu - \delta(B) - \epsilon_{\mathbf{k}}/2 - \hbar\Sigma_{\mathrm{m}}^{\mathrm{MB}}(\mathbf{k},E) + \hbar\Sigma_{\mathrm{m}}^{\mathrm{2B}}(\mathbf{0},0), \quad (82)$$

where the many-body self-energy in the ladder approximation is given by

$$\hbar\Sigma_{\mathrm{m}}^{\mathrm{MB}}(\mathbf{q},E) - \hbar\Sigma_{\mathrm{m}}^{\mathrm{2B}}(\mathbf{0},0) = \frac{1}{V}\sum_{\mathbf{k}} |g^{\mathrm{MB}}(\mathbf{q},2\epsilon_{\mathbf{k}})|^2 \times \left(\frac{1 - N_{\mathbf{q}/2+\mathbf{k}} - N_{\mathbf{q}/2-\mathbf{k}}}{E + 2\mu - 2\epsilon_{\mathbf{k}} - \epsilon_{\mathbf{q}}/2} + \frac{1}{2\epsilon_{\mathbf{k}}} \right). \quad (83)$$

If we neglect the many-body corrections in g^{MB} and the Fermi factors in the numerator of the integrand, we recover the two-body result in Eq. (42). The integral of Eq. (83) cannot be performed analytically but some progress can be made by considering a special limit. Neglecting the many-body effects in the dressed coupling constant g^{MB}, the expression reduces to

$$\hbar\Sigma_{\mathrm{m}}^{\mathrm{MB}}(\mathbf{q},E) - \hbar\Sigma_{\mathrm{m}}^{\mathrm{2B}}(\mathbf{0},0) = \frac{1}{V}\sum_{\mathbf{k}} |g^{\mathrm{2B}}(\mathbf{0},2\epsilon_{\mathbf{k}})|^2 \left(\frac{1 - N_{\mathbf{q}/2+\mathbf{k}} - N_{\mathbf{q}/2-\mathbf{k}}}{E + 2\mu - 2\epsilon_{\mathbf{k}} - \epsilon_{\mathbf{q}}/2} + \frac{1}{2\epsilon_{\mathbf{k}}} \right). \quad (84)$$

In this case, the integral can be integrated analytically at $T=0$ but the solution is rather cumbersome and we do not reproduce it here. The solution at $T=0$ in the limit $a_{\mathrm{bg}} \to 0$, is given by [52]

$$\hbar\Sigma_{\mathrm{m}}^{(+)\mathrm{MB}}(\mathbf{q},E) - \hbar\Sigma_{\mathrm{m}}^{\mathrm{2B}}(\mathbf{0},0) = -\eta i \sqrt{E + 2\mu - \frac{\epsilon_{\mathbf{q}}}{2}} + 2\eta\frac{\sqrt{2\mu}}{\pi} + \eta\frac{E}{\pi\sqrt{2\epsilon_{\mathbf{q}}}} \ln\left(\frac{E - \epsilon_{\mathbf{q}} + 2\sqrt{\mu\epsilon_{\mathbf{q}}}}{E - \epsilon_{\mathbf{q}} - 2\sqrt{\mu\epsilon_{\mathbf{q}}}} \right) + \frac{\eta}{\pi}\sqrt{E + 2\mu - \frac{\epsilon_{\mathbf{q}}}{2}} \left(\ln \frac{\sqrt{E + 2\mu - \frac{\epsilon_{\mathbf{q}}}{2}} - \left(\sqrt{2\mu} + \sqrt{\frac{\epsilon_{\mathbf{q}}}{2}} \right)}{\sqrt{E + 2\mu - \frac{\epsilon_{\mathbf{q}}}{2}} + \left(\sqrt{2\mu} + \sqrt{\frac{\epsilon_{\mathbf{q}}}{2}} \right)} + \ln \frac{\sqrt{E + 2\mu - \frac{\epsilon_{\mathbf{q}}}{2}} - \left(\sqrt{2\mu} - \sqrt{\frac{\epsilon_{\mathbf{q}}}{2}} \right)}{\sqrt{E + 2\mu - \frac{\epsilon_{\mathbf{q}}}{2}} + \left(\sqrt{2\mu} - \sqrt{\frac{\epsilon_{\mathbf{q}}}{2}} \right)} \right). \quad (85)$$

As an important point, we must mention the fact that in Eq. (84) the Galilean invariance is lost. This is because the Fermi sea introduces a preferred coordinate frame in the description of the scattering. Physical insight is gained by observing the $T=0$ solution for $\mathbf{q}=0$. In that case the solution is

$$\hbar\Sigma_{\mathrm{m}}^{\mathrm{MB}}(\mathbf{0},E) - \hbar\Sigma_{\mathrm{m}}^{\mathrm{2B}}(\mathbf{0},0) = \eta\frac{\sqrt{-E-2\mu}}{1 + \sqrt{\frac{-E-2\mu}{\epsilon_{\mathrm{bg}}}}} + \frac{\eta}{1 + \frac{E+2\mu}{\epsilon_{\mathrm{bg}}}} \left[\frac{4}{\pi}\sqrt{\epsilon_{\mathrm{bg}}} \operatorname{Arctan}\left(\frac{\sqrt{2\epsilon_F}}{\sqrt{\epsilon_{\mathrm{bg}}}} \right) - \frac{4}{\pi}\sqrt{-E-2\mu} \operatorname{Arctan}\left(\frac{\sqrt{2\epsilon_F}}{-E-2\mu} \right) \right] \quad (86)$$

or

$$\hbar\Sigma_{\rm m}^{\rm MB}(\mathbf{0},E)-\hbar\Sigma_{\rm m}^{\rm 2B}(\mathbf{0},0)=\eta\sqrt{-2\mu-E}+\frac{4}{\pi}\eta\sqrt{2\epsilon_F}-\frac{4}{\pi}\eta\sqrt{-E-2\mu}\,\mathrm{Arctan}\left(\frac{\sqrt{2\epsilon_F}}{-E-2\mu}\right) \tag{87}$$

in the limit of $a_{\rm bg}\to 0$ when it is possible to neglect the energy dependence of the atom-molecule coupling constant.

Only the imaginary part of the self-energy in Eq. (84) can be calculated by simple analytic methods. In the limit $a_{\rm bg}\to 0$ we find [48]

$$\mathrm{Im}\{\hbar\Sigma_{\rm m}^{\rm MB}(\mathbf{q},E^+)\}=\frac{\eta}{\beta\sqrt{\frac{\epsilon_{\mathbf{q}}}{2}}}\Theta\left(E+2\mu-\frac{\epsilon_{\mathbf{q}}}{2}\right)\times\ln\left(\frac{\cosh\frac{\beta}{2}\left[\frac{E^+}{2}+\sqrt{\left(E^++2\mu-\frac{\epsilon_{\mathbf{q}}}{2}\right)\frac{\epsilon_{\mathbf{q}}}{2}}\right]}{\cosh\frac{\beta}{2}\left[\frac{E^+}{2}-\sqrt{\left(E^++2\mu-\frac{\epsilon_{\mathbf{q}}}{2}\right)\frac{\epsilon_{\mathbf{q}}}{2}}\right]}\right). \tag{88}$$

The real part at nonzero temperatures can only be calculated numerically. The effects of the nonzero temperature corrections are shown in Figs. 10 and 11. Figure 12(a) illustrates the real part of the zero-temperature self-energy in Eq. (85) at different momenta $\mathbf{q}$. Figure 12(b) shows the effect of the corrections introduced by the background scattering length $a_{\rm bg}$. In Fig. 13(a) the real part of the self-energy in Eq. (84) is plotted at fixed energy $\hbar\omega$ as a function of the momentum $\hbar q$ at different temperatures. Finally in Fig. 13(b) the relative dependence between the two variables ω and $\mathbf{q}$ is illustrated. Some physical consequences of this behavior of the molecular self-energy are discussed next.

F. Fermi edge effects for a narrow Feshbach resonance

A two-component Fermi gas with negative s-wave interactions exhibits a superconducting instability when lowering the temperature to $T\ll T_F$. The instability is signaled by a singularity at $\mathbf{K}=\Omega=0$ in the two-particle propagator G_Δ which describes the Cooper channel. For a weak attractive background interaction $a_{\rm bg}<0$, for example, the pair propagator in Eq. (70) of the traditional BCS theory

$$\hbar G_{\Delta_{\rm bg}}^{-1}(\mathbf{0},0)=\mathrm{T}_{\rm bg}^{\rm MB-1}(\mathbf{0},0)=-\frac{1}{V}\sum_{\mathbf{k}}\left(\frac{1-2N_{\mathbf{k}}}{2\mu-2\epsilon_{\mathbf{k}}}+\frac{1}{2\epsilon_{\mathbf{k}}}\right)+\frac{m}{4\pi\hbar^2 a_{\rm bg}} \tag{89}$$

has a pole at [13,103]

$$T_c\simeq\frac{8\epsilon_F}{k_B\pi}e^{\gamma-2}\exp\left(-\frac{\pi}{2k_F|a_{\rm bg}|}\right), \tag{90}$$

where $\gamma=0.5772$ is Euler's constant.

From a mathematical point of view, the logarithmic singularity is generated by the rather sharp Fermi surface in Eq. (89). The same structure occurs in the self-energy in Eq. (84). This is because many-body effects on the propagation of the molecule and the Cooper instability are described by the same ladder diagrams. As a result, the pairing mechanism must be enhanced by the presence of the molecular bound state. The effects of the resonant interaction on the Cooper instability are considered in the next section, by focusing on the singularities of the total many-body T matrix in Eq. (71). Here we follow the opposite logic and concentrate on the effects of the logarithmic singularity, introduced by the atomic Fermi sea, on the molecular field.

The bare molecular field is a true independent degree of freedom. Even at the lowest order in the self-energy, its propagator

$$\hbar G_0^{-1}(\mathbf{K},\Omega_n)=\left(i\hbar\Omega_n-\frac{\epsilon_{\mathbf{K}}}{2}+2\mu-\delta_{\rm bare}\right) \tag{91}$$

is dynamical. This is in contrast with the auxiliary pairing field $\Delta_{\rm bg}$ of BCS theory, which, at lowest order, is described by a static propagator

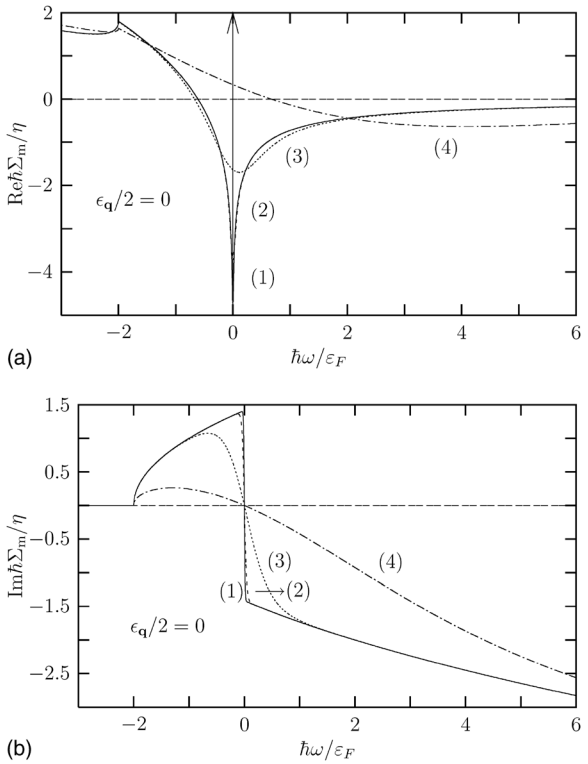

FIG. 10. Real part (a) and imaginary part (b) of the molecular self-energy in Eq. (84), with $\mathbf{q}=0$ and $|g^{\rm 2B}(\mathbf{0},2\epsilon_{\mathbf{k}})|^2\simeq|g^{\rm 2B}(\mathbf{0},\mathbf{0})|^2=g^2$, and at different temperatures: (1) $T\simeq 0$, (2) $T=10^{-2}T_F$, (3) $T=10^{-1}T_F$, (4) $T=T_F$.

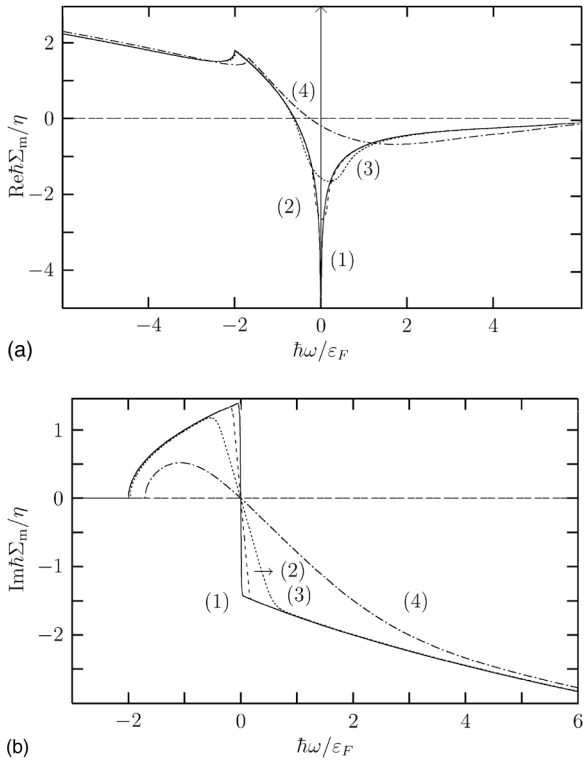

FIG. 11. Real part (a) and imaginary part (b) of the molecular self-energy in Eq. (84), with $|g^{2B}(\mathbf{0},2\epsilon_\mathbf{k})|^2 \simeq |g^{2B}(\mathbf{0},\mathbf{0})|^2 = g^2$, and at different momenta and temperatures: (1) $k_BT = \epsilon_\mathbf{q}/2 \simeq 0$, (2) $k_BT = \epsilon_\mathbf{q}/2 = 3\times10^{-3}k_BT_F$, (3) $k_BT = \epsilon_\mathbf{q}/2 = 3\times10^{-2}k_BT_F$, (4) $k_BT = \epsilon_\mathbf{q}/2 = 3\times10^{-1}k_BT_F$.

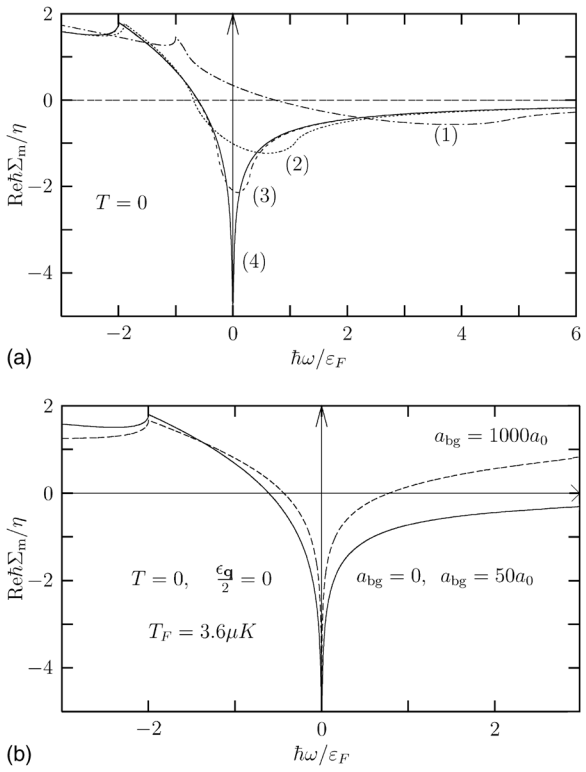

FIG. 12. (a) Real part of the molecular self-energy (85), at different momenta: (1) $\epsilon_\mathbf{q}/2 = \epsilon_F$, (2) $\epsilon_\mathbf{q}/2 = 10^{-1}\epsilon_F$, (3) $\epsilon_\mathbf{q}/2 = 10^{-2}\epsilon_F$, (4) $\epsilon_\mathbf{q} = 0$. (b) Real part of the molecular self-energy in Eq. (86) for different values of the background scattering length a_{bg}.

$$\hbar G^{-1}_{\Delta_{bg}} = \frac{1}{V_{bg}}. \tag{92}$$

This explains why we expect the logarithmic singularity to have nontrivial effects on the molecule thermodynamics. It turns out that it can lead to important consequences, expecially in the case of a narrow resonance $\eta^2 \ll \epsilon_F$. Surprisingly, the bare molecular component of the gas becomes strongly enhanced by the presence of a sharp Fermi surface when approaching the resonance from positive detuning. The mechanism underlying this effect can be better understood when examining the analogy with other well-known phenomena in condensed-matter physics. In particular, the resonant molecular level embedded in the continuum of the atoms is reminescent of the Anderson model for a quantum dot, where a localized electron level is located just below the Fermi energy of the metal leads.

Quantum dots are small solid-state devices in which the number of electrons is a well-defined integer N [104,105]. In Fig. 14 the quantum dot is sketched as an electron box, separated from the leads by tunable tunnel barriers and with a number of spin-degenerate energy states that can be single or doubly occupied by electrons of either spin up or down. An electron on the leads cannot tunnel onto the dot because it would cost an energy $E_C - \epsilon_F$, which is assumed to be much larger than the thermal energy k_BT of the leads. The inhibition of such a transition, called the Coulomb blockade, suppresses exponentially the conduction through the dot at low temperature. This suppression occurs because the process of electron transport through the dot involves a real transition to the state in which the charge of the dot differs by one unit from the thermodynamically most probable value. However, the Heisenberg uncertainty principle allows higher-order processes for short durations, in which virtual states participate in the tunneling process. The leading contributions to this activationless transport are provided by the inelastic and elastic cotunneling processes described in Fig. 14.

It turns out that in a quantum dot the amplitude of the elastic cotunneling process with a singly occupied level of Fig 14(c) diverges logarithmically when the energy $\hbar\omega \simeq k_BT$ of an incoming electron approaches zero. The singularity in the transition amplitude gives a dramatic enhancement of the conductance through the dot. In the elastic cotunneling process (c) the electron on the dot is quickly replaced by another electron, when the electron on the dot tunnels to one of the leads. The characteristic time scale for such a cotunneling is about $\hbar/E_C$. Events of type (c) also effectively flip the spin on the dot. Successive spin-flip processes screen the local spin on the dot until a spin singlet is formed by the electrons in the leads and on the dot. Macroscopically, the system enters in a many-body correlated quantum state. The formation of this entangled state, which is a pure many-body effect, represents the Kondo effect in quantum dots [104,106]. If we interpret the tunneling as an effective magnetic-exchange coupling, the physics of a quantum dot between two leads becomes analogous to the origi-

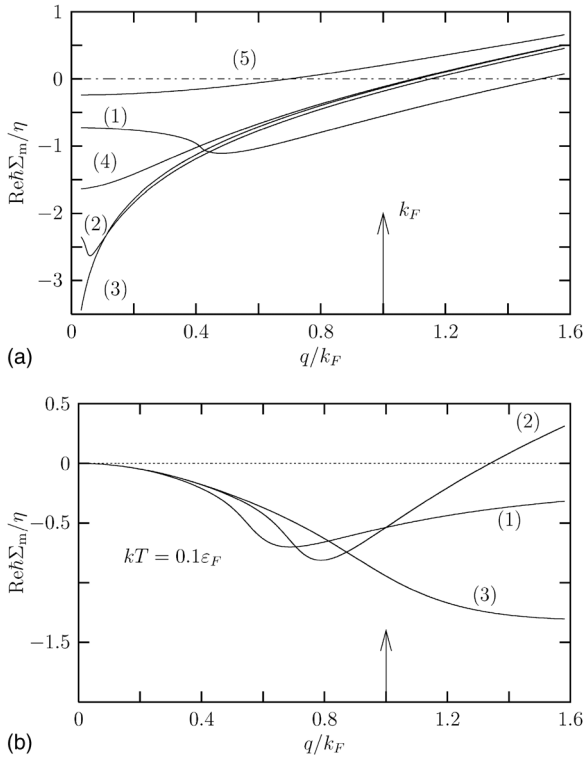

FIG. 13. (a) Real part of the molecular self-energy in Eq. (84) as a function of the momentum $\mathbf{q}$, at different energies and temperatures. The various curves are (1) $k_BT=0, \hbar\omega=\epsilon_F$; (2) $k_BT=0, \hbar\omega=0.1\epsilon_F$; (3) $k_BT=0, \hbar\omega=0.01\epsilon_F$; (4) $k_BT=0.1k_BT_F, \hbar\omega=0.01\epsilon_F$; (5) $k_BT=k_BT_F, \hbar\omega=0.01\epsilon_F$; (b) Real part of the molecular self-energy in Eq. (84) as a function of the scaling variable $\hbar\omega/\epsilon_\mathbf{q}$. The curves are (1) $\mathrm{Re}\,\hbar\Sigma_m(\omega/\epsilon_\mathbf{q}, \mathbf{q})/\eta$, (2) $\mathrm{Re}\,\hbar\Sigma_m(\omega/\epsilon_\mathbf{q}, \mathbf{k}_F)/\eta$, (3) $\mathrm{Re}\hbar\Sigma_m(\omega/\epsilon_\mathbf{q}, 0.3\mathbf{k}_F)/\eta$.

nal Kondo effect [107] for magnetic impurities coupled to conduction electrons in a metal host. As shown in Fig. 15(a), the Kondo effect is signaled by a narrow resonance at the Fermi energy in the density of states of the dot.

Returning back to our model, we expect something similar to happen when the molecular level is located at somewhat more than twice the Fermi energy above the threshold of the atomic continuum. Differently than in quantum dots, the molecular state has to lie above twice the Fermi energy of the atoms, because otherwise the ground state of the gas would contain a Bose-Einstein condensate of molecules. The atom-molecule coupling produces virtual transitions between the molecules and two atoms above and two holes below the

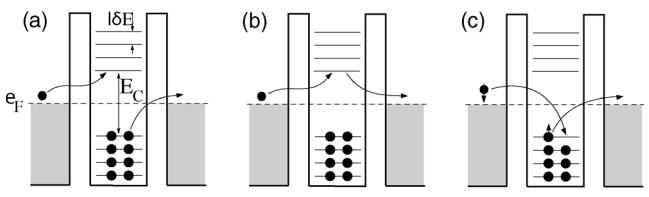

FIG. 14. Examples of cotunneling processes: (a) inelastic cotunneling transferring an electron between the leads leaves behind an electron-hole pair in the dot; (b) elastic cotunneling; (c) elastic cotunneling with a flip of the spin. This figure is taken from [105].

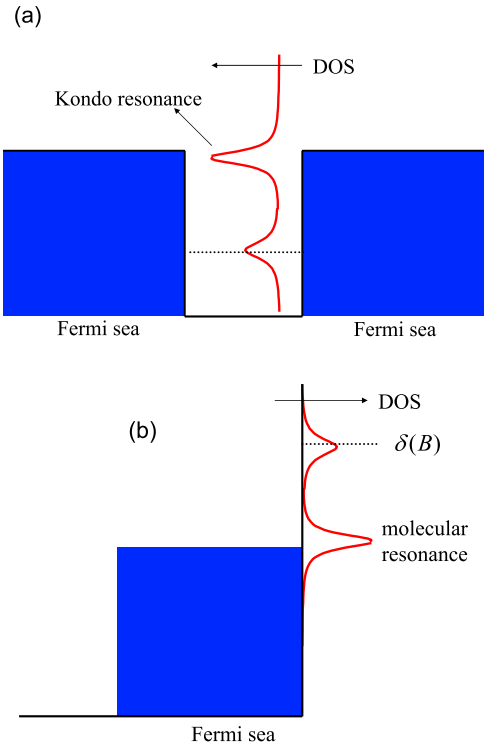

FIG. 15. (Color online) (a) Kondo resonance in quantum dots. (b) Many-body resonance in the molecular density of states near the Feshbach resonance. Note that, in order to make more evident the analogy with (a), we have plotted in (b) the quantity $\rho(\omega)/\omega$ [see also Fig. 18(a)].

Fermi sea, as is shown in Fig. 16. In this case the virtual cotunneling of pairs of atoms to the molecular level is indeed reminiscent of the inelastic cotunneling of Fig. 14(c). However, in our case, no Coulomb blockade is required. The Fermi sea removes the symmetry between scattering to and from the virtual molecular level, because atoms can tunnel only in pairs. This leads to the logarithmic singularity in the self-energy in Eq. (84) as mentioned above. The onset of a singularity in the self-energy signals the formation of a new many-body collective state. Taking the lowest-order precesses shown in Fig. 16 this many-body resonant state can be written as a linear superposition

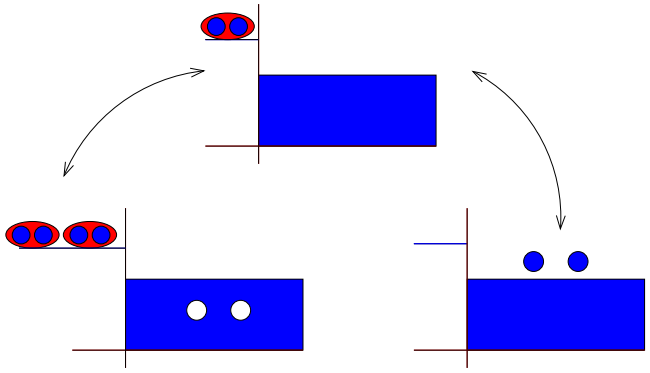

FIG. 16. (Color online) Virtual tunneling of pairs of atoms to the molecular level in the Fermi gas near a Feshbach resonance.

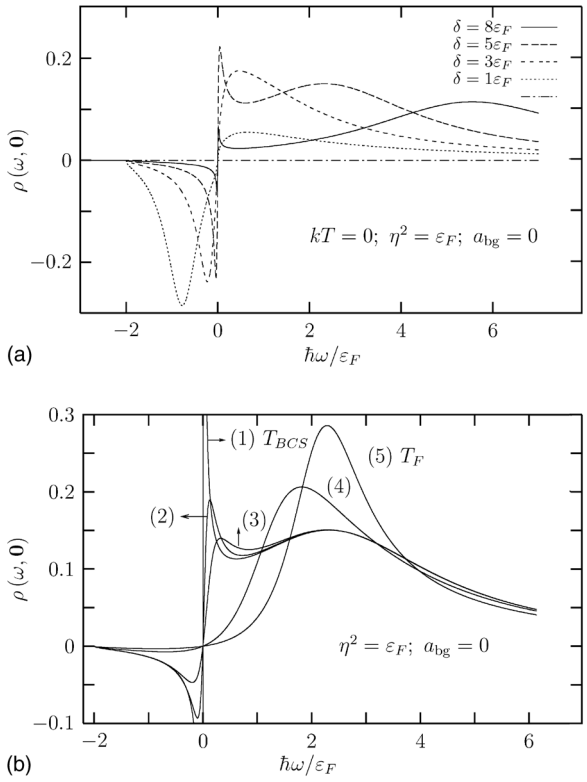

FIG. 17. Molecular spectral density (a) calculated from the self-energy in Eq. (87) at different detunings. Molecular spectral density (b) calculated from the self-energy in Eq. (84) at $\delta=5\epsilon_F$ for different temperatures: (1) $T_{BCS}\simeq 0.02T_F$, (2) $T=0.06T_F$, (3) $T=0.1T_F$, (4) $T=0.5T_F$, (5) $T=T_F$.

$$|\Psi_{\mathrm{K}}\rangle \simeq \sqrt{Z_{\mathrm{K}}}\Big(b_{\mathbf{0}}^{\dagger}|\Phi_{\mathrm{F}}\rangle + \sum_{|\mathbf{k}|>k_{\mathrm{F}}} \alpha_{\mathbf{k}} a_{\mathbf{k},\uparrow}^{\dagger} a_{-\mathbf{k},\downarrow}^{\dagger}|\Phi_F\rangle + \sum_{|\mathbf{k}|<k_{\mathrm{F}}} \beta_{\mathbf{k}} b_{\mathbf{0}}^{\dagger} b_{\mathbf{0}}^{\dagger} a_{\mathbf{k},\uparrow} a_{-\mathbf{k},\downarrow}|\Phi_{\mathrm{F}}\rangle\Big), \tag{93}$$

where $|\Phi_{\mathrm{F}}\rangle$ indicates the filled Fermi sea and the molecular field is treated in the zero-mode approximation that considers only the lowest molecular state. This is justified at very low temperatures. In the formation of the many-body coherent state the system gains an energy

$$\Delta E_K = \langle\Psi_{\mathrm{K}}|H|\Psi_{\mathrm{K}}\rangle - E_G, \tag{94}$$

where $E_G=2\Sigma_{|\mathbf{k}|<k_{\mathrm{F}}}(\epsilon_{\mathbf{k}}-\mu)$ is the ground state of the Fermi mixture in absence of the Feshbach resonance. This shift can be calculated variationally [108,109] as follows.

First we evaluate $H|\Psi_{\mathrm{K}}\rangle$ considering the Hamiltonian given in Eq. (102). Then we project this state on the three different components of the ground-state ansatz of Eq. (93). As a result Eq. (94) is turned in three equations for the variables ΔE_{K}, $\alpha_{\mathbf{k}}$, $\beta_{\mathbf{k}}$. The variable Z cancels out because it is the normalization constant. Eliminating $\alpha_{\mathbf{k}}$ and $\beta_{\mathbf{k}}$ we obtain at $T=0$ a self-consistent equation for ΔE_{K}. This is

$$\Delta E_K + 2\mu - \delta(B) \simeq \eta\frac{4\sqrt{2\mu}}{\pi} + \eta\frac{2}{\pi}\sqrt{\Delta E_K + 2\mu}\,\ln\frac{\sqrt{\Delta E_K+2\mu}-\sqrt{2\mu}}{\sqrt{\Delta E_K+2\mu}+\sqrt{2\mu}}, \tag{95}$$

where we have used that $\mu=\epsilon_F=\hbar^2k_F^2/2m$. At large detunings $\delta\gg 2\mu$ this equation has only one solution at $\Delta E_K\simeq\delta(B)$ as expected when resonance effects can be neglected. However, when $\delta\gtrsim 2\mu$, we have three solutions. The lowest-energy solution defines the ground state of the systems and occurs when $\Delta E_K\simeq 0$. The logarithm in the last term diverges when $\Delta E_K\to 0$. Therefore, we have that $2\mu\gg\Delta E_K$, $|\ln\Delta E_K|\gg\Delta E_K$ and we can approximate Eq. (95) as

$$2\mu - \delta(B) \simeq \eta\frac{2\sqrt{2\mu}}{\pi}\left[2+\ln\left(\frac{|\Delta E_K|}{8\mu}\right)\right]. \tag{96}$$

This leads to a nonperturbative expression for the energy shift of the ground state given by

$$|\Delta E_K| \simeq \frac{8\mu}{e^2}e^{(\pi/2)(\sqrt{2\mu}/\eta)}e^{-(\pi/2)[\delta(B)/\eta\sqrt{2\mu}]}. \tag{97}$$

The change in the ground-state energy defines a temperature, i.e., the analogous of the Kondo temperature.

The singular behavior of the self-energy is associated with the occurrence of a resonance in the spectral density $\rho(\mathbf{q},\omega)$ of the molecular bosons given by

$$\rho_{\mathrm{m}}(\mathbf{q},\omega) = -\,\mathrm{Im}[G_{\mathrm{m}}^{(+)}(\mathbf{q},\omega)]/\pi\hbar. \tag{98}$$

This feature is clearly illustrated in Fig. 15(b). Figure 17 shows the function $\rho_{\mathrm{m}}(\mathbf{q},\omega)$ for different detunings and momenta $\mathbf{q}$ both at nonzero and zero temperature. At large positive detuning, the spectral function shows just a single broad peak centered around the detuning. This is the expected situation for a single molecular state with a finite lifetime. As the detuning gets closer to twice the Fermi energy, the spectral density shows two other sharp peaks slightly above and below the zero frequency. When approaching the resonance, the spectral density of the molecular field at low momenta and temperatures does no longer satisfy the unitarity sum rule [110]

$$\int_{-\infty}^{\infty} d(\hbar\omega)\rho_{\mathrm{m}}(\mathbf{q},\omega) = 1, \tag{99}$$

despite the fact that the self-energy in Eq. (84) is analytic in the upper-half complex plane. This happens already above the BCS critical temperature and is due to the appearance of a complex pole in the upper-half plane in the propagator. This feature is an artifact of the weak-coupling approximation, which neglects self-consistency effects on the Fermi propagators in the calculation of the molecular self-energy when the gas enters the strong-coupling regime $k_Fa(B)<-1$. For fermions, Luttinger's theorem [111] shows that the causality of the self-energy is a sufficient condition to have also a causal propagator. We are not aware of an analogous theorem in the case of bosons and our findings indeed

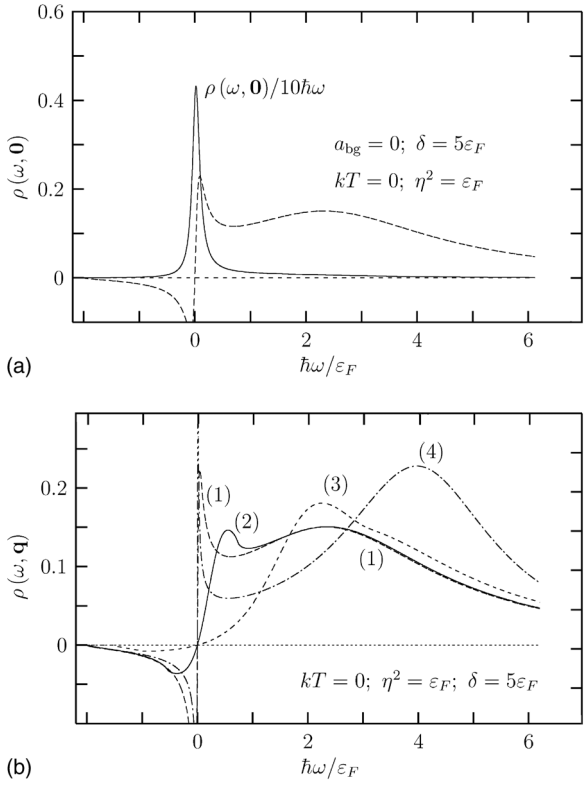

FIG. 18. (a) The spectral density is plotted together with $\rho(\omega)/\omega$. At small frequencies, the latter quantity is proportional to the density of states times the occupation number. The double structure of the molecular resonance merges then into a single Kondo-like resonance. (b) Effects on the molecular spectral density, calculated from the self-energy in Eq. (87), of the kinetic energy of the molecules: (1) $q=0$, (2) $q\sim 0.3k_F$, and (3) $q=k_F$. The curve (4) is calculated from the self-energy (86) using $q=0$, $a_{bg}\sim 10^3\ a_0$, $\epsilon_F \sim 3.6\ \mu$K. It shows the corrections given on the density of states by a large background scattering length.

present a counter example [112]. The double-peak feature arises because the spectral density must be negative at negative frequencies for a bosonic field. By plotting the quantity $\rho_m(\omega)/\omega$ [113], as shown in Fig. 18(a), a single peak at zero frequency is obtained.

We call this a molecular Kondo resonance. The effects of nonzero momentum and of corrections due to a nonzero background scattering lenght a_{bg} are shown in Fig. 18(b). Both tend to suppress the resonance. Nonzero momentum corrections spoil the coherence of the many-body virtual cotunneling events similarly as BCS pairing is suppressed at nonzero total momentum. A large background scattering length means that there is a bound state in the open channel potential [100]. This induces some density of states at large energy. Because the total density of states is normalized to 1, this results in an effective reduction of the resonance peak.

The additional spectral weight at low frequencies, induced by the above-mentioned many-body effects, leads to an increase of the bare molecular component in the gas, calculated by means of

$$n_B(T)=\int_{-\infty}^{+\infty} d(\hbar\omega)\int \frac{d\mathbf{q}}{(2\pi)^3}\rho_m(\mathbf{q},\omega)N\left(\frac{\hbar\omega}{k_BT}\right) \quad (100)$$

with respect to that estimated from two-body physics. The enhancement of the bare molecular components for realistic resonance parameters is discussed in detail in [52].

G. Exact mapping to the anisotropic Kondo Hamiltonian

The analogy with the Kondo effect in a quantum dot, introduced in the previous section, requires a more formal analysis. It is very desirable to search for an exact mapping from the atom-molecule Hamiltonian to the Hamiltonian of the Kondo problem.

The physics of the Kondo effect is described by a model Hamiltonian based on the assumption that the magnetic moment of a local impurity is coupled via an antiferromagnetic exchange interaction J with the conduction electrons. This is known as the Kondo Hamiltonian and reads

$$H=\sum_{\mathbf{k},\sigma}(\epsilon_{\mathbf{k}}-\mu)c^\dagger_{\mathbf{k},\sigma}c_{\mathbf{k},\sigma}+\sum_{\mathbf{k},\mathbf{k}'}[J_+S^+c^\dagger_{\mathbf{k},\downarrow}c_{\mathbf{k}',\uparrow}+J_-S^-c^\dagger_{\mathbf{k},\uparrow}c_{\mathbf{k}',\downarrow}$$
$$+J_zS_z(c^\dagger_{\mathbf{k},\uparrow}c_{\mathbf{k}',\uparrow}-c^\dagger_{\mathbf{k},\downarrow}c_{\mathbf{k}',\downarrow})], \quad (101)$$

where $\epsilon_{\mathbf{k}}$ is the energy of the conduction electrons and S_z and $S^\pm(\equiv S_x\pm iS_y)$ are the spin operators for the impurity with spin 1/2. The operators $c_{\mathbf{k},\alpha}$ and $c^\dagger_{\mathbf{k},\alpha}$ correspond to the creation and annihilation operators of conduction electrons with momenta $\mathbf{k}$ and one of the possible spin states $\alpha=|\uparrow\rangle$ or $|\alpha=\downarrow\rangle$ which scatters of the impurity. The coupling constants $J_\pm$ and J_z describe spin-flip and non-spin-flip scattering, respectively.

The Hamiltonian of our model in Eq. (20) appears rather different than the Hamiltonian in Eq. (101), but it becomes more similar when a restricted many-body Fock space is considered [114]. For our present purpose, we can in first instance consider only the zero-momentum molecular state [115]. We can also neglect the effects of the background interaction. Within these approximations, the atom-molecule Hamiltonian in Eq. (20) becomes

$$H=\sum_{\mathbf{k},\sigma\in\{\uparrow,\downarrow\}}(\epsilon_{\mathbf{k}}-\mu)a^\dagger_{\mathbf{k},\sigma}a_{\mathbf{k},\sigma}+[\delta(B)-2\mu]b_0^\dagger b_0$$
$$+\frac{1}{\sqrt{V}}\sum_{\mathbf{k}}(g^*b_0^\dagger a_{\mathbf{k},\downarrow}a_{-\mathbf{k},\uparrow}+\text{H.c.}). \quad (102)$$

The bosonic number operator $b_0^\dagger b_0$ acts on the occupied (unoccupied) lowest energy molecular state $|1\rangle$ ($|0\rangle$) according to $b_0^\dagger b_0|1\rangle=1|1\rangle$ and $b_0^\dagger b_0|0\rangle=0$. Hence, in this reduced Hilbert space, we can formally identify the molecular operators $b_0^\dagger$ and b_0 with spin 1/2 raising and lowering operators $S^+=S^x+iS^y$ and $S^-=S^x-iS^y$, which satisfy analogous relations

$$S^+S^-|+1/2\rangle=\left(\frac{1}{2}+S^z\right)|+1/2\rangle=1|+1/2\rangle, \quad (103)$$

$$S^+S^-|-1/2\rangle=\left(\frac{1}{2}+S^z\right)|-1/2\rangle=0 \quad (104)$$

in the two-dimensional Hilbert space $\{|+1/2\rangle,|-1/2\rangle\}$.

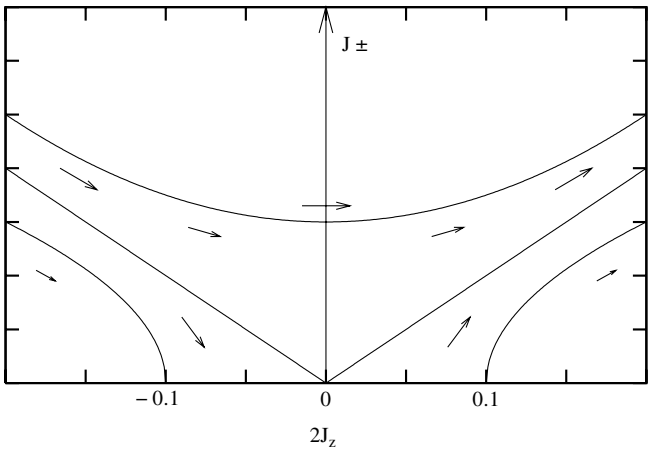

FIG. 19. Scaling trajectories for the anisotropic Kondo model in Eq. (101) [117].

More progress can be made by rewriting the atom-molecular coupling in terms of the symmetrized atom-pair operators $d_{\mathbf{k}}=[a_{-\mathbf{k},\downarrow}a_{\mathbf{k},\uparrow}+a_{\mathbf{k},\downarrow}a_{-\mathbf{k},\uparrow}]/\sqrt{2}$ and $d_{\mathbf{k}}^{+}=[a_{\mathbf{k},\uparrow}^{\dagger}a_{-\mathbf{k},\downarrow}^{\dagger}+a_{-\mathbf{k},\uparrow}^{\dagger}a_{\mathbf{k},\downarrow}^{\dagger}]/\sqrt{2}$, which satisfy the commutation relation

$$[d_{\mathbf{k}}^{+},d_{\mathbf{k}}]=\frac{1}{2}(N_{\mathbf{k},\uparrow}+N_{-\mathbf{k},\downarrow}+N_{-\mathbf{k},\uparrow}+N_{\mathbf{k},\downarrow}-2). \quad (105)$$

In the restricted two-dimensional Hilbert space, defined by the condition that the eigenvalues of $N_{\mathbf{k},\uparrow}+N_{-\mathbf{k},\downarrow}$ and $N_{-\mathbf{k},\uparrow}+N_{\mathbf{k},\downarrow}$ are either 2 or 0, the commutator in Eq. (105) can be put [116] into the matrix form $[d_{\mathbf{k}}^{+},d_{\mathbf{k}}]=\sigma_{\mathbf{k}}^{z}$, by means of the z-component Pauli matrix

$$\begin{pmatrix}1 & 0\\ 0 & -1\end{pmatrix}=\sigma_{\mathbf{k}}^{z}. \quad (106)$$

This suggests the correspondence $d_{\mathbf{k}}\rightarrow\sigma_{\mathbf{k}}^{+}\equiv\frac{1}{2}(\sigma_{\mathbf{k}}^{x}+i\sigma_{\mathbf{k}}^{y})$ and $d_{\mathbf{k}}^{+}\rightarrow\sigma_{\mathbf{k}}^{-}\equiv\frac{1}{2}(\sigma_{\mathbf{k}}^{x}-i\sigma_{\mathbf{k}}^{y})$. Finally, by rewriting the spin ladder operators $\sigma_{\mathbf{k}}^{\pm}$, by means of the Abrikosov representation [118], in terms of anticommuting fermionic operators $\sigma_{\mathbf{k}}^{+}=c_{\mathbf{k},\uparrow}^{\dagger}c_{\mathbf{k},\downarrow}$ and $\sigma_{\mathbf{k}}^{-}=c_{\mathbf{k},\downarrow}^{\dagger}c_{\mathbf{k},\uparrow}$ the atom-molecule Hamiltonian in Eq. (20) can finally be transformed into

$$H=\sum_{\mathbf{k},\alpha}(\epsilon_{\mathbf{k}}-\mu)c_{\mathbf{k},\alpha}^{\dagger}c_{\mathbf{k},\alpha}+(\delta-2\mu)S_{z}+\frac{g}{\sqrt{2V}}\sum_{\mathbf{k}}[S^{+}c_{\mathbf{k},\uparrow}^{\dagger}c_{\mathbf{k},\downarrow}+S^{-}c_{\mathbf{k},\downarrow}^{\dagger}c_{\mathbf{k},\uparrow}]. \quad (107)$$

When $\delta=2\mu$, this Hamiltonian is equivalent of the anisotropic Kondo Hamiltonian in Eq. (101) if we state the correspondence $g/\sqrt{2}=J_{+}=J_{-}$ and $J_{z}=0$. At nonzero detuning but larger than 2μ, the term $(\delta-2\mu)S_{z}$ represents an external magnetic field applied on the localized spin, which removes its degeneracy and ultimately destroys the Kondo effect. Moreover, it is important to realize that the lack of the non-flipping spin-interaction term, signaled by the condition $J_{z}=0$, does not rule out the possibility that such a term is generated by higher-order processes. As illustrated in the example of Fig. 19, the renormalization group flow in the solution of the Kondo problem can generate nonzero values of J_{z} starting from a point with $J_{z}=0$ [117]. A renormalization group analysis of the coupling constants flow reveals that this occurs also in Eq. (107).

H. Fermi-liquid description of the normal state in the weak-coupling regime

In the absence of the Feshbach resonance, the ultracold dilute fermionic mixture weakly interacting in the background scattering channel above some certain critical temperature T_{c}, is a Fermi liquid [119]. In this section, we consider the weak-coupling regime $1/k_{F}a(B)\leqslant -1$ in the presence of the Feshbach resonance from the point of view of the Fermi-liquid theory [50]. The thermodynamics of a normal-fluid Fermi liquid is determined by the fermionic Green's function

$$G_{\sigma}(\mathbf{k},\omega_{n})=\frac{\hbar}{i\hbar\omega_{n}-(\epsilon_{\mathbf{k}}-\mu)-\hbar\Sigma_{\sigma}^{f}(\mathbf{k},\omega_{n})}. \quad (108)$$

In a self-consistent approach, the fermionic self-energy $\hbar\Sigma_{\sigma}^{f}(\mathbf{k},\omega_{n})$ is calculated in the ladder approximation from

$$\hbar\Sigma_{\sigma}^{f}(\mathbf{k},\omega_{n})=-\frac{1}{(2\pi)^{3}}\int d^{3}\mathbf{k}'\frac{1}{\beta\hbar}\sum_{\omega_{n'}}\times \mathrm{T}^{\mathrm{MB}}(\mathbf{k}+\mathbf{k}',\omega_{n}+\omega_{n}')G_{-\sigma}(\mathbf{k}',\omega_{n}'), \quad (109)$$

where the many-body T matrix of Eq. (33) is determined by Eqs. (82), (83), and (70). From the self-energy $\hbar\Sigma_{\sigma}^{f}(\mathbf{k},\omega_{n})$ we can calculate the atomic spectrum given by the poles of the fermionic propagator in Eq. (108) [90,119] according to the equation

$$\hbar\omega_{\mathbf{k}}=\frac{\hbar k^{2}}{2m}+\hbar\Sigma^{f}(\mathbf{k},\omega_{\mathbf{k}})=\epsilon_{\mathbf{k}}+\hbar\Sigma^{f}(\mathbf{k},\omega_{\mathbf{k}}), \quad (110)$$

where we have suppressed the spin indices because the two-species have the same mass and chemical potential. This equation can be simplified in the weak-coupling limit as

$$\hbar\omega_{\mathbf{k}}\simeq\epsilon_{\mathbf{k}}+\hbar\Sigma^{f}(\mathbf{k},p_{\mathbf{k}}), \quad (111)$$

because we expect a quasiparticle spectrum for the single particle excitations of the type $\hbar\omega_{\mathbf{k}}=\epsilon_{\mathbf{k}}[1+O(k_{F}a(B))]$ and the self-energy $\hbar\Sigma^{f}(\mathbf{k},\omega_{\mathbf{k}})$ to be of the order of $O(k_{F}a(B))$. The real part $\mathrm{Re}[\hbar\Sigma^{f}(\mathbf{k},\epsilon_{\mathbf{k}})]$ gives a shift in the single-particle energies of momentum $\mathbf{k}$, while the imaginary part $\mathrm{Im}[\hbar\omega_{\mathbf{k}}]\equiv\hbar\gamma_{\mathbf{k}}$ leads to a finite lifetime proportional to $1/\gamma_{\mathbf{k}}$. Since the lifetime becomes infinite at k_{F}, the chemical potential is defined by

$$\mu\equiv\hbar\omega_{k_{F}}=\epsilon_{k_{F}}+\hbar\Sigma^{f}(k_{F},\epsilon_{k_{F}}). \quad (112)$$

Close to the Fermi surface the energy spectrum can be expanded into a Taylor series

$$\mathrm{Re}[\hbar\omega_{\mathbf{k}}]=\epsilon_{k_{F}}+\frac{\hbar^{2}k_{F}}{m^{*}}(k-k_{F})+O((k-k_{F})^{2}), \quad (113)$$

which defines the effective mass

$$m^* = \hbar^2 k_F \left(\left. \frac{\partial \mathrm{Re}[\hbar\omega_{\mathbf{k}}]}{\partial k} \right|_{k=k_F} \right)^{-1}. \tag{114}$$

The effective mass determines the properties of the system in the zero-temperature limit.

In presence of the resonance it is important to distinguish [50] between the weak-coupling regime near a broad and a narrow resonance. For a broad resonance the condition $\eta^2 \gg \epsilon_F$ implies that in the weak-coupling regime $1/k_F a(B) \leqslant -1$ we have $\delta(B) \gg \epsilon_F$. Therefore, we can neglect the retardation effects on the atom-atom interaction induced by the dynamics of the bare molecular boson. According to the discussion of Sec. III D, near a broad resonance, the many-body T matrix of Eq. (33) can be approximated by the single-channel expression of Eq. (78). Then the atomic self-energy becomes

$$\hbar\Sigma^f(\mathbf{k},\omega_n) = -\int \frac{d^3\mathbf{k}'}{(2\pi)^3} \frac{1}{\beta\hbar} \sum_{\omega_{n'}} \frac{4\pi\hbar^2}{m} \left[\frac{1}{a(B)} - \frac{4\pi\hbar^2}{m} \frac{1}{V} \sum_{\mathbf{p}} \left(\frac{1 - N_{(\mathbf{k}+\mathbf{k}')/2+\mathbf{p}} - N_{(\mathbf{k}+\mathbf{k}')/2-\mathbf{p}}}{i\omega_n + 2\mu - 2\epsilon_{\mathbf{p}} - \epsilon_{(\mathbf{k}+\mathbf{k}')/2}} + \frac{1}{2\epsilon_{\mathbf{p}}} \right) \right]^{-1} G_\sigma(\mathbf{k}', \omega_n'). \tag{115}$$

In the weak-coupling limit the many-body T matrix in Eq. (115) can be expanded in powers of $a(B)$ and we obtain

$$\hbar\Sigma^f(\mathbf{k},\omega_n) = \frac{n}{2} \frac{4\pi\hbar^2 a(B)}{m} + \hbar\tilde{\Sigma}^f(\mathbf{k},\omega_n), \tag{116}$$

where n is the total atomic density of the gas and $\hbar\tilde{\Sigma}^f(\mathbf{k},\omega_n)$ represents a correction of order $[k_F a(B)]^2$. Calculating the self-energy $\hbar\tilde{\Sigma}^f(\mathbf{k},\omega_n)$ in the limit of zero temperature one finds the expression of $\hbar\omega_{\mathbf{k}}$, $\gamma_{\mathbf{k}}$, and m^* up to order $[k_F a(B)]^2$ of a dilute Fermi-liquid theory [14,28,32,50,90]

$$\hbar\omega_{k_F} = \frac{\hbar^2 k_F^2}{2m} \left(1 + \frac{4}{3\pi}[k_F a(B)] + \frac{4}{15\pi^2}(11 - 2\ln 2)[k_F a(B)]^2 \right)$$

$$\frac{m^*}{m} = 1 + \frac{8}{15\pi^2}(7\ln 2 - 1)[k_F a(B)]^2$$

$$\gamma_{\mathbf{k}} = -\frac{\hbar k_F^2}{2m} \frac{2}{\pi} \left(\frac{k_F - k}{k_F} \right)^2 \tag{117}$$

for $|k - k_F|/k_F \ll 1$.

In the case of a narrow resonance the bare dynamics of the molecular propagator cannot be neglected in the weak-coupling limit $1/k_F a(B) \leqslant -1$. Therefore, we have to retain the full expression of the molecular propagator in the many-body T matrix of Eq. (33). Using the formal definition of the effective mass in Eq. (114) and calculating the integral in Eq. (109), we recover the additional contribution to the effective mass of Eq. (117)

$$\frac{\delta m^*}{m} \simeq \frac{g^2}{2\delta(B)^2} n, \tag{118}$$

calculated by Bruun and Pethick in [50]. However, we have seen that, in the weak-coupling regime $1/k_F a(B) \leqslant -1$ on the positive side of the resonance, non-trivial correlations arise in the molecular degree of freedom. These correlations induce a resonance in the molecular spectral function. As a result the finite-lifetime molecule on the positive side of the resonance cannot be pictured as a well-defined quasiparticle, as one would naively think in the case of a narrow resonance. Therefore, it is reasonable to ask if it is not possible that the Fermi-liquid description could partially break down in the case of a narrow resonance in combination with the onset of the molecular resonance at the Fermi surface. This requires a more detailed analysis of the fermionic Green's function in Eq. (108) and will be addressed elsewhere.

IV. THE EQUATION FOR THE CRITICAL TEMPERATURE T_c IN THE BEC-BCS CROSSOVER IN RESONANT ATOMIC FERMI GASES

The ability to control experimentally the strength of the interactions between ultracold atoms offers the exciting possibility to study in detail the crossover between the Bose-Einstein condensation (BEC) of diatomic molecules and the Bardeen-Cooper-Schrieffer (BCS) transition of atomic pairs [10–13,44,46,48,60].

According to the Thouless criterion [120], the superfluid phase transition in a Fermi system with attractive interactions occurs at the temperature for which the many-body T matrix in Eq. (33) develops a pole at $(\mathbf{K},\omega)=(\mathbf{0},0)$. At large positive detuning, i.e., in the weak-coupling BCS limit, the Thouless criterion yields the equation for the determination of the BCS critical temperature of a Fermi gas with attractive interactions. However, when approaching the resonance, the attraction increases and the Fermi surface of the gas gets strongly renormalized. Hence, the approximation $\mu \simeq \epsilon_F$, valid in the weak-coupling BCS limit, is no longer valid. Particle number conservation gives the desired condition on the chemical potential of the gas under equilibrium conditions [10–12]. This leads to a set of two coupled equations for T_c and μ. In the opposite BEC limit the role of the two equations is inverted. The equation of state determines the critical temperature for the Bose-Einstein condensation of dressed molecules. The pole of the many-body T matrix becomes two-body in nature. This fixes the chemical potential to half the binding energy of a dressed molecule.

The equation of state can be determined in different approximations. The simplest mean-field theory at nonzero temperature neglects finite-lifetime effects of the molecules and does not reproduce the correct binding energy of the dressed molecules. The latter problem can be repaired by replacing in the equation of state the bare energy of the molecular level with its dressed value calculated at Sec. III B in the two-body scattering approximation. This leads to the modified mean-field description [49] discusssed in Sec. IV A. However, this mean-field approach still neglects finite-lifetime effects of the molecules. As a result, it exhibits a

phase transition between the BCS phase and the BEC phase. Since we expect, from symmetry principles, a smooth curve for T_c and μ, this must be considered to be an artifact of the mean-field theory. The inclusion of Gaussian fluctuations on top of the mean-field solution, according to the Nozieres-Schmitt-Rink approach [12,13], is sufficient to obtain a smooth crossover in the two-channel model [46,48,51]. This approximation is described in Sec. IV B. A comparison of the critical temperature as a function of the magnetic field for a broad resonance reveals that our modified mean-field approach agrees quantitatively fairly well with the Nozieres-Schmitt-Rink result. The Gaussian approximation exhibits a maximum in the curve for T_c [46,51,121]. It has been shown that, in a self-consistent approach, this maximum in the curve for T_c disappears both in a single-channel [14] and in a two-channel model [61]. In Sec. IV C, we discuss the self-consistent equations in connection with our dressed-molecule picture through a systematic analysis of the BEC limit where analytical calculation are possible.

A. Modified mean-field equations

In order to study the pole structure of the many-body T matrix in Eq. (33), it is crucial to consider explicitly the many-body corrections of the atom-molecule coupling constant in the calculation of the self-energy of the dressed molecular propagator in Eq. (83). However, a more transparent derivation of the equation for the critical temperature can be obtained by rewriting the many-body T matrix in Eq. (33) in terms of the simpler two-body T matrix in Eq. (35). We start by considering the definition of the many-body T matrix in Eq. (27)

$$\mathrm{T}^{\mathrm{MB}}(\mathbf{K},E) = \mathrm{V}_{\mathrm{eff}} + \mathrm{V}_{\mathrm{eff}}\Pi(\mathbf{K},E)\mathrm{T}^{\mathrm{MB}}(\mathbf{K},E),$$

with $\mathrm{V}_{\mathrm{eff}}$ given in Eq. (26). Then we replace the kernel in Eq. (28)

$$\hbar\Pi(\mathbf{K},E) = -\frac{k_B T}{\hbar V}\sum_{\mathbf{k},\omega_n} G_{\uparrow}\left(\frac{\mathbf{K}}{2}+\mathbf{k},\frac{E}{2}+\omega_n\right) \times G_{\downarrow}\left(\frac{\mathbf{K}}{2}-\mathbf{k},\frac{E}{2}-\omega_n\right) \tag{119}$$

with the result of Eq. (67)

$$\hbar\Pi_0(\mathbf{K},E) = -\frac{k_B T}{\hbar V}\sum_{\mathbf{k},\omega_n} G_{0,\uparrow}\left(\frac{\mathbf{K}}{2}+\mathbf{k},\frac{E}{2}+\omega_n\right) \times G_{0,\downarrow}\left(\frac{\mathbf{K}}{2}-\mathbf{k},\frac{E}{2}-\omega_n\right) = \frac{\hbar}{V}\sum_{\mathbf{k}}\left(\frac{1-N_{\mathbf{K}/2+\mathbf{k}}-N_{\mathbf{K}/2-\mathbf{k}}}{E+2\mu-2\epsilon_{\mathbf{k}}-\epsilon_{\mathbf{K}}/2}\right), \tag{120}$$

as we have done in the calculation of the molecular self-energy in Eq. (83). Subtracting from the many-body T matrix equation in Eq. (27) the two-body limit

$$\mathrm{T}^{\mathrm{2B}}(E) = \mathrm{V}_{\mathrm{eff}} + \mathrm{V}_{\mathrm{eff}}\frac{1}{V}\sum_{\mathbf{k}}\left(\frac{1}{E-2\epsilon_{\mathbf{k}}}\right)\mathrm{T}^{\mathrm{2B}}(E) \tag{121}$$

at $E=2\mu$, the many-body T-matrix can be put into the form

$$\mathrm{T}^{\mathrm{MB}}(\mathbf{K},E) = \frac{\mathrm{T}^{\mathrm{2B}}(2\mu^+)}{1-\mathrm{T}^{\mathrm{2B}}(2\mu^+)\left[\Pi_0(\mathbf{K},E)-\frac{1}{V}\sum_{\mathbf{k}}\left(\frac{1}{2\mu^+-2\epsilon_{\mathbf{k}}}\right)\right]}, \tag{122}$$

where the two-body T matrix $\mathrm{T}^{\mathrm{2B}}(E)$ is known from Eqs. (35)–(43). At $\mathbf{K}=\omega=0$ this becomes

$$\mathrm{T}^{\mathrm{MB}}(\mathbf{0},0) = \frac{\mathrm{T}^{\mathrm{2B}}(2\mu^+)}{1+\mathrm{T}^{\mathrm{2B}}(2\mu^+)\Xi(\mathbf{0},0^+)}, \tag{123}$$

where

$$\Xi(\mathbf{K},E) = \frac{1}{V}\sum_{\mathbf{k}}\left(\frac{N_{\mathbf{K}/2+\mathbf{k}}+N_{\mathbf{K}/2-\mathbf{k}}}{E+2\mu-2\epsilon_{\mathbf{k}}-\epsilon_{\mathbf{K}}/2}\right). \tag{124}$$

According to the Thouless criterion the denominator of Eq. (123) vanishes at the critical temperature. To illustrate more clearly the physics involved we consider first a system when the background interaction can be neglected, i.e., the limit $a_{\mathrm{bg}}\to 0$. This is the case, for example, in ^{40}K mixtures where the background scattering length is small and does not contribute to the pairing mechanism because is positive. In that case the condition to have a pole in Eq. (123) becomes

$$\delta(B) - 2\mu + \eta\sqrt{-2\mu} - g^2\Xi(\mathbf{0},0^+) = 0. \tag{125}$$

The critical temperature T_c and the chemical potential μ are determined at every magnetic field in the mean-field approximation by solving self-consistently Eq. (125) together with the equation of state. At the mean-field level, neglecting the finite lifetime of the molecules, the latter is calculated from the thermodynamic potential Ω [87] according to the formula

$$n = -\frac{1}{V}\frac{\partial\Omega}{\partial\mu} = -\frac{1}{\beta V}\frac{\partial}{\partial\mu}\left(-\sum_{\sigma}\mathrm{Tr}[\ln(\beta\hbar G_{\sigma,0}^{-1})] + \mathrm{Tr}[\ln(\beta\hbar G_0^{-1})]\right) = \frac{1}{V}\sum_{\mathbf{k}}\{2N(\epsilon_{\mathbf{k}}-\mu) + 2N_B[\epsilon_{\mathbf{k}}/2+\delta(B)-2\mu]\}, \tag{126}$$

where the free-particle atomic and molecular propagators are given by $G_0/\hbar=[i\hbar\omega-\epsilon_{\mathbf{k}}/2+2\mu-\delta(B)]^{-1}$ and $G_{\sigma,0}/\hbar=(i\hbar\omega-\epsilon_{\mathbf{k}}+\mu)^{-1}$, $N(\epsilon_{\mathbf{k}}-\mu)$ is the Fermi distribution $N_{\mathbf{k}}$, and N_B is the Bose distribution function. However, to neglect completely self-energy effects in the molecular propagator is not consistent. This can be repaired in a first approximation by replacing the detuning δ in the free molecular propagator occurring in Eq. (126) with the two-body curve of Eq. (58)

$$\epsilon_{\mathrm{m}} = \frac{1}{3}\left(\delta - \frac{\eta^2}{2} + \sqrt{\frac{\eta^4}{4}-\eta^2\delta+4\delta^2}\right), \tag{127}$$

which we have discussed in Sec. II C. This replacement is necessary because the energy of the dressed molecule in the equation of state must be the same as the binding energy resulting from the chemical potential in the BEC limit from the gap equation. As we shall see, this is crucial in the case of a crossover near a broad resonance where the binding energy is quadratic in the detuning in a large part of the crossover region. For a very narrow resonance, when η^2

$\ll \epsilon_F$, the binding energy of the dressed molecule can be approximated as $\epsilon_m \simeq \delta(B)$ except on a small range of magnetic field close to resonance, and the equation of state in Eq. (126) turns out to be a good approximation. However, the resonances used in current experiments on the BEC-BCS crossover are broad in nature. Therefore, the mean-field equation of state has to be modified to

$$n = \frac{1}{V}\sum_{\mathbf{k}} [2N(\epsilon_{\mathbf{k}} - \mu) + 2N_B(\epsilon_{\mathbf{k}}/2 + \epsilon_m - 2\mu)]. \quad (128)$$

Note that the two-body quantity ϵ_m does not account for a possible many-body shift of the molecular bound state. However, for a broad resonance, this seems to be a smaller correction when compared to the two-body shift.

At positive detuning, in the BCS limit, the chemical potential is positive and the many-body term of Eq. (125) is

$$g^2\Xi(\mathbf{0},0^+) = g^2\,\mathrm{Re}[\Xi(\mathbf{0},0^+)] + \eta\sqrt{-2\mu}. \quad (129)$$

Therefore we obtain the gap equation

$$\delta(B) - 2\mu = g^2\,\mathrm{Re}[\Xi(\mathbf{0},0^+)]. \quad (130)$$

Note that our derivation is based on the many-body T matrix calculated in the ladder approximation. Therefore, it neglects the Gorkov correction [103] to the transition temperature introduced by the effects of the density fluctuations of the medium on the effective two-body interactions.

It turns out that for a narrow Feshbach resonance with $\eta^2 \simeq \epsilon_F$, we can be in the weak-coupling regime $k_F|a(B)| \leqslant 1$ at magnetic fields such that $\delta \simeq 2\mu \simeq \epsilon_F$. In this case the BCS critical temperature is given by

$$T_c \simeq \frac{8\epsilon_F}{k_B\pi} e^{\gamma-2} e^{\frac{2}{\pi}\frac{\sqrt{2\mu}}{\eta}} \exp\left(-\frac{\pi}{2k_F|a(B)|}\right). \quad (131)$$

When the resonance is broad and $\eta^2 \gg 2\epsilon_F$, the detuning is always $\delta \gg 2\mu \simeq \epsilon_F$ in the weak-coupling range $k_F|a(B)| \leqslant 1$, and the term $e^{2\sqrt{2\mu}/\pi\eta}$ can be neglected. In this limit the BCS critical temperature can be approximated by

$$T_c \simeq \frac{8\epsilon_F}{k_B\pi} e^{\gamma-2} \exp\left(-\frac{\pi}{2k_F|a(B)|}\right). \quad (132)$$

This is the same result that one would obtain by looking at the pole of the the *single-channel* many-body T matrix given by Eq. (77). Therefore, we conclude that the positive shift of the weak-coupling BCS critical temperature by the factor $e^{2\sqrt{2\mu}/\pi\eta}$, characteristic of the resonant superfluidity, can be observed only in narrow resonances.

At large negative detuning, the pole of the many-body T matrix in Eq. (27) determines the chemical potential 2μ of the dressed molecule, i.e., the energy we need to make a dressed molecule from two atoms at zero momenta. In the BEC limit this is very large and negative and corresponds to the binding energy of the dressed molecule. Indeed the pole of the many-body T matrix becomes two-body in nature because, for negative μ, the many-body factor is

$$g^2\Xi(\mathbf{0},0^+) = g^2\,\mathrm{Re}[\Xi(\mathbf{0},0^+)] \quad (133)$$

and vanishes exponentially as $|2\mu|/k_BT \to \infty$. The condition (125) becomes

$$\delta(B) - 2\mu + \eta\sqrt{-2\mu} \simeq 0, \quad (134)$$

which is the same algebraic equation as in Eq. (46), again in the limit of $a_{bg} \to 0$, satisfied by the binding energy in Eq. (49)

$$\epsilon_m(B) = \delta(B) + \frac{\eta^2}{2}\left(\sqrt{1 - \frac{4\delta(B)}{\eta^2}} - 1\right). \quad (135)$$

Notice that the curve ϵ_m of Eq. (127) that we have replaced in the equation of state coincides with the binding energy of Eq. (135) at zero detuning.

Once more, it is instructive to distinguish between the two limits of narrow $\eta^2 \ll \epsilon_F$ and broad $\epsilon_F \ll \eta^2$ resonances. On the BEC side of a narrow resonance, when the chemical potential approaches half the binding energy, we have $\mu \simeq \epsilon_m/2 \simeq \delta/2$, and the dressed molecular wavefunction has only a small amplitude in the open channel, that is, $Z \simeq 1$. This can be checked easily if we assume that the chemical potential approaches half the molecular binding energy $\mu \simeq \epsilon_m/2$ approximatively at some value B_{BEC} when $k_F|a(B_{BEC})| \simeq 1$. From the definition of the resonant scattering length in Eq. (44), we have that $|\delta(B_{BEC})| \simeq \eta\sqrt{\epsilon_F}$. Then we can evaluate with the help of the formula in Eq. (135) the binding energy for this value of the magnetic field. This gives

$$\epsilon_m(B_{BEC}) \simeq -\eta\sqrt{\epsilon_F} + \frac{\eta^2}{2}\left(\sqrt{1 + \frac{4\sqrt{\epsilon_F}}{\eta}} - 1\right). \quad (136)$$

Substituting this expression in the definition of Z in Eq. (52) and expanding the result in the small parameter η^2/ϵ_F, we obtain

$$Z(B_{BEC}) \simeq 1 - \frac{1}{2}\left(\frac{\eta^2}{\epsilon_F}\right)^{1/4} \simeq 1. \quad (137)$$

Therefore, for a narrow resonance the bare component of the dressed molecule cannot be neglected. It turns out that also in the so-called universal region, where $k_F|a(B)| \gg 1$, we have $0 < Z < 1$ and the thermodynamics is actually not universal [39].

For a very broad resonance, the bare component Z in the universal region $k_F|a(B)| \gg 1$, is not strictly zero but it is rather small. When the chemical potential approaches half the binding energy, the bare component weight is still $Z \simeq 0$. In fact, expanding Eq. (136) in ϵ_F/η^2 we find

$$Z(B_{BEC}) \simeq 2\frac{\epsilon_F}{\eta^2} \ll 1. \quad (138)$$

This implies that at magnetic fields where the BEC-BCS crossover takes place, the dressed molecule is almost completely in the open channel component. Furthermore, the binding energy in Eq. (135) can be approximated like in Eq. (50) by

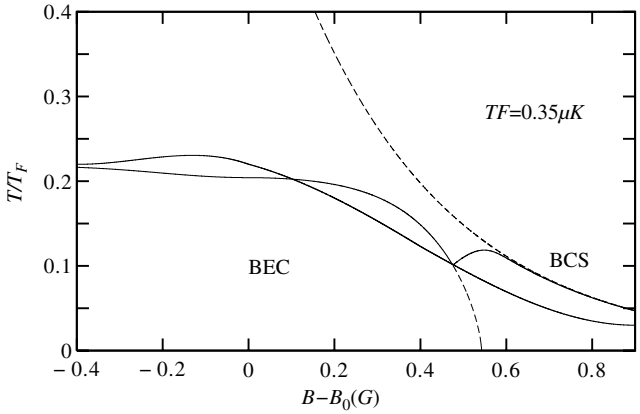

FIG. 20. Phase diagram of atomic ^{40}K near the broad resonance near 201.2 G, as a function of magnetic field and temperature for a Fermi temperature of the gas of $T_F=0.35$ μK. The solid line exhibiting a kink at about 0.5 G gives the critical temperature for either a Bose-Einstein condensation of dressed molecules or a Bose-Einstein condensation of atomic Cooper pairs. The critical temperature for the latter is calculated by simultaneously solving the BCS gap equation of Eq. (125) and the equation of state of an ideal mixture of atoms and dressed molecules as in Eq. (128). For comparison, the upper dashed curve is the analytical BCS result of Eq. (132). The lower dashed line is the crossover between the two Bose-Einstein condensed phases. The other solid smooth line describes the result of the Nozieres-Schmitt Rink approximation.

$$\epsilon_{\rm m}(B) = -\frac{\hbar^2}{ma^2(B)} \propto \delta^2 \tag{139}$$

which is equivalent to neglecting the term 2μ in Eq. (134). Note that this is the same solution determined by the pole of the the many-body T matrix in the *single-channel* approximation of Eq. (77). It is also clear now why, in the case of a broad resonance, it is essential to replace in the equation of state the detuning with the curve of Eq. (127) in order to avoid inconsistency in the BEC limit between the two crossover equations. In conclusion, in the case of a broad resonance, we can, roughly speaking, distinguish between two different crossovers. At detunings where the many-body crossover to a Bose-Einstein condensate of dressed molecules takes place, the dressed molecules live essentially in the states of the atomic continuum. At larger negative detuning, the wavefunction of the dressed molecules undergoes a second two-body crossover to the bare closed-channel eigenstate. The energy scale of this second crossover is η^2 as mentioned above.

In general, as far as the background interaction satisfies the weak-coupling condition $k_F|a_{\rm bg}|<1$, the above discussion does not change qualitatively if we extend the analysis of the many-body T matrix in Eq. (123) without taking the limit $a_{\rm bg}=0$. The gap equation in Eq. (130) in the BCS weak-coupling regime modifies to

$$1+\left(\mathrm{T}_{\rm bg}^{\rm 2B}(0)+g^2\frac{1}{2\mu-\delta(B)}\right)\Xi(\mathbf{0},0^+)\simeq 0. \tag{140}$$

In the case of a broad resonance the weak-coupling solution is again given by Eq. (132) and can now be written as

$$T_{\rm c}\simeq\frac{8\epsilon_F}{k_B\pi}e^{\gamma-2}\exp\left(-\frac{\pi}{2k_F(|a_{\rm res}|+|a_{\rm bg}|)}\right). \tag{141}$$

At large negative detuning the pole of the many-body T-matrix (123) reproduces the correct two-body physics of the dressed molecules. The equation for the chemical potential in Eq. (134) assumes the general form as in Eq. (46)

$$\delta(B)-2\mu+\frac{\eta(B)}{1+|a_{\rm bg}(B)|\sqrt{\frac{-2\mu m}{\hbar^2}}}\sqrt{-2\mu}\simeq 0. \tag{142}$$

Therefore the chemical potential goes to half the binding energy of the dressed molecules $\epsilon_{\rm m}$ given by the more general solution (47). The analysis concerning the differences between the broad and narrow resonances remains unchanged, except that the energy of the second two-body crossover defined above is now near $\hbar^2/ma_{\rm bg}^2$. This analysis holds in general for the resonances currently used in experiments. One exception, however, concerns the region at large positive detuning of the broad resonance at 834 G in a gas of of ^{6}Li atoms. In that case the background interactions turn out to be so large that $\hbar^2/ma_{\rm bg}^2\simeq\epsilon_F$. In other words, the gas never enters a weak-coupling regime at positive detuning and the gap equation in Eq. (140) is not expected to be valid.

Figure 20 shows the mean-field curve for the critical temperature for a gas of ^{40}K atoms near the broad resonance near 201.2 G. The mean-field approach based on Eqs. (125) and (128) does not describe a smooth BEC-BCS crossover because it neglects finite lifetime effects of the molecules. The curve for T_c exibits a sharp phase transition between a Bose-Einstein condensation phase of dressed molecules with binding energy $\epsilon_{\rm m}$ to a Bardeen-Cooper-Schriffer superfluid. This phase transition is only an artifact of the mean-field aproximation because the two phases break the same $U(1)/Z_2$ symmetry [11]. However, the dressed-molecules are the real physical components of the system. Therefore, the location of the kink in the curve for T_c of Fig. 20 leads to an interesting interpretation. According to the poor man's approach of [49], it fixes a scale in the magnetic field below which, the superfluid transition temperature is determined by the condensation temperature of the dressed molecules. Note that this value of the magnetic field coincides also with the magnetic field value at which the size of the dressed-molecule, that is equal to $a(B)$, approaches the interparticle separation k_F^{-1} [38]. It is important to stress that, without the replacement in the equation of state of the detuning with the true location of the molecular level in presence of coupling described by Eq. (127), this scale would have been orders of magnitudes smaller. Interestingly, the location of the crossover line in our mean-field picture that is shown in the dashed curve of Fig. 20, coincides with the threshold for the nonzero condensate fraction in the $(T/T_C,\Delta B)$ plane found by Regal *et al.* in the experiment of [15] that we have discussed in Sec. II.

B. Theory of Gaussian fluctuations

A smooth curve for the critical temperature T_c can be obtained by including finite lifetime effects of the molecular

field in the theory. This can be achieved by considering the quadratic fluctuations on top of the mean-field, according to the Nozieres-Schmitt Rink approach [12,13,46,48,51]. In the Nozieres-Schmitt Rink approximation, one equation is still determined by the Thouless condition expressed by Eq. (140). The equation of state, however, is modified because it has to incorporate the effects of Gaussian fluctuations around the saddle point. The new equation of state reads [48]

$$n = -\frac{1}{V}\frac{\partial \Omega}{\partial \mu} = -\frac{\partial}{\partial \mu}\left(-\frac{1}{\beta V}\sum_{\sigma} \mathrm{Tr}[\ln(\beta\hbar G_{\sigma,0}^{-1})] + \frac{1}{\beta V}\mathrm{Tr}[\ln(\beta\hbar G^{-1})]\right), \tag{143}$$

where the full molecular propagator G is given by Eqs. (82) and (83) and the symbol Tr[ ] denotes the sum over the Matsubara frequencies and momenta. This equation describes a gas of atoms and dressed molecules [122]. Using the definition of the full molecular propagator Eq. (143) can be rewritten as

$$n = \frac{1}{\hbar\beta V}\sum_{\sigma} \mathrm{Tr}[G_{\sigma,0}] - 2\frac{1}{\hbar\beta V}\mathrm{Tr}[G] + \frac{1}{\hbar\beta V}\mathrm{Tr}\left[G\frac{\partial}{\partial \mu}\hbar\Sigma_{\mathrm{m}}\right]. \tag{144}$$

The partition of the different contributions in this equation of state suggests a possible interpretation of each term on the right-hand side of Eq. (144). The first term denotes the number of unbound atoms. The second term describes the contribution of the bare molecular component while the third one defines the open-channel component of the dressed molecules. The analysis of the BEC extreme of the crossover reveals that this interpretation is correct in that regime. In the BEC limit the chemical potential approaches half the binding energy of the dressed molecules, i.e., $\mu \simeq \epsilon_{\mathrm{m}}/2$. Therefore, the chemical potential becomes large and negative and the contribution of the unbound atoms can be neglected. In first approximation the gas constituted mainly of dressed molecules

$$n \simeq 2n_{\mathrm{m}}. \tag{145}$$

We thus want to show that in that limit

$$-2\frac{1}{\hbar\beta V}\mathrm{Tr}[G] + \frac{1}{\hbar\beta V}\mathrm{Tr}\left[G\frac{\partial}{\partial \mu}\hbar\Sigma_{\mathrm{m}}\right] = 2n_{\mathrm{m}}. \tag{146}$$

Taking the contribution of the pole of the dressed molecular propagator we have

$$-2\frac{1}{\hbar\beta V}\mathrm{Tr}[G] + \frac{1}{\hbar\beta V}\mathrm{Tr}\left[G\cdot\frac{\partial}{\partial \mu}\hbar\Sigma_{\mathrm{m}}\right] = \frac{1}{V}\sum_{\mathbf{k}}\left(2ZN(\epsilon_{\mathbf{k}}/2 + \epsilon_{\mathrm{m}} - 2\mu) + ZN_B(\epsilon_{\mathbf{k}}/2 + \epsilon_{\mathrm{m}} - 2\mu)\cdot\frac{\partial}{\partial \mu}\hbar\Sigma_{\mathrm{m}|E=\epsilon_{\mathrm{m}}}\right)$$
$$= \frac{1}{V}\sum_{\mathbf{k}}\left[2ZN(\epsilon_{\mathbf{k}}/2 + \epsilon_{\mathrm{m}} - 2\mu) + 2(1-Z)N_B(\epsilon_{\mathbf{k}}/2 + \epsilon_{\mathrm{m}} - 2\mu)\right] = 2Zn_{\mathrm{m}} + 2(1-Z)n_{\mathrm{m}} = 2n_{\mathrm{m}}, \tag{147}$$

where we have used the definition of the residue Z given in Eq. (52), and that in the BEC limit we have $\partial/\partial\mu \simeq 2\partial/\partial E$ because the many-body molecular self-energy approaches its two-body limit given by Eq. (43).

In the remaining part of this section we want to show that in the limit of a very broad resonance our two-channel model reproduces the results for T_c found by Sa De Meló *et al.* in [13] based on a *single-channel* model [12]. As we have shown in Sec. III E, in the case of a broad resonance, the general expression for the pairing field propagator $\hbar G_{\Delta}$ given in Eq. (71) reduces to that given in Eq. (78). The latter corresponds exactly to that defined by Sa De Meló *et al.* in [13]. This argument is sufficient to proof that our two-channel model is able to reproduce the results of the single-channel model in the limit of a very broad resonance when $\eta^2 \gg \epsilon_F$. However, a detailed analysis of our crossover equations for a broad resonance, gives us more insight about the two different descriptions. When $\eta^2 \gg \epsilon_F$, the gap equation in Eq. (140) can be approximated with

$$1 + \left(\mathrm{T}_{\mathrm{bg}}^{2\mathrm{B}}(0) + g^2\frac{1}{-\delta(B)}\right)\Xi(\mathbf{0},0^+) \simeq 0, \tag{148}$$

along the full range of magnetic fields where the BCS-BEC crossover takes place. This is possible because, as we have explain in Sec. III E, in the case of a broad resonance we have $|\delta(B)| \gg |2\mu|, \epsilon_{\mathrm{m}}$ except of course very close to resonance. However, in that region the gas becomes essentially universal and it can be shown that the nonuniversal correction term 2μ can also be neglected [39]. By using Eq. (44), Eq. (148) can be rewritten as

$$1 + \left(\frac{4\pi\hbar^2 a(B)}{m}\right)\Xi(\mathbf{0},0^+) \simeq 0, \tag{149}$$

which corresponds to the single-channel gap equation of Sa De Meló *et al.* in [13]. A similar analysis concerns the equation of state in Eq. (144). In the case of a broad resonance the weight of the bare molecular component remains quite small such that $Z \simeq 0$ even when the chemical potential approaches half the binding energy $\mu \simeq \epsilon_{\mathrm{m}} \simeq \hbar^2/ma^2$. Therefore we can neglect completely the bare molecular contribution to the number of particles and the equation of state reduces to

$$n \simeq \frac{1}{\hbar\beta V}\sum_{\sigma} \mathrm{Tr}[G_{\sigma,0}] + \frac{1}{\hbar\beta V}\mathrm{Tr}\left[G\frac{\partial}{\partial \mu}\hbar\Sigma_{\mathrm{m}}\right]. \tag{150}$$

Furthermore, in the crossover near a broad resonance the bare dynamics of the molecular field can be neglected and the molecular propagator in Eq. (150) can be approximated as in Eq. (75). Therefore Eq. (150) can be rewitten as

$$n \simeq \frac{1}{\hbar\beta V}\sum_{\sigma} \mathrm{Tr}[G_{\sigma,0}] + \frac{1}{\hbar\beta V}\mathrm{Tr}\left[\frac{\hbar}{-\delta(B) - \hbar\Sigma_{\mathrm{m}}}\frac{\partial}{\partial \mu}\hbar\Sigma_{\mathrm{m}}\right], \tag{151}$$

or

$$n \simeq \frac{\partial}{\partial \mu}\left\{ 2\frac{1}{\beta V}\sum_{\sigma} \mathrm{Tr}[\ln(\beta\hbar G_{\sigma,0}^{-1})] - \frac{1}{\beta V}\mathrm{Tr}\left[\ln\left(\beta\hbar\frac{-\delta(B)-\hbar\Sigma_{\mathrm{m}}}{\hbar}\right)\right]\right\}. \quad (152)$$

At this point, to make this part of the derivation more transparent we consider the special case when $a_{\mathrm{bg}} \to 0$. In that case the molecular self-energy of Eq. (83) is

$$\hbar\Sigma_{\mathrm{m}}(\mathbf{q},\omega_n) = g^2\frac{1}{V}\sum_{\mathbf{k}}\left(\frac{1-N_{\mathbf{q}/2+\mathbf{k}}-N_{\mathbf{q}/2-\mathbf{k}}}{i\hbar\omega_n+2\mu-2\epsilon_{\mathbf{k}}-\epsilon_{\mathbf{q}}/2}+\frac{1}{2\epsilon_{\mathbf{k}}}\right). \quad (153)$$

Using the expression of the total scattering length in Eq. (44) this can be rewritten as in [13]:

$$n = \frac{\partial}{\partial\mu}\left(\frac{1}{\beta V}\sum_{\sigma}\mathrm{Tr}[\ln(\beta\hbar G_{\sigma,0}^{-1})] + \frac{1}{\beta V}\mathrm{Tr}[\ln(\beta\hbar {G_{\Delta}}^{-1})]\right), \quad (154)$$

where G_{Δ} is the pairing field propagator in the Gaussian approximation defined in Eq. (78). In the general case when a_{bg} is finite, the derivation is analogous but more involved because of the energy dependence of the atom-molecule coupling [123].

By comparing Eq. (150) and Eq. (154) we argue that the propagator G_{Δ} of the composite boson in the single-channel picture contains the open-channel contribution of the dressed-molecules. The precise mathematical relation between the two entities will be discussed further in one of the following sections where we give a detailed analysis of the BEC limit in the superfluid state.

The curve of the critical temperature T_c for the broad resonance in ^{40}K atoms based on the crossover Eqs. (149) and (154) is shown also in Fig. 20. This result shows that our modified mean-field approach, based on the two-body physics of the dressed molecules, can be considered a rather good approximation in view of its simplicity.

C. Beyond Gaussian fluctuactions

The curve of T_c in Fig. 20 calculated according the Nozieres-Schmitt Rink approximation exhibits a maximum. This maximum disappears in the self-consistent approach of [14]. The latter includes some fluctuations that lead to an increase of the effective mass of the dressed molecules and therefore to a descrease of the transition temperature. This self-consistent approach for the calculation of T_c in a dilute gas of fermions interacting with strong attractive interactions has been developed by Haussmann in [14] in relation with a single-channel model, and has been extended by Xiang and Ji in [61] to the two-channel Feshbach model. Their numerical results shows clearly that the curve for T_c in the BEC-BCS crossover evolves monotonically from one limit to the other when self-energy effects between atoms and molecules are treated self-consistently. In this self-consistent approach, the conservation of the number of total particle in the BEC-BCS crossover is given by the equation

$$n = \frac{1}{\hbar\beta V}\sum_{\sigma}\mathrm{Tr}[G_{\sigma}] - 2\frac{1}{\hbar\beta V}\mathrm{Tr}[G], \quad (155)$$

where the full atomic Green's function is calculated from the many-body T matrix as in Eq. (109) but including to all order the self-energy effects in the fermionic and molecular propagators. In this section we want to discuss the two coupled Eqs. (155) and (140) in connection with our dressed-molecules picture. The analysis of the BEC limit is particularly illuminating in this respect. We consider here the case when the background interaction can be neglected. However, as we have seen, it is always straightforward to generalize our result including the effect of the nonresonant interactions.

In the BEC limit we have $2\mu \simeq \epsilon_{\mathrm{m}}$ and $\epsilon_{\mathrm{m}} \gg k_B T, \epsilon_F$ and the fermionic self-energy

$$\hbar\Sigma_{\sigma}^{f}(\mathbf{k},\omega_n) = -\int\frac{d^3\mathbf{k}'}{(2\pi)^3}\frac{1}{\beta\hbar^2}\sum_{\omega_n'} g^2 \times G(\mathbf{k}+\mathbf{k}',\omega_n+\omega_n')G_{-\sigma}(\mathbf{k}',\omega_n') \quad (156)$$

can be approximated to the lowest order in the fermionic propagator as [14]

$$\hbar\Sigma_{\sigma}^{f}(\mathbf{k},\omega_n) \simeq -G_{-\sigma,0}(\mathbf{k},\omega_n)g^2\int\frac{d^3\mathbf{k}'}{(2\pi)^3}\frac{1}{\beta\hbar^2}\sum_{\omega_{n'}} G(\mathbf{k}',\omega_n'), \quad (157)$$

$$\simeq \frac{G_{-\sigma,0}(\mathbf{k},\omega_n)}{\hbar}g^2 Z n_{\mathrm{m}}(T),$$

where Z in the BEC limit is given by taking the limit $a_{\mathrm{bg}} \to 0$ in Eq. (52), that is [47],

$$Z = \left[1+\frac{\eta}{2\sqrt{|\epsilon_{\mathrm{m}}|}}\right]^{-1}. \quad (158)$$

This means that the fermionic propagator assumes a double fraction structure as

$$G_{\sigma}(\mathbf{k},\omega_n) = \hbar \Big/ \left(i\hbar\omega_n - (\epsilon_{\mathbf{k}}-\mu) - \frac{g^2 Z n_{\mathrm{m}}(T)}{i\hbar\omega_n-(\epsilon_{\mathbf{k}}-\mu)}\right), \quad (159)$$

which is equivalent to a fermionic BCS propagator characterized by a "gap" in the spectrum defined as

$$|\Delta_{\mathrm{pg}}|^2 \equiv g^2 Z n_{\mathrm{m}}(T). \quad (160)$$

Therefore the equation of state in Eq. (155) can be rewritten as

$$n = -2\frac{1}{\hbar\beta V}\mathrm{Tr}[G] - 2\int\frac{d^3\mathbf{k}'}{(2\pi)^3}\frac{1}{\beta\hbar}\sum_{\omega_{n'}}\frac{\hbar[i\hbar\omega_n+(\epsilon_{\mathbf{k}}-\mu)]}{(\hbar\omega_n)^2+(\epsilon_{\mathbf{k}}-\mu)^2+|\Delta_{\mathrm{pg}}|^2} = 2Zn_{\mathrm{m}}(T) - 2\int\frac{d^3\mathbf{k}'}{(2\pi)^3}\frac{1}{\beta\hbar}\sum_{\omega_{n'}}\frac{\hbar[i\hbar\omega_n+(\epsilon_{\mathbf{k}}-\mu)]}{(\hbar\omega_n)^2+(\epsilon_{\mathbf{k}}-\mu)^2+|\Delta_{\mathrm{pg}}|^2}. \quad (161)$$

Far enough in the BEC limit, it is always possible to expand

the second term on the right-hand side in powers of $\Delta_{pg}/|\mu| \simeq \Delta_{pg}/\epsilon_m$ and we get

$$n = 2Zn_m(T) + |\Delta_{pg}|^2 \frac{m^2}{4\pi\hbar^3\sqrt{2m|\mu|}}, \tag{162}$$

which can be rewritten as

$$n = 2(1-Z)n_m(T) + 2Zn_m(T) = 2n_m(T). \tag{163}$$

Therefore, at sufficiently negative detuning we find a gas of thermal dressed molecules. However, we have not specified the approximation of the molecular self-energy in the molecular propagator G. To lowest order, the molecular self-energy $\hbar\Sigma_m$ is given by the expression in Eq. (83) calculated taking two free fermionic propagators $G_{\sigma,0}G_{-\sigma,0}$. In this approximation, Eq. (163) reproduces the gas of noninteracting dressed molecules as in the Nozieres-Schmitt Rink approach found in Eq. (146).

The interaction between the dressed molecules at $T \geqslant T_c$ is introduced by calculating the molecular self-energy to the lowest order in the fermionic self-energy. This requires to take one free and one dressed fermionic propagator $(G_{\sigma,0}G_{-\sigma})$ in the diagram of the molecular self-energy. Taking, in the lowest order, the self-energy in the fermionic propagator G_σ given by Eq. (156)

$$\hbar\Sigma_\sigma^f(\mathbf{k},\omega_n) \simeq -\int \frac{d^3\mathbf{k}'}{(2\pi)^3}\frac{1}{\beta\hbar^2}\sum_{\omega_{n'}} g^2 \times G(\mathbf{k}+\mathbf{k}',\omega_n+\omega_n')G_{-\sigma,0}(\mathbf{k}',\omega_n'), \tag{164}$$

the molecular propagator assumes the form

$$\hbar G^{-1}(\mathbf{K},\Omega_n) = i\hbar\Omega_n - \frac{\epsilon_\mathbf{K}}{2} + 2\mu - \delta(B) - \hbar\Sigma_m(\mathbf{K},\Omega_n) - \hbar\Delta\Sigma_m(\mathbf{K},\Omega_n). \tag{165}$$

The first-order correction $\hbar\Delta\Sigma_m$ is given by

$$\hbar\Delta\Sigma_m(\mathbf{K},\Omega_n) = \int \frac{d^3\mathbf{K}'}{(2\pi)^3}\frac{1}{\beta\hbar}\sum_{\Omega_{n'}} G(\mathbf{K}',\Omega_n') \times \Gamma_m^{\mathrm{Born}}(\mathbf{K}+\mathbf{K}',\mathbf{K}+\mathbf{K}',(\mathbf{K}+\mathbf{K}')/2, (\Omega_n+\Omega_n')/2), \tag{166}$$

with the many-body molecule-molecule vertex given by

$$\Gamma_m^{\mathrm{Born}}(\mathbf{K}+\mathbf{K}',\mathbf{K}+\mathbf{K}',(\mathbf{K}+\mathbf{K}')/2,(\Omega_n+\Omega_n')/2) = 2g^4\int \frac{d^3\mathbf{k}}{(2\pi)^3}\frac{1}{\beta\hbar^4}\sum_{\omega_n} G_{\uparrow,0}(\mathbf{K}-\mathbf{k},\Omega_n-\omega_n) \times G_{\downarrow,0}(\mathbf{k},\omega_n)G_{\uparrow,0}(\mathbf{k},\omega_n)G_{\downarrow,0}(\mathbf{K}'-\mathbf{k},\Omega_n'-\omega_n). \tag{167}$$

In the BEC limit at temperature near T_c, we have $|\epsilon_m(B)| \gg \hbar\Omega, \hbar^2\mathbf{K}^2/4m$ and $|\Delta\Sigma_m| \ll |\Sigma_m|$ and the molecular propagator of Eq (165) can be expanded around the pole of the molecular propagator without the $\hbar\Delta\Sigma_m$ correction. This gives

$$\hbar G^{-1}(\mathbf{K},\Omega_n) \simeq \frac{1}{Z}\left(i\hbar\Omega_n - \frac{\epsilon_\mathbf{K}}{2} + 2\mu - \epsilon_m(B) - Z\hbar\Delta\Sigma_m(\mathbf{K},\Omega_n)\right) \tag{168}$$

$$= \frac{1}{Z}\left(i\hbar\Omega_n - \frac{\epsilon_\mathbf{K}}{2} + \mu_m - Z\hbar\Delta\Sigma_m(\mathbf{K},\Omega_n)\right), \tag{169}$$

where we have defined the dressed-molecule chemical potential as

$$\mu_m \equiv 2\mu - \epsilon_m(B). \tag{170}$$

Furthermore, the zero momentum and zero energy correction to the molecular self-energy in Eq. (168) is given by

$$Z\hbar\Delta\Sigma_m(\mathbf{0},0) = Z\Gamma_m^{\mathrm{Born}}(\mathbf{0},\mathbf{0},\mathbf{0},0)\int \frac{d^3\mathbf{K}'}{(2\pi)^3}\frac{1}{\beta\hbar}\sum_{\Omega_{n'}} G(\mathbf{K}',\Omega_n') = \Gamma_m^{\mathrm{Born}}(\mathbf{0},\mathbf{0},\mathbf{0},0)Z^2n_m(T). \tag{171}$$

Evaluating the Matsubara summation and the momentum integral of Eq. (167) in the BEC limit where $2\mu \simeq \epsilon_m$ we find

$$Z\hbar\Delta\Sigma_m(\mathbf{0},0) = g^4\frac{m^{3/2}}{8\pi\hbar^3|\epsilon_m(B)|^{3/2}}Z^2n_m(T) = g^2\frac{1-Z}{Z|\epsilon_m(B)|}Z^2n_m(T), \tag{172}$$

where we have used the definition of Z in Eq. (158). In the case of a very broad resonance at large negative detuning, when the gas of dressed molecules enters the weak-coupling regime $k_Fa(B) \leqslant 1$ and the chemical potential is essentially equal to half the binding energy of the two-body dressed molecules, the wavefunction in Eq. (53) of the dressed molecule can still contain only a very small amplitude in the closed bare molecular channel. This means that the binding energy is in the quadratic regime in the magnetic field given by Wigner's formula $\epsilon_m \simeq -\hbar^2/ma^2(B)$ and that $Z \simeq 0$. In this case Eq. (172) can be written as

$$Z\hbar\Delta\Sigma_m(\mathbf{0},0) \simeq 2\frac{4\pi\hbar^2 2a(B)}{2m}n_m(T) \equiv 2\Gamma_m^{\mathrm{Born}}(\mathbf{0},\mathbf{0},\mathbf{0},0)n_m(T). \tag{173}$$

This term in the dressed molecular propagator of Eq. (168) represents a many-body mean-field shift of a dilute gas of molecules interacting with positive scattering length $2a(B)$.

The interaction energy of the dressed molecular gas has been measured [18] by fitting a Thomas-Fermi profiles to the spatial distributions of the trapped ultracold Fermi gas at densities of about 10^{13} cm^{-3} in the BEC limit. These experiments consider the crossover across the broad resonance at about 834 G in atomic ^{6}Li atoms. They assume, for magnetic fields between 600 and 780 G, a dilute gas of tightly bound interacting molecules. They find that the molecule-molecule scattering length is in agreement with $a_m(B) \simeq 0.6a(B)$. The origin of the value of $0.6a(B)$ has been explained by solving directly the Schrödinger equation of the four-body problem [79] and also in terms of Feynmann diagrams in [40,41] by

using a single-channel model. In the latter approach, the authors of [40,41] have identified the exact equation for the generalized molecule-molecule vertex Γ_m that contains the dominant fluctuations in the BEC limit leading to the value found in the experiment. Considering the same class of diagrams in our two-channel formulation for the vertex Γ_m introduced in Eq. (167) would also lead to a dressed molecule-molecule T matrix $\Gamma_m(\mathbf{0},\mathbf{0},\mathbf{0},0) \simeq 4\pi\hbar^2 0.6a(B)/2m$. For example, by summing over all the ladder diagrams in the particle-particle channel beyond the Born approximation described by Γ_m^{Born} we would recover the result $\Gamma_m(\mathbf{0},\mathbf{0},\mathbf{0},0) \simeq 4\pi\hbar^2 0.75a(B)/2m$ found by Pieri and Strinati in [33].

The interaction between dressed molecules introduced in Eq. (173) does not cause any shift on the critical temperature of the Bose-Einstein condensation of the dressed molecules because it does not shift the effective mass of the dressed molecules. Therefore, we have to consider the momentum and frequency dependence in the interaction vertex Γ_m^{Born} in Eq. (167). Following the analysis of the BEC limit given by Haussmann [14], we consider the ansatz

$$\hbar G^{-1}(\mathbf{K},\Omega_n) \simeq \frac{1}{ZZ_1}\left(i\hbar\Omega_n - \frac{\hbar^2\mathbf{K}^2}{4m^*} + \mu_m\right) \tag{174}$$

for the dressed-molecular propagator. The Nozieres-Schmitt Rink approximation corresponds clearly to the case $Z_1=1$ and $m^*=m$. To find the first-order corrections to Z_1 and m^*, we substitute the ansatz of Eq. (174) in Eqs. (166)–(168), we perform the frequency sum and the momentum integral in Eq. (167), and finally we expand the resulting expression up to the first order in $\mathbf{K}^2$ and Ω_n. Ultimately, in the case of a broad resonance, we find [14]

$$m^* \simeq m\{1 + 2\pi[n_m a(B)^3]\}, \tag{175}$$

$$Z_1 \simeq 1 + 6\pi n_m a(B)^3, \tag{176}$$

$$\mu_m \simeq 2\Gamma_m^{\mathrm{Born}}(\mathbf{0},\mathbf{0},\mathbf{0},0) n_m(T). \tag{177}$$

The critical temperature in the BEC limit is determined by the equation of state. For a broad resonance, one generally has still $Z \simeq 0$ when the gas enters the BEC limit of the crossover. In that case, the number of particles in the equation of state of Eq. (155) is determined mainly by the fermionic Green's function

$$n \simeq \frac{1}{\hbar\beta V}\sum_{\sigma} \mathrm{Tr}[G_{\sigma,0}]. \tag{178}$$

The evaluation of this term given in Eq. (163) is calculated by taking for the fermionic propagator G_σ only the zeroth- and first-order correction in the self-energy into account. Expanding the fermionic Green's function up to the second order in its self-energy, one can show [14] that the result of Eq. (163) is modified as

$$n \simeq -\frac{1}{Z_1} 2 \frac{1-Z}{Z} \frac{1}{\hbar\beta V} \mathrm{Tr}[G] \simeq -\frac{1}{Z_1} 2 \frac{1}{Z} \frac{1}{\hbar\beta V} \mathrm{Tr}[G]. \tag{179}$$

Substituting in this equation the propagator of Eq. (174) the Z and Z_1 factors drop out. Therefore the equation of state describes effectively an ideal gas of dressed molecules with renormalized mass m^*. The critical temperature is calculated from the relation

$$n \simeq 2n_m(T) = \int \frac{d^3\mathbf{K}}{(2\pi)^3} N_B\left(\frac{\hbar^2\mathbf{K}^2}{4m^*}\right) = 2\zeta(3/2) \times (2m^* k_B T_c/2\pi\hbar^2). \tag{180}$$

This leads to the negative shift of the critical temperature T_c with respect to the ideal Bose-Einstein critical temperature T_{BEC}

$$\Delta T_c/T_{\mathrm{BEC}} = m/m^* - 1 = -\frac{1}{(3\pi)[k_F a(B)]^3} \tag{181}$$

found by Haussmann.

Although the above self-consistent calculation is more general than the Nozieres-Schmitt Rink approximation, we believe that the correct theory should lead to a positive shift and then to a maximum in the curve of T_c. In fact, according to the theory of dilute weakly interacting Bose gases [124–126], the repulsive interactions between the molecules in the asymptotic BEC limit are expected to enhance the value of the critical temperature. The physical origin of this maximum, therefore, is clearly different than that described by the Nozieres-Schmitt Rink approach, as the latter neglects the interactions between the noncondensed molecules.

V. BEC-BCS CROSSOVER BELOW T_c

In this section, we consider the BEC-BCS crossover in the broken symmetry state. The Gross-Pitaevskii theory at $T=0$ of the dressed-molecule condensate and the Bogoliubov theory at nonzero temperature are derived in the BEC limit by means of analytical methods. As before, the single-channel results are derived as a special case in the limit of very broad resonances. Moreover, the relation between the composite boson of the single-channel model and the dressed-molecule of the two-channel model is clearly formulated.

A. Mean-field theory at $T=0$

At $T=0$ a set of two self-consistent equations for the BCS energy gap and the chemical potential can be derived generalizing the variational approach introduced by Leggett [11] to our two-channel atom-molecule Hamiltonian given by Eq. (20). The zero-temperature ground state can be written [58] as a product state of both a bare molecular and an atomic contribution, i.e.,

$$|\Psi_0\rangle = |\Phi_0^F\rangle \otimes |\Phi_0^B\rangle, \tag{182}$$

where the normalized fermionic wavefunction is the standard crossover ground state [10,11]

$$|\Phi_0^F\rangle = \prod_{\mathbf{k}>0} (u_\mathbf{k} + v_\mathbf{k} c_k^\dagger c_{-k}^\dagger)|0\rangle, \tag{183}$$

and the normalized bare molecular contribution $|\Phi_0^B\rangle$ is given by

$$|\Phi_0^B\rangle = e^{-n_0/2+\sqrt{n_0}b_0^\dagger}|0\rangle. \tag{184}$$

The real variational parameters are $u_\mathbf{k}$, $v_\mathbf{k}$, and $\sqrt{n_0}$. Minimizing the grand-canonical energy with respect to the parameter $\sqrt{n_0}$, we find the constraint

$$\langle b_0\rangle \equiv \sqrt{n_0} = \frac{g_{\text{bare}}\Delta_{\text{bg}}}{(\delta_{\text{bare}} - 2\mu)\mathrm{V}_{\text{bg}}}, \tag{185}$$

where Δ_{bg} is the order parameter related to the attractive background interaction

$$\Delta_{\text{bg}} \equiv -\frac{1}{V}\sum_\mathbf{k} \mathrm{V}_{\text{bg}} u_\mathbf{k} v_\mathbf{k} = -\frac{1}{V}\sum_\mathbf{k} \mathrm{V}_{\text{bg}} \langle a_{-\mathbf{k}\downarrow} a_{\mathbf{k}\uparrow}\rangle. \tag{186}$$

The variation with respect to $v_\mathbf{k}$, under the normalization constraint $v_\mathbf{k}^2 + u_\mathbf{k}^2 = 1$, yields

$$u_\mathbf{k}^2 = \frac{1}{2}\left(1 + \frac{\epsilon_\mathbf{k} - \mu}{\sqrt{(\epsilon_\mathbf{k} - \mu)^2 + |\Delta|^2}}\right),$$

$$v_\mathbf{k}^2 = \frac{1}{2}\left(1 - \frac{\epsilon_\mathbf{k} - \mu}{\sqrt{(\epsilon_\mathbf{k} - \mu)^2 + |\Delta|^2}}\right), \tag{187}$$

where the total gap of the theory Δ is defined as

$$\Delta = \Delta_{\text{bg}} - g_{\text{bare}}\sqrt{n_0}. \tag{188}$$

Substituting these results in the definition in Eq. (186) and using the constraint in Eq. (185), we arrive at the gap equation in the compact form

$$-\frac{1}{\mathrm{V}_{\text{bg}} - \dfrac{g_{\text{bare}}^2}{\delta_{\text{bare}} - 2\mu}} = \frac{1}{V}\sum_\mathbf{k} \frac{1}{2\sqrt{(\epsilon_\mathbf{k} - \mu)^2 + |\Delta|^2}}. \tag{189}$$

This equation can be rewritten in terms of the renormalized quantities as

$$-\frac{1}{\mathrm{T}_{\text{bg}}^{2\text{B}} - \dfrac{g^2}{\delta - 2\mu}} = \frac{1}{V}\sum_\mathbf{k}\left(\frac{1}{2\sqrt{(\epsilon_\mathbf{k} - \mu)^2 + |\Delta|^2}} - \frac{1}{2\epsilon_\mathbf{k}}\right), \tag{190}$$

where now

$$\Delta \equiv \Delta_{\text{bg}} - g\sqrt{n_0} \tag{191}$$

and

$$\Delta_{\text{bg}} = \frac{\sqrt{n_0}(\delta - 2\mu)\mathrm{T}_{\text{bg}}^{2\text{B}}}{g}, \tag{192}$$

as a consequence of the general result for the many-body T matrix in Eq. (33), combined with the fact that the gap equation in Eq. (190) must be equivalent to a sum over all ladder diagrams. The description of the BEC-BCS crossover at the mean-field level of approximation is completed by the equation of state

$$n = 2n_0 + \int \frac{d^3\mathbf{k}}{(2\pi)^3}\left(1 - \frac{\epsilon_\mathbf{k} - \mu}{\sqrt{|\Delta|^2 + (\epsilon_\mathbf{k} - \mu)^2}}\right). \tag{193}$$

Equations (190)–(193) represent a set of coupled equations in Δ and μ at fixed density. Note that in contrast to the normal-state result, the analysis at zero temperature in the broken symmetry state does not require any modification of the equation of state in order to get the proper two-body physics of the dressed molecules in the BEC limit. This is because the equation of state of BCS mean-field theory at $T=0$ sums automatically over the ladder diagrams. As a result, we expect also to have smooth crossover curves for Δ and μ already at the mean-field level.

At positive detuning, in the weak-coupling regime $k_F|a(B)| \lesssim 1$, the binding is a cooperative effect in the

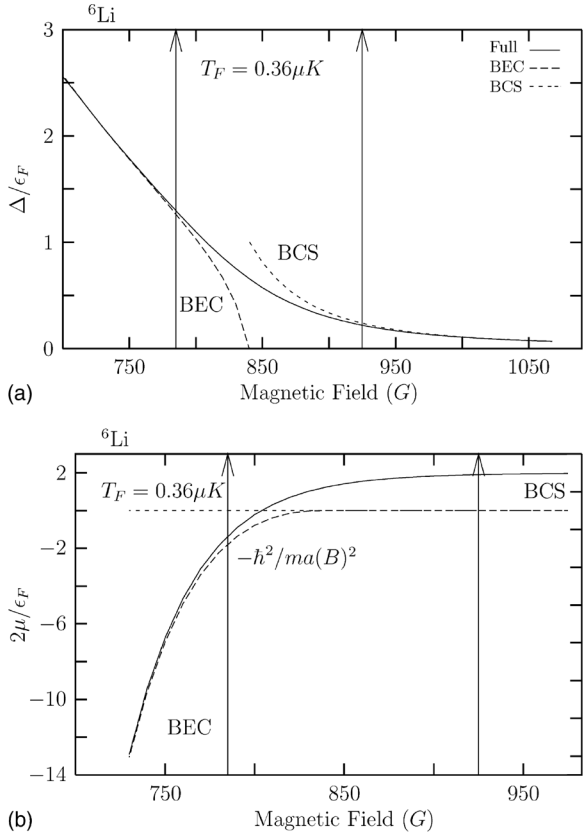

FIG. 21. BCS energy gap (a) and chemical potential (b) as a function of the magnetic field for the very broad resonance at 834 G in a ^{6}Li mixture at low density. Full lines are obtained by solving numerically the crossover equations of Eqs. (190)–(193) or equivalently by Eqs. (197) and (198). Both quantities are rescaled in unit of the Fermi energy of the noninteracting Fermi mixture. In (a), the dashed line called "BEC" shows the aymptotic BEC limit of the energy gap given by $\Delta = \sqrt{(16/3\pi)}\epsilon_F/\sqrt{k_F a(B)}$, while the dotted line called "BCS" describes the BCS asymptotic solution given by Eq. (194). In (b) the dashed line shows the two-body binding energy $\epsilon_\text{m} \simeq \hbar^2/ma(B)^2$. The region inside the two vertical arrows represents the strong-coupling regime $k_F|a(B)| > 1$.

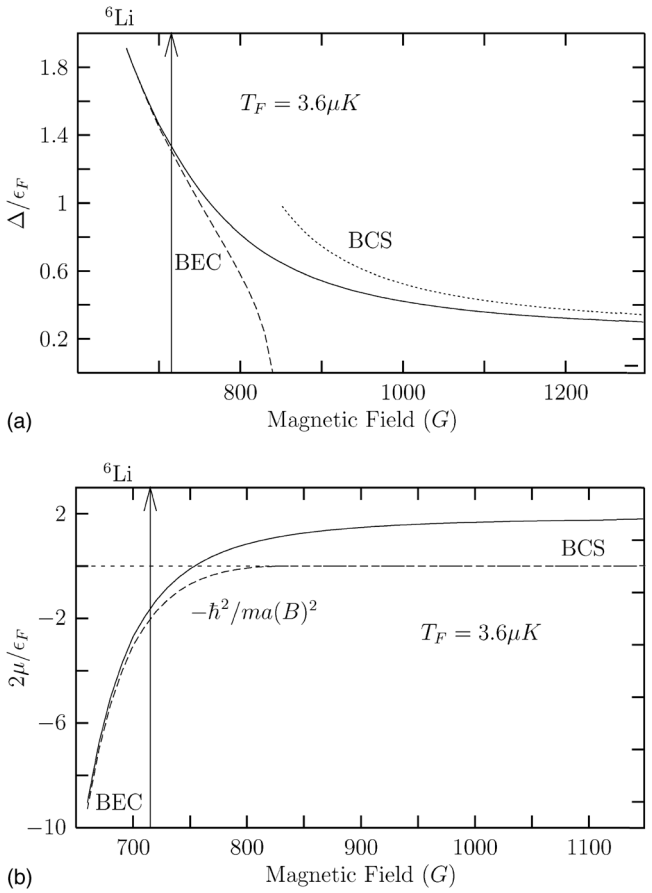

FIG. 22. BCS energy gap (a) and chemical potential (b) as a function of the magnetic field for the very broad resonance at 834 G in a ^{6}Li mixture at high density. Full lines are obtained by solving numerically the crossover equations of Eqs. (190)–(193) or equivalently by Eqs. (197) and (198). Both quantities are rescaled in unit of the Fermi energy of the noninteracting Fermi mixture. In (a), the dashed line called "BEC" shows the aymptotic BEC limit of the energy gap given by $\Delta=\sqrt{(16/3\pi)}\epsilon_F/\sqrt{k_F a(B)}$, while the dotted line called "BCS" describes the BCS asymptotic solution given by Eq. (194). In (b) the dashed line shows the two-body two-body binding energy $\epsilon_m \simeq \hbar^2/ma(B)^2$. The vertical arrow at negative detuning indicates the value of the magnetic field for which $k_F a(B)=1$. Note that due to the large background scattering length a_{bg} of the ^{6}Li atoms, at high density, the gas never enters the weak-coupling regime $k_F a(B)<-1$ at positive detuning.

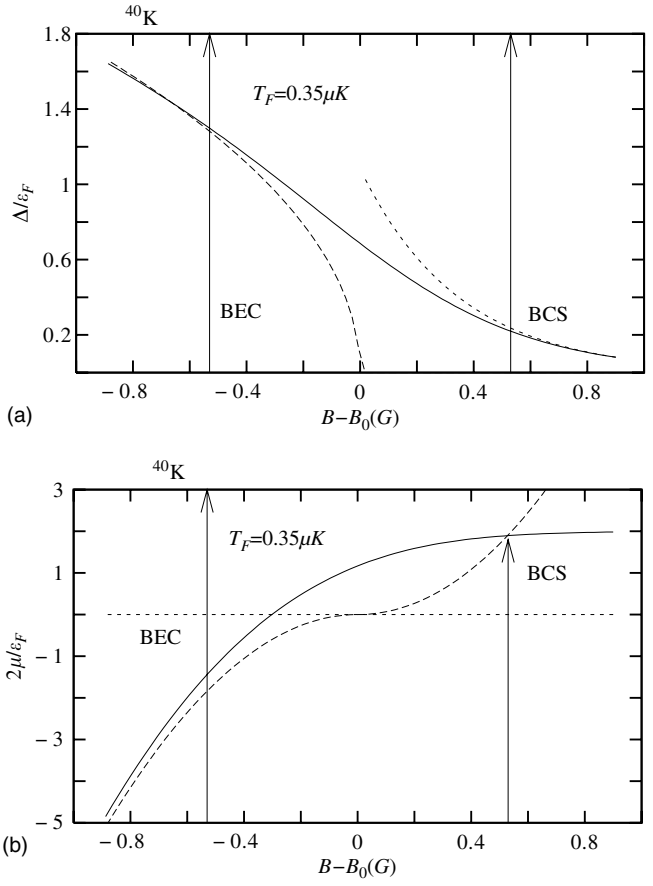

FIG. 23. BCS energy gap (a) and chemical potential (b) as a function of the magnetic field for the broad resonance at 202.1 G in a ^{40}K mixture at low density. Full lines are obtained by solving numerically the crossover equations of Eqs. (190)–(193) or equivalently by Eqs. (197) and (198). Both quantities are rescaled in unit of the Fermi energy of the noninteracting Fermi mixture. In (a), the dashed line called "BEC" shows the aymptotic BEC limit of the energy gap given by $\Delta=\sqrt{(16/3\pi)}\epsilon_F/\sqrt{k_F a(B)}$, while the dotted line called "BCS" describes the BCS asymptotic solution given by Eq. (194). In (b) the dashed line shows the two-body two-body binding energy $\epsilon_m \simeq \hbar^2/ma(B)^2$. The curve for the two-body binding energy is continued at positive detuning by the location of the maximum in the molecular density of states given in Eq. (58). The region inside the two vertical arrows represents the strong-coupling regime $k_F|a(B)|>1$. Note the at positive magnetic field, the condition $k_F a(B)=-1$ coincides with the magnetic field where the energy of the maximum in the density of states of the molecules is equal to twice the Fermi energy of the atoms. Significantly, this value of the magnetic field coincides also with the value where, in the experiment at Jila of [15], the condensation of pairs begins to be observed.

vicinity of the Fermi surface. The gas consists of largelyoverlapping weakly bound Cooper pairs. The chemical potential is fixed at $\mu=\epsilon_F$ by the equation of state in Eq. (193). The solution of Eq. (190) is then easy calculated analytically with the result

$$\Delta \simeq 8\epsilon_F e^{-2} e^{\frac{2}{\pi}\frac{\sqrt{2\mu}}{\eta}} \exp\left\{-\frac{\pi}{2k_F|a(B)|}\right\}. \qquad (194)$$

The energy gap is related to the BCS critical temperature (131) by the relation $k_B T_c=(e^\gamma/\pi)\Delta$, as is expected for weak-coupling superconductivity. Note that the energy gap of Eq. (194) coincides formally with the shift in the ground-state energy of Eq. (97). This is not surprising because the singularity in the molecular self-energy discussed in Sec. III F and the Cooper pairing occur in the same diagram.

At negative detuning, the system evolves to a Bose-Einstein condensate of tightly bound dressed molecules. The roles of the gap equation and the number equation are exchanged. In the BEC limit, the chemical potential becomes large and negative. The crossover equations then can be expanded in powers of $|\Delta|/|\mu|$ as

$$\frac{1}{\mathrm{T}_{\mathrm{bg}}^{2\mathrm{B}} - \dfrac{g^2}{\delta - 2\mu}} = \left(\frac{2m}{\hbar^2}\right)^{3/2} \frac{\sqrt{|\mu|}}{8\pi}\left(1 + \frac{1}{16}\frac{|\Delta|^2}{\mu^2}\right) \tag{195}$$

and

$$n = 2n_0 + |\Delta|^2 \frac{m^2}{4\pi\sqrt{2m|\mu|}\hbar^3}. \tag{196}$$

Neglecting the term quadratic in $|\Delta|/|\mu|$, Eq. (195) becomes equivalent to Eq. (142). Thus the chemical potential approaches half the binding energy of Eq. (47) of a Bose-Einstein condensed dressed molecule, as expected.

The curves for μ and Δ obtained by solving numerically the mean-field crossover Eqs. (190)–(193) are shown in Figs. 21 and 22 for a gas of ^{6}Li atoms at two different densities and in Fig. 23 for a gas of ^{40}K atoms. In both cases we have $\eta^2 \gg \epsilon_F$. In each figure the vertical lines represent the boundary of the strong coupling regime $k_F|a(B)| > 1$. In the ^{6}Li gas with the high density of Fig. 22, the gas never enters the weak-coupling regime $k_F|a(B)| < 1$ in the range of the magnetic field considered in the figure.

The mean-field curves for Δ and μ do not differ quantitatively from the solutions obtained by the single-channel approximation [11,13] based on the equations

$$-\frac{1}{\mathrm{T}_{\mathrm{bg}}^{2\mathrm{B}} - \dfrac{g^2}{\delta}} = -\frac{1}{\dfrac{4\pi\hbar^2 a(B)}{m}} = \frac{1}{V}\sum_{\mathbf{k}}\left(\frac{1}{2\sqrt{(\epsilon_{\mathbf{k}} - \mu)^2 + |\Delta_{\mathrm{sc}}|^2}} - \frac{1}{2\epsilon_{\mathbf{k}}}\right), \tag{197}$$

and

$$n = \int \frac{d^3\mathbf{k}}{(2\pi)^3}\left(1 - \frac{\epsilon_{\mathbf{k}} - \mu}{\sqrt{|\Delta_{\mathrm{sc}}|^2 + (\epsilon_{\mathbf{k}} - \mu)^2}}\right), \tag{198}$$

where the single-channel gap is defined as $\Delta_{\mathrm{sc}} \equiv \langle (\mathrm{V}_{\mathrm{bg}} + \mathrm{V}_{\mathrm{res}})\psi_\uparrow(\mathbf{x})\psi_\downarrow(\mathbf{x})\rangle$. These equations are obtained from Eqs. (190) and (193) neglecting explicitly the contribution of the bare molecular boson. They can be derived also by integrating out the molecular field in the action of Eq. (60) from the very beginning.

At negative detuning the chemical potential goes to half the binding energy $\epsilon_{\mathrm{m}} \simeq -\hbar^2/ma^2(B)$ described in Figs. 21(b), 22(b), and 23(b) by dotted lines. In Fig. 23(b) the curve of the binding energy of the dressed molecules is continued at positive detuning by the location of the maximum in the molecular density of states given in Eq. (58). This illustrates the main idea of our modified mean-field picture of Sec. IV A. The magnetic field at which this curve crosses 2μ is indicated by a vertical line. At this magnetic field the energy of the two-body dressed molecules approaches the chemical potential of the gas [49].

In Figs. 21–23 the dotted lines represent the two extreme limits of the crossover. The lines denoted as BCS correspond to the BCS solution of Eq. (190). The lines denoted as BEC correspond to the curve $\Delta = \sqrt{(16/3\pi)}\epsilon_F/\sqrt{k_F a(B)}$, which is the asymptotic solution for the energy gap according to the single-channel gap equation in Eq. (197).

B. Asymptotic limit of Z in the deep BEC limit

The analysis of the equation of state in the BEC limit requires some special consideration. The correct picture of the crossover across the Feshbach resonance is based on the dressed molecule, which is the true energy eigenstate of the diatomic molecule in the presence of the atom-molecule coupling. Unfortunately, however, the dressed molecule density does not appear explicitly in the coupled equations of our mean-field treatment and mean-field theory is therefore not able to extract this quantity.

Nevertheless, a gas of weakly interacting closed-channel bare molecules is realized at sufficiently large negative detunings. More precisely, denoting the condensate of bare molecules by n_0, the total density amounts to

$$n \simeq 2n_0 \tag{199}$$

when $k_F a(B) \leqslant 1$ and $|\delta(B)| \geqslant \hbar^2/ma_{\mathrm{bg}}^2$. For less negative detunings we must use [57]

$$n_0 = Zn_{\mathrm{mc}}, \tag{200}$$

where n_{mc} is defined as the condensate density of the dressed molecules. A careful analysis of the equation of state in Eq. (196) shows that this definition is indeed consistent. The proof proceeds as follows. First we assume that in the deep BEC limit the total density can be approximated by the density of the dressed molecules, instead of bare molecules as in Eq. (199),

$$n \simeq 2n_{\mathrm{mc}}, \tag{201}$$

with binding energy $\epsilon_{\mathrm{m}} \simeq 2\mu$ given by Eq. (47). Then, we eliminate the explicit dependence on δ and Δ_{bg} by using Eqs. (192) and (142), to rewrite the equation of state as

$$2n_{\mathrm{mc}} \simeq 2Zn_{\mathrm{mc}} + \frac{2Zn_{\mathrm{mc}}\eta}{2\sqrt{|\epsilon_{\mathrm{m}}|}\left(1 + \sqrt{\dfrac{|\epsilon_{\mathrm{m}}|}{\epsilon_{bg}}}\right)^2}. \tag{202}$$

Solving for Z we recover the correct two-body limit expression of Eq. (52), i.e.,

$$Z = \left(1 + \frac{\eta}{2\sqrt{|\epsilon_{\mathrm{m}}|}\left(1 + \sqrt{\dfrac{|\epsilon_{\mathrm{m}}|}{\epsilon_{bg}}}\right)^2}\right)^{-1}.$$

Putting back this Z in the equation of state we find again Eq. (201).

It is important to stress the fact that the approximation introduced in Eq. (201) is valid only deep in the BEC limit of strongly bound dressed molecules. This can be understood as follows. According to the BCS theory, at zero temperature all the atoms are paired far below resonance. In our case we have a gas of dressed molecules which have an amplitude to be in the open-channel Cooper pairs wavefunction and on the bare closed-channel molecular bound state. However, even at

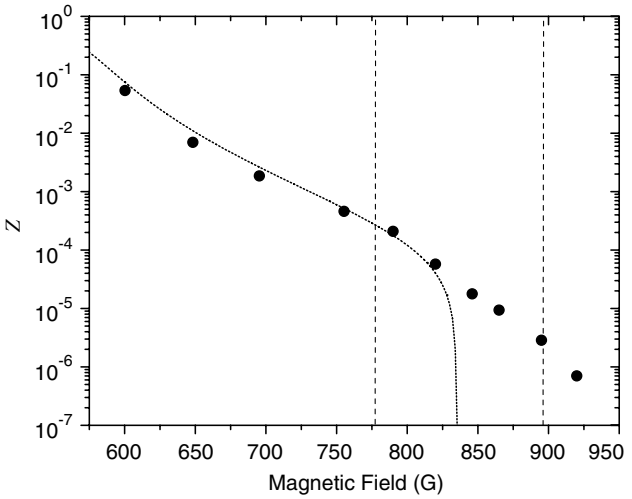

FIG. 24. The value of Z measured in [20] is plotted as function of the magnetic field (dots). The continous line represents the two-body Z given by Eq. (52). The vertical dashed lines represent the boundary of the strong coupling regime $k_F|a(B)|>1$. Below 800 Gauss, we have $2\mu \simeq \epsilon_m$ and the two-body Z matches perfectly with the experimental value. The Fermi energy of the gas is at $T_F = 380nK$.

zero temperature not all the dressed molecules are condensed because interactions deplete the condensate density as the interactions between the Cooper pairs do in the zero-temperature BCS theory. Therefore, Eq. (201) neglects the depletion of the dressed-molecules condensate and is correct only asymptotically in the deep BEC limit when the depletion decreases progressively because the gas becomes more and more dilute.

This means that Eq. (201) is valid only at magnetic fields such that $k_F a(B) \leqslant 1$, when the many-body part of the BEC-BCS crossover has already taken place, and where the chemical potential approaches half the molecular two-body binding energy in Eq. (47). When $k_F|a(B)| \geqslant 1$, the fluctuations in the atomic fields become important and also at $T=0$ the gas cannot be approximated only by a condensate of dressed molecules [57]. As a result, the bare molecular probability Z is not given by $2n_0/n$ [60,127] as in the asymptotic BEC limit. Moreover, Z deviates from its two-body expression of Eq. (52) and the two mean-field equations are not sufficient to calculate its value, because they cannot calculate the depletion of condensate of the dressed-molecules. A more refined approach is needed beyond the saddle-point solution [57]. The quantity Z has been recently measured by Partridge *et al.* [20]. Their data are illustrated in Fig. 24. The experimental data in the BEC limit are in very good agreement with our two-body Z of Eq. (52).

C. Gross-Pitaevskii theory of the dressed-molecule condensate at $T=0$

We show in this section that, in contrast to the normal-state analysis, the Born interactions between the dressed molecules in the BEC limit of the crossover described in the previous section arise already at the mean-field level based on Eqs. (190) and (193). The effective chemical potential for a dilute weakly interacting gas of dressed molecules, is defined, at the leading order, as

$$\mu_m \equiv \frac{4\pi\hbar^2 a_m^{\text{Born}} n_{mc}}{m_m}, \tag{203}$$

where a_m is scattering length of two dressed molecules with mass $m_m = 2m$. The quantity μ_m is given by

$$\mu_m = 2\mu - \epsilon_m, \tag{204}$$

where 2μ is calculated retaining the quadratic term $|\Delta|^2/|\mu|^2$ in the gap equation in Eq. (195). Using Eqs. (200) and (201) and that $2\mu \simeq \epsilon_m$, the gap equation in Eq. (195) can be rewritten as

$$\epsilon_m = 2\mu + n_{mc}\frac{4\pi\hbar^2 a_{\text{eff}}(B)}{m} Z \frac{\eta}{2\sqrt{|\epsilon_m|}\left(1+\sqrt{\frac{|\epsilon_m|}{\epsilon_{bg}}}\right)^2} + O\left(\left(\frac{\Delta}{2\mu}\right)^4\right), \tag{205}$$

or

$$\mu_m \simeq n_{mc}\frac{4\pi\hbar^2 a_{\text{eff}}(B)}{m} Z \frac{\eta}{2\sqrt{|\epsilon_m|}\left(1+\sqrt{\frac{|\epsilon_m|}{\epsilon_{bg}}}\right)^2}, \tag{206}$$

where the binding energy ϵ_m is given by the general solution of Eq. (47), and the quantity a_{eff} has the dimensions of a length and is given by

$$a_{\text{eff}}(B) \equiv \frac{\hbar}{\sqrt{m|\epsilon_m|}}. \tag{207}$$

Using in Eq. (205) the definition of Z in Eq. (52), we find for the effective chemical potential of the dressed molecules at the mean-field level

$$\mu_m \simeq n_{mc}\frac{4\pi\hbar^2}{m_m} 2a_{\text{eff}}(B)(1-Z), \tag{208}$$

which implies

$$a_m^{\text{Born}} = 2a_{\text{eff}}(B)(1-Z). \tag{209}$$

However, for very broad resonances such as that at 834 G in the ^{6}Li gas, when the gas enters the weak-coupling regime $k_F a(B) \leqslant 1$, the wavefunction in Eq. (53) of the dressed molecule still contains only a very small amplitude in the closed bare molecular channel. This implies that the dependence of the binding energy on the magnetic field is still in the quadratic regime by Wigner's formula $\epsilon_m \simeq -\hbar^2/ma^2(B)$. Therefore, in this regime Eq. (208) can be approximated as

$$\mu_m \simeq n_{mc}\frac{4\pi\hbar^2}{m_m} 2a(B)(1-Z). \tag{210}$$

This result is equivalent to that of a Gross-Pitaevskii theory [128,129] for a gas of Bose-Einstein condensed dressed molecules interacting with an effective scattering length

$$a_{\mathrm{m}}^{\mathrm{Born}} \simeq 2a(B)(1-Z). \tag{211}$$

Because in this regime we have $Z \simeq 0$, however, the scattering length between the dressed molecules in the Born approximation and in the mean-field approximation is given essentially by

$$a_{\mathrm{m}}^{\mathrm{Born}} \simeq 2a(B). \tag{212}$$

Such a situation is typical of a very broad resonance.

D. Dressed molecules versus composite bosons

Our derivation in the previous section, has to be considered as an extension of the mean-field analysis of the BEC limit for a single-channel model crossover discussed by Sa de Melo *et al.* in [13] (see also [25]) based on Eqs. (197) and (198). In the mean-field single-channel model the Cooper pairs evolve in the BEC limit toward a dilute gas of weakly interacting *composite bosons* with scattering length $2a(B)$. In the BEC limit, the equation of state of the mean-field single-channel model at zero temperature can be approximated by [14,34,36]

$$n \simeq \frac{m^2 a(B)}{4\pi\hbar^4}|\Delta_{\mathrm{sc}}|^2. \tag{213}$$

The composite boson condensate Ψ_0^B of the single-channel model is defined from [14,34,36]

$$\Delta_{\mathrm{sc}} \equiv \sqrt{\frac{8\pi\hbar^4}{m^2 a(B)}}\Psi_0^B \tag{214}$$

such that the BEC limit of Eq. (213) is characterized by a gas of composite bosons

$$n \simeq 2|\Psi_0^B|^2. \tag{215}$$

The equation of state in Eq. (213) must be compared with its two-channel analogue in the BEC regime where $2\mu \simeq \epsilon_{\mathrm{m}}$. We have

$$n \simeq 2n_0 + |\Delta|^2 \frac{m^2}{4\pi\sqrt{2m|\mu|}\hbar^3} = 2Zn_{\mathrm{mc}} + \frac{2Zn_{\mathrm{mc}}\eta}{2\sqrt{|\epsilon_{\mathrm{m}}|}\left(1+\sqrt{\frac{|\epsilon_{\mathrm{m}}|}{\epsilon_{bg}}}\right)^2}$$

$$= 2n_{\mathrm{mc}}. \tag{216}$$

Moreover, for a very broad resonance, we have $2\mu \simeq \epsilon_{\mathrm{m}} \simeq -\hbar^2/ma^2(B)$ and $Z \simeq 0$. Therefore we have $\epsilon_{\mathrm{m}} \ll \epsilon_{\mathrm{bg}}$, and we find

$$g^2 Z \simeq g^2 \frac{2\sqrt{|\epsilon_{\mathrm{m}}|}}{\eta} = \frac{8\pi\hbar^4}{m^2 a(B)}. \tag{217}$$

This relation between the residues of the poles associated with the composite boson and with the dressed molecule of the two-channel model in the case of a very broad resonance can now be better understood if we remember the physical meaning of Z [47] and of $8\pi\hbar^4/m^2a(B)$ [14,34,36]. The factor $8\pi\hbar^4/m^2a(B)$ reflects the difference between the bosonic propagator of the single-channel composite boson and the particle-particle ladder propagator in Eq. (78) in the BEC limit. In that limit we have $2|\mu| \simeq |\hbar^2/ma(B)^2| \gg k_B T$ and the latter can be approximated as

$$\hbar G_\Delta^{-1}(\mathbf{K},\Omega_n) = \mathrm{T}_{\mathrm{MB}}^{-1}(\mathbf{K},\Omega_n) \simeq \frac{m}{4\pi\hbar^2}\left(\frac{1}{a(B)} - \sqrt{\frac{m}{\hbar^2}}\sqrt{-i\hbar\Omega_n + \frac{\hbar^2\mathbf{K}}{4m} - 2\mu}\right). \tag{218}$$

Expanding for small $a(B)$ this can be rewritten in the *polar* form [36]

$$G_\Delta(\mathbf{K},\Omega_n)/\hbar = \mathrm{T}^{\mathrm{MB}}(\mathbf{K},\Omega_n) \simeq \frac{8\pi\hbar^4}{m^2 a(B)}\frac{1}{i\hbar\Omega_n - \frac{\hbar^2\mathbf{K}}{4m} - \mu_{CB}}, \tag{219}$$

where the chemical potential of the composite boson is defined as $\mu_{\mathrm{CB}} = 2\mu - \hbar^2/ma(B)^2$ and can be calculated from the single-channel gap equation (197) in the BEC limit. We find [14,36]

$$\mu_{\mathrm{CB}} \simeq \frac{4\pi\hbar^2 2a(B)}{2m} \simeq \frac{|\Delta_{\mathrm{sc}}|^2}{4|\mu|}. \tag{220}$$

To be rigorous, we should have considered the particle-particle ladder propagator in the superfluid state. However, in the BEC limit, $\hbar\Omega_n$, $\hbar^2\mathbf{K}/4m$, and μ_{CB} are of the same order or smaller than $\hbar^2/ma(B)^2$. Therefore the mean-field inverse particle-particle propagator $\hbar G_\Delta^{-1}$, up to the first order in $\hbar\Omega_n$ and $\hbar^2\mathbf{K}/4m$, is the same as in the normal state.

The factor Z reflects the difference between the bare and the dressed molecule [47]. The full molecular propagator in Eq. (82)

$$\hbar G^{-1}(\mathbf{K},\Omega_n) = i\hbar\Omega_n - \frac{\hbar^2\mathbf{K}}{4m} + 2\mu - \delta(B) - \frac{1}{V}\sum_{\mathbf{k}} |g^{2\mathrm{B}}(0,2\epsilon_{\mathbf{k}})|^2 \left(\frac{1 - N_{\mathbf{K}/2+\mathbf{k}} - N_{\mathbf{K}/2-\mathbf{k}}}{i\hbar\Omega_n + 2\mu - 2\epsilon_{\mathbf{k}} - \epsilon_{\mathbf{K}}/2} + \frac{1}{2\epsilon_{\mathbf{k}}}\right), \tag{221}$$

can be approximated in the BEC regime, where $2\mu \simeq \epsilon_{\mathrm{m}} \simeq -\hbar^2/ma^2(B)$ and $Z \simeq 0$, as

$$\hbar G^{-1}(\mathbf{K},\Omega_n) = i\hbar\Omega_n - \frac{\hbar^2\mathbf{K}}{4m} + 2\mu - \delta(B) - \frac{1}{V}\sum_{\mathbf{k}} |g^{2\mathrm{B}}(0,2\epsilon_{\mathbf{k}})|^2 \left(\frac{1}{i\hbar\Omega_n + 2\mu - 2\epsilon_{\mathbf{k}} - \epsilon_{\mathbf{K}}/2} + \frac{1}{2\epsilon_{\mathbf{k}}}\right). \tag{222}$$

However, for broad resonances, in this limit we have also that $|\delta(B)| \gg 2|\mu|$, $\hbar^2\mathbf{K}/4m$, and $\hbar\Omega_n$, $\hbar^2\mathbf{K}/4m \ll \hbar\Sigma(\mathbf{K},\Omega_n)$

. Therefore, we can approximate the dressed-molecular propagator further as

$$\hbar G^{-1}(\mathbf{K},\Omega_n) \simeq -\delta(B) - \frac{1}{V}\sum_{\mathbf{k}} |g^{2B}(0,2\epsilon_{\mathbf{k}})|^2 \left(\frac{1}{i\hbar\Omega_n + 2\mu - 2\epsilon_{\mathbf{k}} - \epsilon_{\mathbf{K}/2}} + \frac{1}{2\epsilon_{\mathbf{k}}} \right). \tag{223}$$

Calculating the integral this can be rewritten as

$$\hbar G^{-1}(\mathbf{K},\Omega_n) \simeq \frac{1}{g^2}\frac{m}{4\pi\hbar^2}\left(\frac{1}{a(B)} - \sqrt{\frac{m}{\hbar^2}}\sqrt{-i\hbar\Omega_n + \frac{\hbar^2\mathbf{K}}{4m} - 2\mu} \right) \tag{224}$$

from which, expanding as in Eq. (223), we obtain

$$\hbar^{-1}G(\mathbf{K},\Omega_n) \simeq \frac{1}{g^2}\frac{8\pi\hbar^4}{m^2 a(B)}\frac{1}{i\hbar\Omega_n - \frac{\hbar^2\mathbf{K}}{4m} - \mu_{\mathrm{m}}}, \tag{225}$$

where $\mu_{\mathrm{m}} = \mu_{\mathrm{CB}}$. However, expanding Eq. (223) around the real pole at $\epsilon_{\mathrm{m}} \simeq \hbar^2/ma^2(B)$ the propagator can also be written as

$$\hbar^{-1}G(\mathbf{K},\Omega_n) \simeq Z(B)\frac{1}{i\hbar\Omega_n - \frac{\hbar^2\mathbf{K}}{4m} - \mu_{\mathrm{m}}}. \tag{226}$$

Comparing Eqs. (225) and (226) we find again the relation in Eq. (217). Our above analysis is based on a mean-field approach and due to this reason the propagators of Eq. (225) and (219) describe free bosons. This is because we are considering only the bosonic propagators only up to first order in $\hbar\Omega_n$ and $\hbar^2\mathbf{K}/4m$.

E. Gaussian fluctuations around the saddle-point solution

In order to obtain in the BEC limit a superfluid of interacting bosons, we have to extend our analysis beyond the saddle-point approximation. The nonzero temperature molecular propagator in the broken-symmetry state at the level of Gaussian fluctuations can be approximated in the BEC limit by the matrix

$$-\hbar\mathbf{G}^{-1} \simeq \begin{pmatrix} -i\hbar\omega_n - 2\mu + \epsilon_{\mathbf{K}}/2 + \delta(B) & 0 \\ 0 & i\hbar\omega_n - 2\mu + \epsilon_{\mathbf{K}}/2 + \delta(B) \end{pmatrix} + \begin{pmatrix} \hbar\Sigma_{11}(\mathbf{K},\omega_n) & \hbar\Sigma_{12}(\mathbf{K},\omega_n) \\ \hbar\Sigma_{21}(\mathbf{K},\omega_n) & \hbar\Sigma_{22}(\mathbf{K},\omega_n) \end{pmatrix}, \tag{227}$$

where the molecular self-energies are given by [57]

$$\hbar\Sigma_{11}(\mathbf{q},i\omega_n) \simeq \frac{g^2}{1+|a_{\mathrm{bg}}|\sqrt{-2\mu}}\frac{1}{V}\sum_{\mathbf{k}}\left(\frac{u_{\mathbf{k}}^2 u_{\mathbf{k}-\mathbf{q}}^2}{i\hbar\omega_n - \hbar\omega_{\mathbf{k}} - \hbar\omega_{\mathbf{k}-\mathbf{q}}} - \frac{v_{\mathbf{k}}^2 v_{\mathbf{k}-\mathbf{q}}^2}{i\hbar\omega_n + \hbar\omega_{\mathbf{k}} + \hbar\omega_{\mathbf{k}-\mathbf{q}}} + \frac{1}{2\epsilon_{\mathbf{k}}} \right),$$

$$\hbar\Sigma_{12}(\mathbf{q},i\omega_n) \simeq \frac{g^2}{1+|a_{\mathrm{bg}}|\sqrt{-2\mu}}\frac{2}{V}\sum_{\mathbf{k}}\left[u_{\mathbf{k}}v_{\mathbf{k}}u_{\mathbf{k}-\mathbf{q}}v_{\mathbf{k}-\mathbf{q}}\left(\frac{1}{i\hbar\omega_n - \hbar\omega_{\mathbf{k}} - \hbar\omega_{\mathbf{k}-\mathbf{q}}} + \frac{1}{+i\hbar\omega_n + \hbar\omega_{\mathbf{k}} + \hbar\omega_{\mathbf{k}-\mathbf{q}}} \right) \right], \tag{228}$$

and $\hbar\Sigma_{22}(\mathbf{q},i\omega_n) = \hbar\Sigma_{11}(\mathbf{q},-i\omega_n)$, $\hbar\Sigma_{12}(\mathbf{q},i\omega_n) = \hbar\Sigma_{21}(\mathbf{q},i\omega_n)$, and $\omega_{\mathbf{k}} = \sqrt{\Delta^2 + (\epsilon_{\mathbf{k}} - \mu)^2}$ is the atomic spectrum in the BCS state. Note that the we have neglected the thermal Fermi factors $N_{\mathbf{k}-\mathbf{q}}$ and $N_{\mathbf{k}}$ and that the corrections due to the background interactions to the self-energy (see also [123]) are approximated in the two-body normal state limit. This is justified in the BEC limit where $|\mu| \gg \Delta, k_B T$. To the lowest order in perturbation theory the dressed-molecule propagator given by Eqs. (227) and (228) can be approximated by the matrix

$$-\hbar\mathbf{G}^{-1} \simeq \frac{1}{Z}\begin{pmatrix} -i\hbar\omega_n + \epsilon_{\mathbf{K}}/2 + \frac{|\Delta|^2}{4|\mu|}(1-Z)\left(1+4\sqrt{\frac{|\epsilon_{\mathrm{m}}|}{\epsilon_{\mathrm{bg}}}}\right) & \frac{|\Delta|^2}{4|\mu|}(1-Z)\left(1+4\sqrt{\frac{|\epsilon_{\mathrm{m}}|}{\epsilon_{\mathrm{bg}}}}\right) \\ \frac{|\Delta|^2}{4|\mu|}(1-Z)\left(1+4\sqrt{\frac{|\epsilon_{\mathrm{m}}|}{\epsilon_{\mathrm{bg}}}}\right) & i\hbar\omega_n + \epsilon_{\mathbf{K}}/2 + \frac{|\Delta|^2}{4|\mu|}(1-Z)\left(1+4\sqrt{\frac{|\epsilon_{\mathrm{m}}|}{\epsilon_{\mathrm{bg}}}}\right) \end{pmatrix}$$
$$\simeq \frac{1}{Z}\begin{pmatrix} -i\hbar\omega_n + \epsilon_{\mathbf{K}}/2 + \mathrm{T}_{\mathrm{m}}^{\mathrm{Born}} n_{\mathrm{mc}} & \mathrm{T}_{\mathrm{m}}^{\mathrm{Born}} n_{\mathrm{mc}} \\ \mathrm{T}_{\mathrm{m}}^{\mathrm{Born}} n_{\mathrm{mc}} & i\hbar\omega_n + \epsilon_{\mathbf{K}}/2 + \mathrm{T}_{\mathrm{m}}^{\mathrm{Born}} n_{\mathrm{mc}} \end{pmatrix} \tag{229}$$

with

$$\mathrm{T}_{\mathrm{m}}^{\mathrm{Born}} \equiv \Gamma_{\mathrm{m}}^{\mathrm{Born}}(\mathbf{0},\mathbf{0},\mathbf{0},0) = (4\pi\hbar^2/m_{\mathrm{m}})2a_{\mathrm{eff}}(B)(1-Z)^2\left(1+4\sqrt{\frac{|\epsilon_{\mathrm{m}}|}{\epsilon_{\mathrm{bg}}}}\right). \tag{230}$$

The derivation of Eq. (229) follows essentially from an expansion in $|\Delta|/|\mu|$ of the normal and anomalous molecular self-energies at nonzero energy and momentum retaining only the linear terms in $\hbar\omega_n$ and $\epsilon_{\mathbf{K}}/2$ [130]. A sketch of the derivation is given in Appendix A. Note that in Eq. (230), we have made use of $|\Delta|^2/4|\mu| = (4\pi\hbar^2/m_{\mathrm{m}})2a_{\mathrm{eff}}(B)(1-Z)n_{\mathrm{mc}} \simeq (4\pi\hbar^2/m_{\mathrm{m}})2a(B)n_{\mathrm{mc}}$, where $a_{\mathrm{eff}}(B)$ has been defined in Eq. (207). Clearly, Eq. (230) implies that the molecule-molecule scattering length in the Born approximation is given by

$$a_{\mathrm{m}}^{\mathrm{Born}} = 2a_{\mathrm{eff}}(B)(1-Z)^2\left(1+4\sqrt{\frac{|\epsilon_{\mathrm{m}}|}{\epsilon_{\mathrm{bg}}}}\right). \tag{231}$$

In the BEC regime investigated experimentally until now for the broad resonance in ^{6}Li, where $\epsilon_{\mathrm{m}} \simeq -\hbar^2/ma^2(B)$ this essentially reduces to

$$a_{\mathrm{m}}^{\mathrm{Born}} = 2a(B)(1-Z)^2\left(1+4\sqrt{\frac{|\epsilon_{\mathrm{m}}|}{\epsilon_{\mathrm{bg}}}}\right). \tag{232}$$

However, we know that in that regime we have $Z \simeq 0$ and $\epsilon_{\mathrm{bg}} \gg |\epsilon_{\mathrm{m}}|$, such that

$$a_{\mathrm{m}}^{\mathrm{Born}} \simeq 2a(B) \tag{233}$$

in a very good approximation. The results of Eqs. (231)–(233) have to be compared with the mean-field results we obtained in Eqs. (209), (211), and (212). Moreover, it can be shown that the nonuniversal correction induced by the factor $(1-Z)^2(1+4\sqrt{|\epsilon_{\mathrm{m}}|/\epsilon_{\mathrm{bg}}})$ is independent of the approximation used in the calculation of the molecule-molecule vertex interaction. Therefore we can anticipate that the full dressed-molecule scattering length should obey

$$a_{\mathrm{m}}(B) \simeq 0.6a(B)(1-Z)^2\left(1+4\sqrt{\frac{|\epsilon_{\mathrm{m}}|}{\epsilon_{\mathrm{bg}}}}\right) \tag{234}$$

in the BEC limit of the crossover region after including higher-order corrections [40,41].

For $\delta \leqslant -\epsilon_{\mathrm{bg}}$, the approximation $\epsilon_{\mathrm{m}} \simeq -\hbar^2/ma^2(B)$ is not valid, and the dressed-molecules scattering length is expected to be

$$a_{\mathrm{m}}(B) \simeq 0.6a_{\mathrm{eff}}(B)(1-Z)^2\left(1+4\sqrt{\frac{|\epsilon_{\mathrm{m}}|}{\epsilon_{\mathrm{bg}}}}\right), \tag{235}$$

which scales as $|\epsilon_{\mathrm{m}}|^{-3}$ at larger negative detunings when the wavefunction renormalization factor Z goes fast to $Z \simeq 1$. Unfortunately, the molecule-molecule scattering length of ^{6}Li$_2$ has not been investigated yet at such large negative magnetic fields ($B < 650$ G). Note also that, in the case of ^{6}Li, this formula does not hold for all magnetic fields below the resonance. We have seen (see also Fig. 5) that the molecules never enter in the asymptotic region $\epsilon_{\mathrm{m}} \simeq \delta(B)$. Hence, the formula in Eq. (235) describes the small "nonuniversal" corrections due to the closed-channel in the region just below $B < 650$ G.

From the Bogoliubov propagator of Eq. (229) we find an energy spectrum for the dressed molecules [57] which is linear at low momenta

$$E_{\mathrm{m}}(\mathbf{K}) = \sqrt{(\hbar^2\mathbf{K}^2/2m_{\mathrm{m}})^2 + (\hbar^2\mathbf{K}^2/2m_{\mathrm{m}})2\mathrm{T}_{\mathrm{m}}^{\mathrm{Born}}n_{\mathrm{m}}}. \tag{236}$$

In the remaining part of this section we want to show that in this regime the gas is mainly constituted by a gas of interacting dressed molecules. The mean-field equation of state in Eq. (193), however, needs to be modified after the introduction of the fluctuations that lead to the superfluid dressed-molecule propagator of Eq. (229). In the self-consistent approach of [14], the total number of particles is given by the formula

$$n = 2Zn_{\mathrm{mc}} - 2\frac{1}{\hbar\beta V}\mathrm{Tr}[\mathbf{G}] + 2\frac{1}{\hbar\beta V}\mathrm{Tr}[\mathbf{G}_{\mathrm{f}}], \tag{237}$$

where the fermionic single-particle propagator $\mathbf{G}_{\mathrm{f}}$ is given by the matrix

$$\begin{pmatrix} G_{\mathrm{f},11}^{-1}(\mathbf{k},i\omega_n) & G_{\mathrm{f},12}^{-1}(\mathbf{k},i\omega_n) \\ G_{\mathrm{f},21}^{-1}(\mathbf{k},i\omega_n) & G_{\mathrm{f},22}^{-1}(\mathbf{k},i\omega_n) \end{pmatrix} = \begin{pmatrix} G_{\uparrow,0}(\mathbf{k},i\omega_n)^{-1} & 0 \\ 0 & -G_{\downarrow,0}(-\mathbf{k},i\omega_n)^{-1} \end{pmatrix} - \begin{pmatrix} \hbar\Sigma_{11}^{\mathrm{f}}(\mathbf{k},i\omega_n) & \hbar\Sigma_{12}^{\mathrm{f}}(\mathbf{k},i\omega_n)+\Delta \\ \hbar\Sigma_{21}^{\mathrm{f}}(\mathbf{k},i\omega_n)+\Delta^\star & \hbar\Sigma_{22}^{\mathrm{f}}(\mathbf{k},i\omega_n) \end{pmatrix}, \tag{238}$$

and the fermionic self-energies $\hbar\Sigma_{ij}^{\mathrm{f}}(\mathbf{k},i\omega_n)$ contain the feedback effects of the dressed molecules on the atoms. The term $\mathrm{Tr}[\mathbf{G}]$ is easily evaluated according to the theory of a weakly-interacting Bose gas. We have

$$2Zn_{\mathrm{mc}} - 2\frac{1}{\hbar\beta V}\mathrm{Tr}[\mathbf{G}] = 2Zn_{\mathrm{mc}} + 2Z\int\frac{d\mathbf{q}}{(2\pi)^3}[u_{\mathrm{m}}^2(\mathbf{q})N_B(E_{\mathrm{m}}(\mathbf{q})) - v_{\mathrm{m}}^2(\mathbf{q})N_B(-E_{\mathrm{m}}(\mathbf{q}))] = 2Z[n_{\mathrm{mc}}(T) + n_{\mathrm{m}}'(T)], \tag{239}$$

where

$$v_{\mathrm{m}}^2(\mathbf{q}) = u_{\mathrm{m}}^2(\mathbf{q}) - 1 = \frac{\frac{\mathbf{q}^2}{2m_{\mathrm{m}}} + \mathrm{T}_{\mathrm{m}}^{\mathrm{Born}}n_{\mathrm{mc}} - E_{\mathrm{m}}(\mathbf{q})}{2E_{\mathrm{m}}(\mathbf{q})} \tag{240}$$

are the standard bosonic coherence factors of the Bogoliubov transformation [87] and $n_{\mathrm{m}}'(T)$ is the noncondensed density of dressed molecules at temperature T. The density of Eq. (239) corresponds to the bare-molecular contribution to the total density. It is very small because in the BEC limit that

we are considering for a broad resonance, we have $Z \simeq 0$. Therefore, we have that the main contribution in the equation of state in Eq. (237) comes from $\mathrm{Tr}[\mathbf{G}_{\mathrm{f}}]$. To calculate this trace we have first to calculated the fermionic self-energies. Upon neglecting higher-order contributions, we ultimately find [34]

$$\hbar \begin{pmatrix} G_{\mathrm{f},11}^{-1}(\mathbf{k}, i\omega_n) & G_{\mathrm{f},12}^{-1}(\mathbf{k}, i\omega_n) \\ G_{\mathrm{f},21}^{-1}(\mathbf{k}, i\omega_n) & G_{\mathrm{f},22}^{-1}(\mathbf{k}, i\omega_n) \end{pmatrix} = \begin{pmatrix} i\hbar\omega_n + \mu - \epsilon_{\mathbf{k}} - \dfrac{\Delta'^2}{i\hbar\omega_n - \mu + \epsilon_{\mathbf{k}}} & \Delta \\ \Delta^{\star} & -i\hbar\omega_n - \mu + \epsilon_{\mathbf{k}} - \dfrac{\Delta'^2}{i\hbar\omega_n - \mu + \epsilon_{\mathbf{k}}} \end{pmatrix} \tag{241}$$

where

$$\Delta'^2 = \frac{g^2 Z n'_{\mathrm{m}}}{\left(1 + \sqrt{\dfrac{|2\mu|}{\epsilon_{bg}}}\right)^2}. \tag{242}$$

Note that we have neglected the off-diagonal fermionic self-energies because in the limit under consideration we can show that $\hbar\Sigma_{12}^{\mathrm{f}}(0,0) \simeq |\Delta|(|\Delta|^2/2|\mu|^2)$. From Eq. (241) we get the expression for $G_{\mathrm{f},11}$ in the BEC limit [34]

$$G_{\mathrm{f},11}(\mathbf{k}, \omega_n) \simeq \frac{\hbar}{i\hbar\omega_n + \mu - \epsilon_{\mathbf{k}} - \dfrac{|\Delta|^2 + \Delta'^2}{i\omega_n - \mu + \epsilon_{\mathbf{k}}}}, \tag{243}$$

where we have neglected a term of order $\Delta'^2/|\mu|$ with respect to $|\mu|$. Note that Eq. (243) has the same formal structure of the corresponding BCS expression [87], with the replacement $|\Delta|^2 \to (|\Delta|^2 + \Delta'^2)$. Accordingly, the trace of the fermionic propagator can be rewritten in the BCS-like form

$$\frac{1}{\hbar\beta V} 2\mathrm{Tr}[\mathbf{G}_{\mathrm{f}}] \simeq \int \frac{d^3\mathbf{k}}{(2\pi)^3} \left(1 - \frac{\epsilon_{\mathbf{k}} - \mu}{\sqrt{(|\Delta|^2 + \Delta'^2) + (\epsilon_{\mathbf{k}} - \mu)^2}}\right). \tag{244}$$

Expanding the right-hand side of this equation as we did for the mean-field BCS equation of state in Eq. (196), we have

$$\frac{1}{\hbar\beta V} 2\mathrm{Tr}[\mathbf{G}_{\mathrm{f}}] \simeq (|\Delta|^2 + \Delta'^2) \frac{m^2}{4\pi\sqrt{2m|\mu|}\hbar^3}. \tag{245}$$

Moreover, using $2\mu \simeq |\epsilon_{\mathrm{m}}|$ and the definition of two-body Z we find

$$2\frac{1}{\hbar\beta V}\mathrm{Tr}[\mathbf{G}_{\mathrm{f}}] \simeq \frac{2Z(n_{\mathrm{mc}} + n_{\mathrm{m}'})\eta}{2\sqrt{|\epsilon_{\mathrm{m}}|}\left(1 + \sqrt{\dfrac{|\epsilon_{\mathrm{m}}|}{\epsilon_{bg}}}\right)^2} \simeq 2(1 - Z)(n_{\mathrm{mc}} + n'_{\mathrm{m}}). \tag{246}$$

Joining the two contributions of Eqs. (246) and (239) we have

$$n \simeq 2[n_{\mathrm{mc}}(T) + n'_{\mathrm{m}}(T)]. \tag{247}$$

This result holds asymptotically for $k_B T \ll |\epsilon_{\mathrm{m}}|$ and it represents the extension to a two-channel model in the case of a broad resonance, of the description of the BEC limit in [34,36] based on the composite bosons of the single-channel model. However, it is important to stress that these results are only valid in the lowest order of perturbation theory. Furthermore, we use a definition of the probability Z that is only true in the asymptotic BEC limit. The calculation of Z in the strong-coupling region requires a more general approach as shown in [57].

Nevertheless, our analysis of the BEC limit shows the way to connect the two models in the limit of a very broad resonance, where the single-channel model accounts fairly well for the thermodynamics of the gas inside the BEC-BCS crossover region.

VI. CONCLUSIONS AND OUTLOOK

In this paper we have shown that our dressed-molecule picture represents an effective and consistent approach in order to describe the physics of ultracold Fermi gases near a Feshbach resonance. The dressed molecule is the real physical entity of the BEC-BCS crossover in atomic Fermi gases near a Feshbach resonance, because the wavefunction of the Feshbach molecules is always a coherent superposition. In this formulation the information about the mixing of the two-channels is preserved at each stage in the many-body calculation. Therefore it has the advantage that it can be applied also to medium and narrow resonances, when $\eta^2 \leqslant \epsilon_F$, where the single-channel approximation is expected to fail. However, a proper treatment of the narrow resonance case requires the inclusion of the finite-range corrections in the theory [47,131]. This will be addressed elsewhere.

ACKNOWLEDGMENTS

We are most grateful to R. Duine, B. Farid, P. Pieri, P. Coleman, F. Nogueira, M. Haque, F. Marchetti, B. Marcelis, S. Kokkelmans, T. Köhler, and R. G. Hulet for stimulating discussions and criticisms. We would like also to thank Professor H. Kleinert and his group for the hospitality at the Institute of Theoretical Physics of the Free University of Ber-

lin, and Professor R. Graham for the hospitality at the University of Essen.

APPENDIX

In this appendix we present the detailed calculation which leads to the dressed-molecule propagator of Eq. (229) from Eq. (227). In order to make the derivation more transparent we discuss first the case when $a_{\mathrm{bg}}=0$, because the inclusion of the background interactions does not change qualitatively the discussion. Neglecting the background scattering length corrections, the molecular self-energies of Eq. (228) reduce to

$$\hbar\Sigma_{11}(\mathbf{q},i\omega_n)=\frac{g^2}{V}\sum_{\mathbf{k}}\left(\frac{u_{\mathbf{k}}^2u_{\mathbf{k}-\mathbf{q}}^2}{i\hbar\omega_n-\hbar\omega_{\mathbf{k}}-\hbar\omega_{\mathbf{k}-\mathbf{q}}}-\frac{v_{\mathbf{k}}^2v_{\mathbf{k}-\mathbf{q}}^2}{i\hbar\omega_n+\hbar\omega_{\mathbf{k}}+\hbar\omega_{\mathbf{k}-\mathbf{q}}}+\frac{1}{2\epsilon_{\mathbf{k}}}\right),$$

$$\hbar\Sigma_{12}(\mathbf{q},i\omega_n)=\frac{2g^2}{V}\sum_{\mathbf{k}}\left[u_{\mathbf{k}}v_{\mathbf{k}}u_{\mathbf{k}-\mathbf{q}}v_{\mathbf{k}-\mathbf{q}}\left(\frac{1}{-i\hbar\omega_n+\hbar\omega_{\mathbf{k}}+\hbar\omega_{\mathbf{k}-\mathbf{q}}}+\frac{1}{i\hbar\omega_n+\hbar\omega_{\mathbf{k}}+\hbar\omega_{\mathbf{k}-\mathbf{q}}}\right)\right], \tag{A1}$$

where, in the definition of the gap of Eq. (188) entering the definition of the coherence factors $v_{\mathbf{k}}$ and $u_{\mathbf{k}}$, the contribution due to the background interaction has to be neglected as well. In the BEC limit, where $2\mu\simeq\epsilon_{\mathrm{m}}\gg k_BT$, Δ, we can expand the selfenergies of Eq. (A1) for small values of $|\mathbf{q}|$ and ω_n as

$$\hbar\Sigma_{11}(\mathbf{q},i\omega_n)=A_0+A_1i\hbar\omega_n+A_2\epsilon_{\mathbf{q}}/2+O(\omega_n^2,|\mathbf{q}|^4),$$

$$\hbar\Sigma_{12}(\mathbf{q},i\omega_n)=B_0+O(\omega_n^2,|\mathbf{q}|^2). \tag{A2}$$

with the coefficients of the expansion given by

$$A_0=\frac{g^2}{V}\sum_{\mathbf{k}}\frac{1}{2\epsilon_{\mathbf{k}}}-\frac{1}{2\omega_{\mathbf{k}}}+\frac{g^2}{V}\sum_{\mathbf{k}}\frac{|\Delta|^2}{4\omega_{\mathbf{k}}^3},$$

$$A_1=-\frac{g^2}{V}\sum_{\mathbf{k}}\frac{\epsilon_{\mathbf{k}}-\mu}{4\omega_{\mathbf{k}}^3},$$

$$A_2=\frac{g^2}{V}\sum_{\mathbf{k}}\frac{1}{8}\left\{\frac{(\epsilon_{\mathbf{k}}-\mu)[2(\epsilon_{\mathbf{k}}-\mu)^2-|\Delta|^2]}{4\omega_{\mathbf{k}}^5}+\frac{2\epsilon_{\mathbf{k}}|\Delta|^2[8(\epsilon_{\mathbf{k}}-\mu)^2+3|\Delta|^2]}{3\omega_{\mathbf{k}}^7}\right\},$$

$$B_0=\frac{g^2}{V}\sum_{\mathbf{k}}\frac{|\Delta|^2}{4\omega_{\mathbf{k}}^3}. \tag{A3}$$

Substituting these results in Eq. (227) and using the gap equation of Eq. (190), the dressed-molecule propagator can be rewritten as

$$-\hbar\mathbf{G}^{-1}\simeq\begin{pmatrix}-i\hbar\omega_n+\epsilon_{\mathbf{K}}/2-\frac{g^2}{V}\sum_{\mathbf{k}}\frac{|\Delta|^2}{4\omega_{\mathbf{k}}^3}+A_1i\hbar\omega_n+A_2\epsilon_{\mathbf{K}}/2 & \frac{g^2}{V}\sum_{\mathbf{k}}\frac{|\Delta|^2}{4\omega_{\mathbf{k}}^3}\\ \frac{g^2}{V}\sum_{\mathbf{k}}\frac{|\Delta|^2}{4\omega_{\mathbf{k}}^3} & i\hbar\omega_n+\epsilon_{\mathbf{K}}/2-\frac{g^2}{V}\sum_{\mathbf{k}}\frac{|\Delta|^2}{4\omega_{\mathbf{k}}^3}-A_1i\hbar\omega_n+A_2\epsilon_{\mathbf{K}}/2\end{pmatrix}. \tag{A4}$$

This expression can be simplified further by noting that in the BEC limit one has

$$\frac{g^2}{V}\sum_{\mathbf{k}}\frac{|\Delta|^2}{4\omega_{\mathbf{k}}^3}\simeq\left(\frac{1-Z}{Z}\right)\frac{|\Delta|^2}{4|\mu|},\quad A_1\simeq A_2\simeq\left(\frac{Z-1}{Z}\right) \tag{A5}$$

in the leading order of $|\Delta|^2/|\mu|$. Therefore, we get

$$-\hbar\mathbf{G}^{-1}\simeq\frac{1}{Z}\begin{pmatrix}-i\hbar\omega_n+\epsilon_{\mathbf{K}}/2+\frac{|\Delta|^2}{4|\mu|}(1-Z) & \frac{|\Delta|^2}{4|\mu|}(1-Z)\\ \frac{|\Delta|^2}{4|\mu|}(1-Z) & i\hbar\omega_n+\epsilon_{\mathbf{K}}/2+\frac{|\Delta|^2}{4|\mu|}(1-Z)\end{pmatrix}. \tag{A6}$$

This derivation can be generalized rather straightforwardly in order to include the effects of the background scattering length in the molecular self-energies of Eq. (228). The coefficients of Eq. (A3) differ only by an overall factor $1/(1+|a_{\mathrm{bg}}|\sqrt{-2\mu})$, and Z, ϵ_{m}, Δ, and the gap equation must be replaced everywhere with the more general expressions that include

the background scattering length corrections. Note, however, that the background scattering corrections in the self-energies of Eq. (228) are valid only in the BEC limit. Therefore, in order to simplify the dressed-molecule propagator as we have done in Eq. (A4), we cannot use the general gap equation of Eq. (190). Alternatively, we expand the coefficients of Eq. (A3) in powers of $\Delta/|\mu|$ and then we use the expanded version of the gap equation of Eq. (195). Ultimately we find in this manner that

$$-\hbar\mathbf{G}^{-1} \simeq \frac{1}{Z}\begin{pmatrix} -i\hbar\omega_n + \epsilon_{\mathbf{K}}/2 + \frac{|\Delta|^2}{4|\mu|}(1-Z)\left(1+4\sqrt{\frac{|\epsilon_{\mathrm{m}}|}{\epsilon_{\mathrm{bg}}}}\right) & \frac{|\Delta|^2}{4|\mu|}(1-Z)\left(1+4\sqrt{\frac{|\epsilon_{\mathrm{m}}|}{\epsilon_{\mathrm{bg}}}}\right) \\ \frac{|\Delta|^2}{4|\mu|}(1-Z)\left(1+4\sqrt{\frac{|\epsilon_{\mathrm{m}}|}{\epsilon_{\mathrm{bg}}}}\right) & i\hbar\omega_n + \epsilon_{\mathbf{K}}/2 + \frac{|\Delta|^2}{4|\mu|}(1-Z)\left(1+4\sqrt{\frac{|\epsilon_{\mathrm{m}}|}{\epsilon_{\mathrm{bg}}}}\right) \end{pmatrix}, \tag{A7}$$

as given in Eq. (229).

[1] M. H. Anderson, J. Ensher, M. Matthews, E. A. Cornell, and C. E. Wieman, Science **269**, 198 (1995).
[2] K. B. Davis, M. O. Mewes, M. R. Andrews, N. J. van Druten, D. S. Durfee, D. M. Kurn, and W. Ketterle, Phys. Rev. Lett. **75**, 3969 (1995).
[3] C. C. Bradley, C. A. Sackett, J. J. Tollett, and R. G. Hulet, Phys. Rev. Lett. **75**, 1687 (1995).
[4] H. Feshbach, Ann. Phys. (Paris) **5**, 357 (1958); **19**, 287 (1962).
[5] B. DeMarco and D. Jin, Science **285**, 1703 (1999).
[6] A. G. Truscott, K. E. Strecker, W. I. McAlexander, G. B. Partridge, and R. G. Hulet, Science **291**, 2570 (2001).
[7] F. Schreck, L. Khaykovich, K. L. Corwin, G. Ferrari, T. Bourdel, J. Cubizolles, and C. Salomon, Phys. Rev. Lett. **87**, 080403 (2001).
[8] K. Dieckmann, C. A. Stan, S. Gupta, Z. Hadzibabic, C. H. Schunck, and W. Ketterle, Phys. Rev. Lett. **89**, 203201 (2002).
[9] T. Bourdel, J. Cubizolles, L. Khaykovich, K. M. F. Magalhães, S. J. J. M. F. Kokkelmans, G. V. Shlyapnikov, and C. Salomon, Phys. Rev. Lett. **91**, 020402 (2003).
[10] D. M. Eagles, Phys. Rev. **186**, 456 (1969).
[11] A. J. Leggett, in *Modern Trends in the Theory of Condensed Matter* (Springer-Verlag, Berlin, 1980), pp. 13–27.
[12] P. Nozieres and S. Schmitt-Rink, J. Low Temp. Phys. **59**, 195 (1985).
[13] C. A. R. Sáde Melo, M. Randeria, and J. R. Engelbrecht, Phys. Rev. Lett. **71**, 3202 (1993).
[14] R. Haussmann, Phys. Rev. B **49**, 12975 (1994).
[15] C. A. Regal, M. Greiner, and D. S. Jin, Phys. Rev. Lett. **92**, 040403 (2004).
[16] M. W. Zwierlein, C. A. Stan, C. H. Schunck, S. M. F. Raupach, A. J. Kerman, and W. Ketterle, Phys. Rev. Lett. **92**, 120403 (2004).
[17] J. Kinast, S. L. Hemmer, M. E. Gehm, A. Turlapov, and J. E. Thomas, Phys. Rev. Lett. **92**, 150402 (2004); Science **307**, 1296 (2005).
[18] M. Bartenstein, A. Altmeyer, S. Riedl, S. Jochim, C. Chin, J. H. Denschlag, and R. Grimm, Phys. Rev. Lett. **92**, 120401 (2004); **92**, 203201 (2004).
[19] T. Bourdel, L. Khaykovich, J. Cubizolles, J. Zhang, F. Chevy, M. Teichmann, L. Tarruell, S. J. J. M. F. Kokkelmans, and C. Salomon, Phys. Rev. Lett. **93**, 050401 (2004).
[20] G. B. Partridge, K. E. Strecker, R. I. Kamar, M. W. Jack, and R. G. Hulet, Phys. Rev. Lett. **95**, 020404 (2005).
[21] M. W. Zwierlein, J. R. Abo-Shaeer, A. Schirotzek, C. H. Schunk, and W. Ketterle, Nature (London) **435**, 1047 (2005).
[22] M. W. Zwierlein, J. R. Abo-Shaeer, A. Schirotzek, C. H. Schunk, and W. Ketterle, Science **311**, 492 (2006).
[23] G. B. Partridge, W. Li, R. I. Kamar, Y. Liao, and R. G. Hulet, Science **311**, 503 (2006).
[24] J. J. Sakurai, *Modern Quantum Mechanics* (Addison-Wesley, New York, 1985).
[25] M. Randeria, in *Bose-Einstein Condensation*, edited by A. Griffin, D. W. Snoke, and S. Stringari (Cambridge University Press, Cambridge, 1995), p. 355.
[26] H. T. C. Stoof, M. Houbiers, C. A. Sackett, and R. G. Hulet, Phys. Rev. Lett. **76**, 10 (1996); M. Houbiers, R. Ferwerda, H. T. C. Stoof, W. I. McAlexander, C. A. Sackett, and R. G. Hulet, Phys. Rev. A **56**, 4864 (1997).
[27] H. Heiselberg, C. J. Pethick, H. Smith, and L. Viverit, Phys. Rev. Lett. **85**, 2418 (2000).
[28] H. Heiselberg, Phys. Rev. A **63**, 043606 (2001).
[29] H. Heiselberg, Phys. Rev. A **73**, 013607 (2006).
[30] R. Combescot, Phys. Rev. Lett. **91**, 120401 (2003).
[31] R. Combescot, New J. Phys. **5**, 86 (2003).
[32] R. Combescot, X. Leyronas, and M. Yu. Kagan, Phys. Rev. A **73**, 023618 (2006).
[33] P. Pieri and G. C. Strinati, Phys. Rev. B **61**, 15370 (2000); cond-mat/0307421.
[34] P. Pieri, L. Pisani, and G. C. Strinati, Phys. Rev. B **70**, 094508 (2004); A. Perali, P. Pieri, L. Pisani, and G. C. Strinati, Phys. Rev. Lett. **92**, 220404 (2004).
[35] A. Perali, P. Pieri, and G. C. Strinati, Phys. Rev. Lett. **93**, 100404 (2004).
[36] P. Pieri and G. C. Strinati, Phys. Rev. B **71**, 094520 (2005).
[37] L. Viverit, S. Giorgini, L. P. Pitaevskii, and S. Stringari, Phys. Rev. A **69**, 013607 (2004).
[38] A. V. Avdeenkov and J. L. Bohn, Phys. Rev. A **71**, 023609 (2005).
[39] R. B. Diener and Tin-Lun Ho, cond-mat/0405174; cond-mat/0404517.
[40] I. V. Brodsky, M. Yu. Kagan, A. V. Klaptsov, R. Combescot, and X. Leyronas, Phys. Rev. A **73**, 032724 (2006).
[41] J. Levinsen and V. Gurarie, Phys. Rev. A **73**, 053607 (2006).
[42] P. D. Drummond, K. V. Kheruntsyan, and H. He, Phys. Rev. Lett. **81**, 3055 (1998).

[43] E. Timmermans, P. Tommasini, H. Hussein, and A. Kerman, Phys. Rep. **315**, 199 (1999).
[44] E. Timmermans, K. Furuya, P. W. Milonni, and A. K. Kerman, Phys. Lett. A **285**, 228 (2001).
[45] M. Holland, S. J. J. M. F. Kokkelmans, M. L. Chiofalo, and R. Walser, Phys. Rev. Lett. **87**, 120406 (2001).
[46] J. N. Milstein, S. J. J. M. F. Kokkelmans, and M. J. Holland, Phys. Rev. A **66**, 043604 (2002).
[47] R. A. Duine and H. T. C. Stoof, Phys. Rep. **396**, 115 (2004); R. A. Duine and H. T. C. Stoof, J. Opt. B: Quantum Semiclassical Opt. **5**, S212 (2003); cond-mat/0312254.
[48] Y. Ohashi and A. Griffin, Phys. Rev. Lett. **89**, 130402 (2002); Phys. Rev. A **67**, 033603 (2003); **67**, 063612 (2003).
[49] G. M. Falco, R. A. Duine, and H. T. C. Stoof, Phys. Rev. Lett. **92**, 140402 (2004).
[50] G. M. Bruun and C. J. Pethick, Phys. Rev. Lett. **92**, 140404 (2004).
[51] J. Stajic, J. N. Milstein, Quijn Chen, M. L. Chiofalo, M. J. Holland, and K. Levin, Phys. Rev. A **69**, 063610 (2004).
[52] G. M. Falco and H. T. C. Stoof, Phys. Rev. Lett. **92**, 130401 (2004).
[53] P. D. Drummond and K. V. Kheruntsyan, Phys. Rev. A **70**, 033609 (2004).
[54] S. Diehl and C. Wetterich, Phys. Rev. A **73**, 033615 (2006).
[55] S. Diehl and C. Wetterich, cond-mat/0510407.
[56] M. W. J. Romans, R. A. Duine, S. Sachdev, and H. T. C. Stoof, Phys. Rev. Lett. **93**, 020405 (2004).
[57] M. W. J. Romans and H. T. C. Stoof, Phys. Rev. Lett. **95**, 260407 (2005).
[58] J. Stajic, Quijn Chen, and K. Levin, Phys. Rev. A **71**, 033601 (2005).
[59] G. M. Falco and H. T. C. Stoof, Phys. Rev. A **71**, 063614 (2005).
[60] J. Javanainen, M. Kostrun, M. Mackie, and A. Carmichael, Phys. Rev. Lett. **95**, 110408 (2005).
[61] Xia-Ji Liu and Hui Hu, Phys. Rev. A **72**, 063613 (2005).
[62] W. C. Stwalley, Phys. Rev. Lett. **37**, 1628 (1976).
[63] E. Tiesinga, B. J. Verhaar, and H. T. C. Stoof, Phys. Rev. A **47**, 4114 (1993).
[64] H. T. C. Stoof, J. M. V. A. Koelman, and B. J. Verhaar, Phys. Rev. B **38**, 4688 (1988).
[65] M. Houbiers, H. T. C. Stoof, W. I. McAlexander, and R. G. Hulet, Phys. Rev. A **57**, R1497 (1998).
[66] W. Ketterle, D. Durfee, and D. Kurn, "Making and probing Bose-Einstein condensates," in *Proceedings of the 1998 Enrico Fermi Summer School in Bose-Einstein Condensation* (Societa Italiana di Fisica, Italy, 1998).
[67] A. J. Moerdijk, B. J. Verhaar, and A. Axelsson, Phys. Rev. A **51**, 4852 (1995).
[68] M. Greiner, C. A. Regal, and D. S. Jin, Nature (London) **426**, 537 (2003).
[69] K. E. Strecker, G. B. Partridge, and R. G. Hulet, Phys. Rev. Lett. **91**, 080406 (2003).
[70] J. Cubizolles, T. Bourdel, S. J. J. M. F. Kokkelmans, G. V. Shlyapnikov, and C. Salomon, Phys. Rev. Lett. **91**, 240401 (2003).
[71] S. Jochim, M. Bartenstein, A. Altmeyer, G. Hendl, C. Chin, J. H. Denschlag, and R. Grimm, Phys. Rev. Lett. **91**, 240402 (2003).
[72] S. Jochim, M. Bartenstein, A. Altmeyer, G. Hendl, S. Riedl, C. Chin, J. H. Denschlag, and R. Grimm, Science **302**, 2101 (2003).
[73] M. W. Zwierlein, C. A. Stan, C. H. Schunck, S. M. F. Raupach, S. Gupta, Z. Hadzibabic, and W. Ketterle, Phys. Rev. Lett. **91**, 250401 (2003).
[74] K. M. O'Hara, S. L. Hemmer, M. E. Gehm, S. R. Granade, and J. E. Thomas, Science **298**, 2179 (2002).
[75] J. Herbig, T. Kraemer, M. Mark, T. Weber, C. Chin, H. C. Nagerl, and R. Grimm, Science **301**, 1510 (2003).
[76] S. Durr, T. Volz, A. Marte, and G. Rempe, Phys. Rev. Lett. **92**, 020406 (2004).
[77] K. Winkler, G. Thalhammer, M. Theis, H. Ritsch, R. Grimm, and J. H. Denschlag, Phys. Rev. Lett. **95**, 063202 (2005).
[78] D. B. M. Dickerscheid, U. Al Khawaja, D. van Oosten, and H. T. C. Stoof, Phys. Rev. A **71**, 043604 (2005).
[79] D. S. Petrov, C. Salomon, and G. V. Shlyapnikov, Phys. Rev. Lett. **93**, 090404 (2004).
[80] V. V. Goldman, I. F. Silvera, and A. J. Leggett, Phys. Rev. B **24**, R2870 (1981).
[81] G. Baym and C. J. Pethick, Phys. Rev. Lett. **76**, 6 (1996).
[82] W. Zhang, C. A. Sackett, and R. G. Hulet, Phys. Rev. A **60**, 504 (1999).
[83] M. Rodriguez, G. S. Paraoanu, and P. Törma, Phys. Rev. Lett. **87**, 100402 (2001).
[84] C. Menotti, P. Pedri, and S. Stringari, Phys. Rev. Lett. **89**, 250402 (2002).
[85] G. Orso, L. P. Pitaevskii, and S. Stringari, Phys. Rev. Lett. **93**, 020404 (2004).
[86] H. P. Büchler, P. Zoller, and W. Zwerger, Phys. Rev. Lett. **93**, 080401 (2004).
[87] A. L. Fetter and J. D. Walecka, *Quantum Theory of Many-Particle Systems* (McGraw-Hill, New York, 1964).
[88] H. T. C. Stoof, in *Coherent Atomic Matter Waves*, edited by R. Keiser, C. Westbrook, and F. David (Springer, Berlin, 2001), p. 219; cond-mat/9903029.
[89] S. T. Beliaev, Sov. Phys. JETP **7**, 299 (1958).
[90] V. Galitskii, Sov. Phys. JETP **7**, 104 (1958).
[91] H. T. C. Stoof, M. Bijlsma, and M. Houbiers, J. Res. Natl. Inst. Stand. Technol. **101**, 443 (1996).
[92] S. J. J. M. F. Kokkelmans and M. J. Holland, Phys. Rev. Lett. **89**, 180401 (2002).
[93] M. Mackie, K.-A. Suominen, and J. Javanainen, Phys. Rev. Lett. **89**, 180403 (2002).
[94] T. Köhler, T. Gasenzer, P. S. Julienne, and K. Burnett, Phys. Rev. Lett. **91**, 230401 (2003).
[95] E. G. M. v. Kempen, B. Marcelis, and S. J. J. M. F. Kokkelmans, Phys. Rev. A **70**, 050701(R) (2004).
[96] C. A. Regal, C. Ticknor, J. L. Bohn, and D. S. Jin, Nature (London) **424**, 47 (2003).
[97] H. Moritz, T. Stöferle, K. Guenter, M. Köhl, and T. Esslinger, Phys. Rev. Lett. **94**, 210401 (2005).
[98] D. B. M. Dickerscheid and H. T. C. Stoof, Phys. Rev. A **72**, 053625 (2005).
[99] B. Marcelis and S. J. J. M. F. Kokkelmans, Phys. Rev. A **74**, 023606 (2006).
[100] B. Marcelis, E. G. M. vanKempen, B. J. Verhaar, and S. J. J. M. F. Kokkelmans, Phys. Rev. A **70**, 012701 (2004).
[101] H. Kleinert, Fortschr. Phys. **26**, 565 (1978).
[102] J. W. Negele and H. Orland, *Quantum Many-Particle Systems* (Addison-Wesley, New York, 1987).

[103] L. P. Gorkov and T. K. Melik-Barkhudarov, Sov. Phys. JETP **13**, 1018 (1961).
[104] D. Goldhaber-Gordon, Hadas Shtrikman, D. Mahalu, D. Abusch-Magder, U. Meirav, and M. A. Kastner, Nature (London) **391**, 156 (1998).
[105] M. Pustilnik and L. I. Glazman, J. Phys.: Condens. Matter **16**, R513 (2004).
[106] S. M. Cronenwett, T. H. Oosterkamp, and L. P. Kouwenhoven, Science **281**, 540 (1998).
[107] A. C. Hewson, *The Kondo Problem to Heavy Fermions* (Cambridge University Press, Cambridge, 1993).
[108] G. D. Mahan, *Many Particle Physics* (Plenum, New York, 1990).
[109] O. Gunnarsson and K. Schonhammer, Phys. Rev. B **28**, 4315 (1983).
[110] See, for exanple, B. Farid, Philos. Mag. B **82**, 1413 (2002), and references therein.
[111] J. M. Luttinger, Phys. Rev. **119**, 1153 (1960); **121**, 942 (1961).
[112] A similar problem is discussed in P. Coleman, I. Paul, and J. Rech, Phys. Rev. B **72**, 094430 (2005).
[113] A. C. Hewson (private communication).
[114] A. M. Tsvelik (private communication).
[115] R. A. Barankov and L. S. Levitov, Phys. Rev. Lett. **93**, 130403 (2004).
[116] P. W. Anderson, Phys. Rev. **112**, 1900 (1958).
[117] P. W. Anderson, J. Phys. C **3**, 2436 (1970).
[118] A. A. Abrikosov, Physics (Long Island City, N.Y.) **2**, 5 (1965).
[119] V. Galitskii and A. B. Migdal, Sov. Phys. JETP **7**, 96 (1958).
[120] D. Thouless, Ann. Phys. (N.Y.) **10**, 553 (1960).
[121] This appears to be contradicted by the results obtained in [48], which uses a Gaussian approximation for the two-channel model and finds a monotonic curve for the critical temperature. However, we believe that this is a result of the soft cutoff introduced to regulate the ultraviolet divercencies in the theory.
[122] The dressed-molecular propagator G of our theory corresponds to the *renormalized Boson* propagator D_M defined by Ohashi and Griffin in [48].
[123] The molecular self-energy of Eq. (83) contains the many-body corrections through the energy dependence of the atom-molecule coupling. In [48] the many-body molecular self-energy is derived formally in a RPA-like structure. We use also this latter form systematically in Sec. V to avoid introducing an energy-dependent gap as in [57] that would complicate unnecessarily the variational calculation at $T=0$. We have seen in Eq. (42) that the two formulations are essentially equivalent in the two-body limit. It can also be shown that in the two extremes of the crossover they are essentially equivalent. It must be pointed out, however, that in [48] Ohashi and Griffin use a different cutoff procedure to regularize the ultraviolet divergencies in the momentum integrals. As a final remark, let us observe that the effect of using an energy-dependent atom-molecule coupling as in the definition of the self-energy of Eq. (83) consists in shifting the high-momentum cutoff of the theory from infinity [13] to $1/a_{bg}$. When the background scattering length is very small this of course does not make any difference. However, when it is rather large as in ^{6}Li mixtures it can lead to important differences in the strong coupling region [57].
[124] P. Grüter, D. Ceperley, and F. Laloë, Phys. Rev. Lett. **79**, 3549 (1997).
[125] M. Bijlsma and H. T. C. Stoof, Phys. Rev. A **54**, 5085 (1996).
[126] G. Baym, J. P. Blaizot, M. Holzmann, F. Laloë, and D. Vautherin, Phys. Rev. Lett. **83**, 1703 (1999).
[127] Q. Chen and K. Levin, Phys. Rev. Lett. **95**, 260406 (2005).
[128] L. P. Pitaevskii, Sov. Phys. JETP **13**, 451 (1961).
[129] E. P. Gross, Nuovo Cimento **20**, 454 (1961).
[130] N. Andrenacci, P. Pieri, and G. C. Strinati, Phys. Rev. B **68**, 144507 (2003); M. Marini, F. Pistolesi, and G. C. Strinati, Eur. Phys. J. B **1**, 151 (1998).
[131] L. M. Jensen, cond-mat/0412431.